CRITICAL REVIEW OF N, N+, N2+, N++, And N2++ MAIN PRODUCTION PROCESSES AND REACTIONS OF RELEVANCE TO TITAN'S ATMOSPHERE

Odile Dutuit[1,2], Nathalie Carrasco[3], Roland Thissen[1], Véronique Vuitton[1], Christian Alcaraz[4],
Pascal Pernot[4], Nadia Balucani[5], Piergiorgio Casavecchia[5], André Canosa[6], Sébastien Le Picard[6],
Jean-Christophe Loison[7], Zdenek Herman[8], Jan Zabka[8], Daniela Ascenzi[9], Paolo Tosi[9],
Pietro Franceschi[10], Stephen D. Price[11], and Panayotis Lavvas[12]

[1] Institut de Planétologie et d'Astrophysique de Grenoble, UJF-Grenoble 1/CNRS-INSU, UMR 5274, F-38041 Grenoble, France;
roland.thissen@obs.ujf-grenoble.fr
[2] Space Research Institute, Austrian Academy of Sciences (IWF/OAW), Schmiedlstraße 6, A-8042 Graz, Austria
[3] Laboratoire Atmosphères, Milieux, Observations Spatiales, CNRS, UVSQ/UPMC, F-78280 Guyancourt, France
[4] Laboratoire de Chimie Physique, CNRS/UPS UMR 8000, Bât.349, F-91405 Orsay Cedex, France
[5] Dipartimento di Chimica, Università degli Studi di Perugia, Via Elce di Sotto, 8, I-06123 Perugia, Italy
[6] Département de Physique Moléculaire, Université de Rennes 1, Institut de Physique de Rennes, UMR 6251 CNRS Université,
Campus de Beaulieu-Bat 11C, F-35042 Rennes Cedex, France
[7] Institut des Sciences Moléculaires, Université Bordeaux 1/CNRS, UMR 5255, 351 cours de la Libération, F-33405 Talence Cedex, France
[8] J. Heyrovský Institute of Physical Chemistry, Academy of Sciences of the Czech Republic, Dolejškova 3 CZ-182 23 Prague 8, Czech Republic
[9] Dipartimento di Fisica, Università di Trento, Via Sommarive 14, I-38123 Trento, Italy
[10] Biostatistics and Data Management, IASMA Research and Innovation Centre, Fondazione E. Mach, Via E. Mach, 1 I-38010 S. Michele all'Adige (TN), Italy
[11] Department of Chemistry, UCL, Christopher Ingold Laboratories, 20 Gordon Street, London WC1H 0AJ, UK
[12] Groupe de Spectrométrie Moléculaire et Atmosphérique, CNRS, UMR 6089, Campus Moulin de la Housse-BP 1039,
Université Reims Champagne-Ardenne, F-51687 Reims, France
Received 2012 July 27; accepted 2012 October 30; published 2013 January 29

ABSTRACT

This paper is a detailed critical review of the production processes and reactions of N, N+, N2+, N++, and N2++ of relevance to Titan's atmosphere. The review includes neutral, ion–molecule, and recombination reactions. The review covers all possible active nitrogen species under Titan's atmospheric conditions, specifically N_2 ($A\ ^3\Sigma_u^+$), N (^4S), N (^2D), N (^2P), N_2^+, N^+ (^3P), N^+ (^1D), N_2^{++}, and N^{++} species, and includes a critical survey of the reactions of N, N+, N2+, N++, and N2++ with N_2, H_2, D_2, CH_4, C_2H_2, C_2H_4, C_2H_6, C_3H_8 and the deuterated hydrocarbon analogs, as well as the recombination reactions of N_2^+, N^+, N_2^{++}, and N^{++}. Production processes, lifetimes, and quenching by collisions with N_2 of all reactant species are reviewed. The N (^4S) state is reactive with radicals and its reactions with CH_2, CH_3, C_2H_3, and C_2H_5 are reviewed. Metastable states N_2 ($A\ ^3\Sigma_u^+$), N (^2D), and N (^2P) are either reactive or quenched by collisions with the target molecules reviewed. The reactions of N^+ (^1D) have similar rate constants as N^+ (^3P), but the product branching ratios differ significantly. Temperature effects and the role of the kinetic energy content of reactants are investigated. In all cases, experimental uncertainties of laboratory data are reported or estimated. Recommended values with uncertainties, or estimated values when no data are available, are given for rate constants and product branching ratios at 300 K and at the atmospheric temperature range of Titan (150–200 K for neutral reactions and 150 K for ion reactions).

Key words: atomic data – atomic processes – molecular data – molecular processes – planets and satellites: atmospheres – planets and satellites: individual (Titan)

1. INTRODUCTION

1.1. Chemistry in Titan's Atmosphere

The atmosphere of Titan is mainly composed of molecular nitrogen, with 2%–5% methane (Niemann et al. 2010; Yelle et al. 2008) and small amounts of hydrocarbons such as acetylene, ethylene, ethane, and propane, as well as traces of nitrogen and oxygen-bearing species (Cui et al. 2009; Koskinen et al. 2011; Vinatier et al. 2010; Vuitton et al. 2007). The heaviest neutral molecule that has unambiguously been detected to date in Titan's atmosphere is benzene (Vinatier et al. 2010; Vuitton et al. 2008). In addition, Titan's atmosphere also contains a large number of aerosol particles, suggested to be composed of organic material, which form a thick haze layer (Tomasko et al. 2008) as well as a detached thin layer in the stratosphere (Lavvas et al. 2009). The *Cassini* space probe, which in 2005 performed the first ever in situ measurements of Titan's atmosphere, revealed an extraordinarily complex ionospheric chemical composition. The Ion and Neutral Mass Spectrometer (INMS) detected about

50 positive ions in the 1–99 m/z mass range (Cravens et al. 2006) and the *Cassini* Plasma Spectrometer–Ion Beam Spectrometer (CAPS-IBS) provided evidence for even heavier positive ions with m/z up to ~350 (Crary et al. 2009). Another striking result came from another sensor of the CAPS instrument, namely the Electron Spectrometer, which reported the presence of negatively charged ions with m/z up to ~4000 (Coates et al. 2007). These heavy ions could be intermediate species leading to the formation of the aerosols which have been observed at altitudes as high as 900 km by the Ultraviolet Imaging Spectrograph (Koskinen et al. 2011). In Titan's atmosphere, the temperature varies from 93 K at the surface to about 250 K at the top of the ionosphere at ~1600 km (Fulchignoni et al. 2005). In the atmosphere at altitudes between 250 km and 900 km where chemistry is dominated by neutral reactions, the HASI instrument on board Huygens registered wave-like variations in the temperature profile in the 150–200 K range, with a mean value of ~170 K (Fulchignoni et al. 2005). In the ionosphere, at altitudes between 900 and 1600 km, where chemistry is dominated by ion–molecule reactions, the ion (Crary et al. 2009)

and neutral (De la Haye et al. 2007) temperatures are not exactly equal and vary in the ranges 100–200 K and 145–160 K, respectively. Thus, one can conclude that the characteristic average temperature for ion–molecule reactions is about 150 K. In Titan's atmosphere, the electron temperature ranges from 150 to 10,000 K (Edberg et al. 2010), lying between 150 K and 1000 K range in the ionosphere (Richard et al. 2011), where ion–electron recombination plays a major role.

The first results of the *Cassini*–Huygens mission triggered a tremendous modeling effort to interpret the probe's data. This modeling effort used the most complex chemical models employed to date to represent a planetary atmosphere (Cravens et al. 2009; Krasnopolsky 2009; Lavvas et al. 2008a, 2008b; Robertson et al. 2009; Vuitton et al. 2009; Westlake et al. 2012). N_2 neutral molecules in their ground electronic state are non-reactive and therefore, the first steps of molecular growth are mainly due to chemically active nitrogen species. These active nitrogen species come from the dissociation and (dissociative) ionization of N_2 by ultraviolet photons and supra-thermal electrons in the upper atmosphere (Lavvas et al. 2011). An extensive recent review on the chemistry of Titan's atmosphere can be found in the book on Titan to be published by Cambridge University Press (Vuitton et al. 2012).

1.2. Aim and Outline of the Paper

The aim of the present paper is to present a critical review of the reactions of all the possible chemically active nitrogen species playing an important role in Titan's atmospheric chemistry; specifically the reactions of N_2 ($A\,^3\Sigma_u^+$), N (^4S), N (^2D), N (^2P), N_2^+, N^+ (^3P), N^+ (^1D), N_2^{++}, and N^{++} with the main constituents of Titan's atmosphere, N_2, H_2, CH_4, as well as several minor hydrocarbons, i.e., C_2H_2, C_2H_4, C_2H_6, and C_3H_8. In the literature, there are several review papers that study these chemical reactions. These papers are currently widely used by planetary scientists to build their chemical atmospheric models. For neutral reactions, Herron (1999) published a complete critical evaluation of the reactions of N (^2D), N (^2P), and N_2 ($A\,^3\Sigma_u^+$) with many different molecules. For reactions between singly charged ions and neutrals, Anicich & McEwan (Anicich 2003, 1993; McEwan & Anicich 2007; McEwan et al. 1998) published several review papers considering all ion–molecule reactions, at room temperature, which can play a role in Titan's atmospheric chemistry. Electron–ion recombination reactions (Adams et al. 2006; Florescu-Mitchell & Mitchell 2006; Johnsen 2011; Thomas 2008; Vigren et al. 2012) were considered in several recent review papers. For doubly charged ion reactions, Thissen et al. (2011) published a recent review which gives a more general overview of this class of reactions and their possible role in planetary atmospheres. All these earlier compilations are incomplete and more recent work is now available. The current paper provides the necessary update to these earlier reports and also includes the urgently required critical evaluation of the available data.

Due to the lack of relevant experimental studies, predominantly reaction rates for ground state species at room temperature have been used in atmospheric models, or at best Arrhenius-based extrapolations of these rates to temperatures of interest (Hébrard et al. 2009). In this review, we specifically investigate the effects of temperature, as well as internal and kinetic energy of the reactant species, on the observed reactivity. We also emphazise effects which can play a significant role in influencing the reactivity to be expected under Titan's atmospheric conditions and make remarks on factors which do not influence the

reactivity, within experimental uncertainties. Let us note that it has been shown experimentally and theoretically in the last two decades that many neutral–neutral reactions have no barrier on the minimum energy path leading from reactants to products. Therefore, especially in the low temperature range of Titan's atmosphere (150–200 K), the temperature dependence of their rate constants can follow only in some cases the simple Arrhenius law:

$$k = A \exp[-E_a/(k_b T)],$$

where A is the pre-exponential factor, E_a is the activation energy, and k_b is the Boltzmann constant. See the paper of Smith (2008) for a discussion about the factors that control the rates of "non-Arrhenius" reactions.

Temperature has little effect on the values of the rate constants of ion–molecule reactions, as most reactions are already fast. Such reactions usually proceed at close to the collision rate, which is given by the Langevin expression for exothermic reactions assuming reaction after reactant capture:

$$k_L = 2\pi e(\alpha/\mu)^{1/2},$$

where e is the elementary charge, α is the polarizability of the neutral molecule, and μ is the reduced mass of the ion neutral pair. The Langevin rate is independent of temperature and is the maximum value for the rate constant when the target molecule has no permanent dipole, as is the case for all reactions considered in this paper. When the rate constant at 300 K is smaller than the Langevin rate, it may increase when the temperature decreases. This increase at lower temperatures can reasonably be neglected in a first approximation for most exothermic reactions (Wakelam et al. 2010). However, the effect of temperature on the product branching ratios of ion–molecule reactions is much more significant. Surprisingly, Carrasco et al. (2008a) showed, in a study of uncertainty propagation in a Titan's ionospheric model, that large uncertainties on branching ratios affect the calculated density of only a few major ions, but they strongly affect many minor ions. Considering the lack of experimental data on such temperature effects, uncertainty management should be an intrinsic component of atmospheric chemistry modeling.

For some applications involving modeling the upper atmosphere of a planet (study of the atmospheric escape for example), it is important to know how reaction cross sections vary with collision energy. Such considerations are necessary because reactant ions can possess significant kinetic energies. For exoergic ion–molecule reactions, the reaction cross sections σ have been found to decrease with collision energy, roughly as

$$\sigma = A E_{CM}^{-1/2}$$

where A is a constant and E_{CM} is the energy in the center of mass frame. This expression has been used in this paper to make estimates of the rate constant at 150 K, when no experimental data were available.

Each section of this paper focuses on a particular nitrogen chemical species: Section 2 on N_2 ($A\,^3u^+$), Section 3 on N (^4S) ground state as well as N (^2D) and N (^2P) metastable atoms, Section 4 on N_2^+ ions, Section 5 on N^+ (^3P) ground state and N^+ (^1D) metastable atomic ions, Section 6 on N_2^{++} molecular doubly charged ions, and Section 7 on N^{++} atomic doubly charged ions. For each chemical species, we first describe its production from N_2 by both ultraviolet photons (50–3000 Å) and the impact of supra-thermal electrons (15–1000 eV). We then move

Table 1
Dissociation and Ionization Thresholds of N_2, as well as Lifetimes of Excited States

Species	Threshold Energy (eV)	Remarks
N_2 $(X\,^1\Sigma_g^+)$	0	
N_2 $(A\,^3\Sigma_u^+)$	6.22	N_2 (A) lifetime = 2.37 s (a)
N (^4S) + N (^4S)	9.76	Not observed
N (^2D) + N (^4S)	12.14	N (^2D) lifetime = 13.6 hr and 36.7 hr * (b)
N (^2P) + N (^4S)	13.33	N (^2P) lifetime = 11.1 s and 10.5 s ** (b)
N (^2D) + N (^2D)	14.52	
N_2^+ $(X\,^2\Sigma_g^+)$	15.58	
N_2^+ $(A\,^2\Pi_u)$	16.93	N_2^+ (A) lifetime = 13.9 – 7.3 ms *** (c)
N_2^+ $(B\,^2\Sigma_u^+)$	18.75	N_2^+ (B) lifetime = 67 ns (d)
N^+ (^3P) + N (^4S)	24.29	
N^+ (^1D) + N (^4S)	26.19	N^+ (^1D) lifetime = 258 s (e)
N^+ (^3P) + N (^2D)	26.68	
N^+ (^3P) + N (^2P)	27.87	Not observed
N^+ (^1S) + N (^4S)	28.35	Not observed
N_2^{++} $(X\,^1\Sigma_g^+)$	42.88	N_2^{++} lifetime = 3 s (f)
N^+ (^3P) + N^+ (^3P)	44.5	
N^{++} (^2P) + N (^4S)	53.9	Appearance energy is 55.2 eV (g)

Notes. * Lifetimes for the N $(^2D_{3/2})$ and N $(^2D_{5/2})$ sub-states, respectively. ** Lifetimes for the N $(^2P_{1/2})$ and N $(^2P_{3/2})$ sub-states, respectively. *** The lifetime decreases with increasing vibrational level.
References. (a) Piper 1993; (b) Ralchenko et al. 2011; (c) Peterson & Moseley 1973; (d) Wuerker et al. (1988); (e) Wiese & Fuhr 2007; (f) Mathur et al. 1995; (g) Franceschi et al. 2007.

on to considering the lifetime of the chemical species and any relevant quenching reactions, before considering its chemical reactions including ion–electron recombination reactions. We also provide an estimate of the percentage of N and N^+ species that reside in atomic metastable states, given the production of these species by photodissociation, N_2 dissociation by electron impact, dissociative ionization of N_2, and electron–ion recombination reactions. Best estimates of rate constants and product branching ratios, with uncertainties, are given for all reactions at 300 K. We also give, when possible, the temperature dependence of the rate constant for neutral reactions and an estimate of the rate constants of ion–molecule reactions at 150 K, which is the representative of Titan's ionospheric temperature.

This review work has been initiated as the result of an interdisciplinary effort within the European Network Europlanet RI (Research Infrastructure), focusing on employing the expertise of physical chemists to improve the first steps of the chemistry in the models of Titan's atmosphere developed by planetary scientists. The authors are experts in the different topics reviewed in this paper (see Annex). Let us note that the present critical review can also be useful for other planetary atmospheres or even other applications outside planetary sciences. Our work on this review is linked to the effort to build the KIDA (KInetic Database for Astrochemistry) database of neutral and ion reactions, which includes an evaluation of the data from the literature for applications in astrophysics and planetary sciences (Wakelam et al. 2012).

1.3. Active Nitrogen

Dissociation and ionization thresholds of N_2, as well as the lifetime of the excited states are gathered in Table 1. Figure 1 shows schematic potential energy curves of N_2, N_2^+, and N_2^{++}, with the main dissociation channels, which are relevant for the present paper.

N_2 is characterized by a strong triple bond with associated dissociation energies of 9.76 eV, 8.71 eV, and 1.63 eV, for
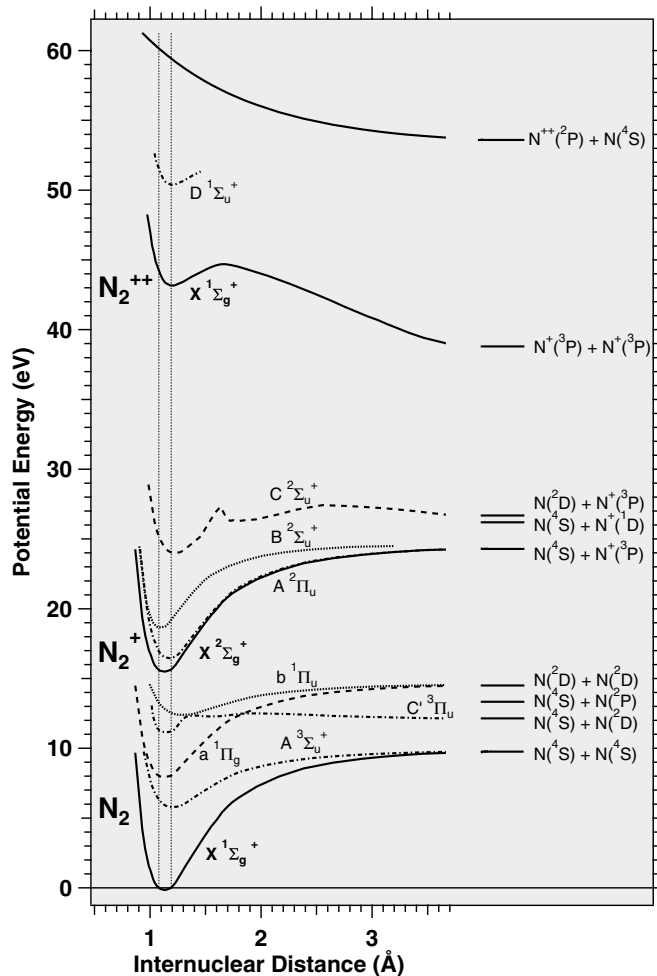

Figure 1. Schematic potential energy curves of N_2, N_2^+, and N_2^{++}. Adapted from references (Franceschi et al. 2007; Gilmore 1965; Hiyama & Iwata 1993; Lewis et al. 2005; Nicolas et al. 2003a).

neutral N_2, N_2^+, and N_2^{++} ions, respectively. As a consequence, chemical reactions involving an N–N bond cleavage are unlikely for N_2 and N_2^+ reactions. Such reactions are only possible for reactions of doubly charged N_2^{++} ions. Such molecular dications are much less stable and most probably play a minor role in Titan's atmosphere due to their low density (Lilensten et al. 2005). Consequently chemical reactions in Titan's atmosphere are mainly induced by N and N^+ fragment ions. However, N_2^+ reactants can generate very reactive species *via* dissociative charge transfer or by capture of a hydrogen atom from hydrocarbons forming N_2H^+ ions. Reactions of all nitrogen active species with N_2 are mainly quenching reactions, whereas reactions with hydrocarbon molecules initiate the complex chemistry of Titan's atmosphere. Among the electronic excited species, only the long-lived N_2 ($A\ ^3\pi_u^+$), N (^2D), N (^2P), and N^+ (^1D) excited species have a lifetime much longer than the time between collisions ($\sim$1 s at 1000 km). However, except for N (^2D) metastable atoms, the reactivity of these species have not been included in photochemical models as yet. The very reactive N_2^{++} and N^{++} doubly charged ions have also not yet been introduced in models of Titan's chemistry, due to a lack of information, both on the double ionization cross sections for dication production and on the chemical reaction rate constants.

1.4. Uncertainties, Data Representation, and Key Reactions

1.4.1. Uncertainties

A series of studies on the photochemical modeling of Titan's atmospheric chemistry has demonstrated that model predictions were affected by large uncertainties, due to both structural uncertainty (incompleteness of the chemical scheme) and parametric uncertainty (limited precision of physico-chemical parameters) (Carrasco et al. 2007, 2008a, 2008b; Dobrijevic et al. 2008; Hébrard et al. 2006, 2007, 2009, 2012; Plessis et al. 2012). On the structural side, a lot of data are presently missing concerning the reaction rates (1) of heavier species (neutrals and ions) and the associated products (2) of excited states of primary species, (3) of isomers, and (4) of negative ions. On the parametric side, besides the unavoidable experimental uncertainty of measured rate constants, a major source of uncertainty is due to the necessity to extrapolate rate parameters to temperatures representative of Titan's atmosphere. The extrapolation uncertainty for Arrhenius-type laws can amount to several orders of magnitude (Hébrard et al. 2009). Moreover, less than 10% of all rate constants in the models of Titan's neutral chemistry have been measured at the required temperatures (Hébrard et al. 2009). This fraction is even lower for products branching ratios, where in fact only a handful of determinations have been made. In order to alleviate this problem, it is necessary to install a constructive dialog between modelers and experimentalists/theorists, for which the methodology of Key Reactions Improvement (KRI) is an optimal tool.

1.4.2. Key Reactions Improvement Strategy

A key reaction is a reaction for which, at a given stage of a model's development, the reaction parameters need to be known with better accuracy in order to optimally improve the precision of model predictions (Dobrijevic et al. 2010). A list of key reactions can be generated by sensitivity analysis, which requires the implementation of sound uncertainty management

in the modeling procedure (Carrasco et al. 2008b; Hébrard et al. 2009). Given these considerations, the outlook might appear hopeless (several hundreds to thousands of reactions, depending on the model), but all the previous studies show that the Pareto principle, or "80/20 rule," is at work here (Juran & Godfrey 1999). It states that roughly 80% of the effects come from 20% of the causes, which means in the present setup that only a small set of reactions is probably responsible for the major part of prediction uncertainty. One can thus expect to improve significantly the precision of the model's predictions through a few, well-targeted, experimental studies on the most influential key reactions. Incidentally, the work by Hébrard et al. (2009) confirms that the updating, in a model, of reactions not identified as key has no or little impact on the precision of model's predictions.

KRI is an iterative procedure, and new key reactions will be identified once the previous ones have been updated in the model. The process can be stopped when the model predictions are deemed precise enough to achieve a specific goal (such as comparison with observations). However, even if one were to loop indefinitely, and because of experimental precision limits, one should not expect to increase the predictions precision beyond a certain threshold: it has been shown for a Titan photochemical model that when all reaction parameters are allotted a *very optimistic* 10% relative uncertainty, the mole fractions of the heavier species are still predicted with sizeable relative uncertainty (up to 50%; Peng et al. 2010).

Global sensitivity analysis based on Monte Carlo uncertainty propagation has been used for the identification of key reactions in Titan's atmosphere (Carrasco et al. 2008b; Hébrard et al. 2009). This method requires that all uncertain reaction parameters are represented by a probability density function which describes as faithfully as possible the available information (Dobrijevic et al. 2010). Under- or overestimation of the uncertainty of the reactions parameters is counter-productive, because they can significantly bias the sensitivity analysis and produce "false" key reactions. In order to minimize the investment in long and costly studies of low-temperature kinetics, the uncertainty budget has to be as accurate as possible. This adds a significant load to the modeling task, but it is a necessity for the KRI procedure to be efficient.

1.4.3. Data Representation

A few methodological rules should ideally be respected by all actors in the KRI loop (experimentalists, data analysts, database managers, modelers, . . .). (1) Experimentalists should provide detailed uncertainty budget, discriminating the systematic and random contributions. (2) The full variance/covariance matrix of the parameters resulting from the fit of a rate law to the experimental data should be published along with the best values of these parameters. This is necessary to derive extrapolation uncertainty (Hébrard et al. 2009); (3) sources of uncertainty coming from independently measured properties should not be mixed. There is a strong case against the use of partial reaction rates when they derive from the product of a global reaction rate and a product branching ratio. Branching ratios require specific probabilistic representations in order to account for their sum-to-one constraint. This intrinsic constraint cannot be preserved at the level of partial reactions (Carrasco & Pernot 2007; Plessis et al. 2010).

As a consequence, in the following, the separation between rate constants and product branching ratios is explicitly

preserved. Best estimates of rate constants and product branching ratios, with their uncertainties, are given for all reactions under Titan's atmospheric conditions. Reported uncertainties are the standard relative uncertainties u_x on the reference values x_0 (rate constant or branching ratio). To exclude negative values from the confidence intervals resulting from large relative uncertainties (above 30%), one uses a multiplicative representation: a 67% (1σ) confidence interval (CI) can be estimated as $[x_0/(1 + u_x), x_0 \times (1 + u_x)]$ and a ($n\sigma$) CI as $[x_0/(1 + u_x)^n, x_0 \times (1 + u_x)^n]$.

Uncertainties on ion–molecule reaction branching ratios are almost never given by the authors. We have estimated them to be $\pm 5\%$ for yields higher than 0.1 and to be $\pm 10\%$ for those which are lower. However, the dispersion of the yields measured by different groups is sometimes outside this uncertainty range, due to other factors, for example, the occurrence of secondary reactions which can alter the product branching ratios.

For the implementation of uncertainty management in chemical models from the data provided in the present paper, we invite the reader to refer to Hébrard et al. (2006, 2007, 2009) for reaction rates of neutrals, to Carrasco et al. (Carrasco et al. 2007, 2008a; Carrasco & Pernot 2007) for ion reactions and to Plessis et al. (2010, 2012) for dissociative recombination reactions, and more generally for the treatment of branching ratios.

1.4.4. Key Reactions Related to the Present Review

Some reactive forms of nitrogen have been found to participate in a set of key reactions for Titan's atmospheric chemistry. For neutrals, photolysis of N_2 appears to be an important source of uncertainty at a global level, i.e., having an influence on a large number of species in the upper atmosphere (Hébrard et al. 2009). Recently, Lavvas et al. (2011) have shown that the use of high-resolution N_2 photolysis cross sections has a strong impact on the altitude-dependent photolysis rate. A detailed study on the production of HCN/HNC in Titan's upper atmosphere identified N (^2D) as a key reactant, notably through its reaction with CH_4 (Hébrard et al. 2012). For ions, a set of reactions necessary to reproduce the INMS ions mass spectrum at 1200 km during the T5 flyby was identified by Carrasco et al. (2008b). In this restricted set, N^+ (^3P) and N_2^+ play an important role through their reactions with H_2, CH_4, C_2H_2, and C_2H_4. However, it is certain that other reactions involving reactive forms of nitrogen still require review.

1.5. Definitions and Notations

In this paper, the experimental methods used to study the reactions are indicated by acronyms. We used the same acronyms as in the review of Herron (1999) and as in the compilation of Anicich (2003) for neutral reactions and ion–molecule reactions, respectively. All acronyms are listed in Table 2.

We note that in the literature, the probability of reactions is often expressed as reaction cross sections σ, instead of rate constants k, in particular for reactant ions having some initial kinetic energy. The conversion between these two quantities can easily be made in first approximation by $k = \sigma \langle v \rangle$, where k is the rate constant in cm^3 s^{-1}, σ is the reaction cross section in cm^2, and $\langle v \rangle$ is the average relative velocity in cm s^{-1}. A more precise treatment can be found in the paper from Ervin & Armentrout (1985). Reactions can either be measured at a given temperature T (with a Boltzmann distribution of reactant velocities at T) or at given collision energies in the center-of-mass frame (E_{CM}), i.e.,

Table 2
Acronyms for the Experimental Methods Cited in the Text and in the Tables

CL	Chemi-luminescence
CRESU	Cinétique de Réactions en Ecoulement Supersonique Uniforme
DF	Discharge flow
DT	Drift tube
ES	Emission spectroscopy
ESR	Electron spin resonance
FA	Flowing afterglow
FJFR	Free jet flow reactor
FP	Flash photolysis
GIB	Guided ion beams
GIB-TOF	Guided ion beams-time of flight
ICR	Ion cyclotron resonance
LIF	Laser-induced fluorescence
LP	Laser photolysis
LPI	Laser photo-ionization
Opt	Optical methods
P	Steady-state photolysis
PD	Pulsed discharge
PIMS	Photo-ionization mass spectrometry
PR	Pulsed radiolysis
RA	Resonance absorption
REMPI	Resonance enhanced multiphoton ionization
RF	Resonance fluorescence
SIFDT	Selected ion flow drift tube
SIFT	Selected ion flow tube
SIFT-LIF	Selected ion flow tube–Laser-induced fluorescence
TPEPICO	Threshold photo-electron photo-ion coincidences

when reactants have a velocity in the laboratory frame, defined with an uncertainty by experimental conditions.

2. METASTABLE N_2 (A $^3\Sigma_u^+$) MOLECULES

2.1. Production of N_2 (A $^3\Sigma_u^+$) Molecules

This triplet metastable state cannot be efficiently produced by photoexcitation of N_2, because the optical transition from the N_2 (X $^1\Sigma_g^+$) ground state is dipole forbidden. However, it can be produced by electron excitation, either directly from the N_2 (X $^1\Sigma_g^+$) ground state or by cascades from higher molecular excited states, in particular by the N_2 (C $^3\Pi_u \rightarrow B$ $^3\Pi_g$) emission, followed by the N_2 (B $^3\Pi_g \rightarrow A$ $^3\Sigma_u^+$) emission. The N_2 (A) metastable state is indeed observed in terrestrial aurorae with the N_2 (A $^3\Sigma_u^+ \rightarrow X$ $^1\Sigma_g^+$) Vegard–Kaplan forbidden emission in the infrared, and several atmospheric models have been developed to fit the observations (see, for example, Morrill & Benesch 1996 and Broadfoot et al. 1997). Very recently Jain et al. (Jain & Bhardwaj 2011) modeled the N_2 Vegard–Kaplan emission observed in the Mars dayglow by the SPICAM instrument on board Mars Express (Leblanc et al. 2006, 2007). This emission had been predicted a long time ago by Fox & Dalgarno (1979), but only observed recently. Bhardwaj & Jain (2012) now predict its presence in the Venus dayglow and it could also be the case for Titan.

2.2. Lifetime and Quenching

Among the N_2 molecular excited states which can be formed, only the $N_2(A)$ state has a sufficiently long lifetime, equal to 2.37 s (Piper 1993), to be able to contribute to Titan's

atmospheric chemistry through chemical reactions. Its quenching by collisions with N_2 is very inefficient, the rate constant being in the range of 10^{-18} cm^3 s^{-1} (see the discussion in the review of Herron 1999 and our discussion in Section 2.3.1).

2.3. N_2 ($A\,^3\Sigma_u^+$) Chemical Reactions

Collisions of the N_2 ($A\,^3\Sigma_u^+$) molecular excited state with molecular targets do not produce the N_2 bond breakage, but they result either in quenching of this excited state or in the excitation or dissociation of the target molecule via dissociative energy transfer (see the reviews of Golde 1988 and Herron 1999). In the following tables, we report the rate constant measured for the ground vibrational level of N_2 ($A\,^3\Sigma_u^+$). Our recommended rate constant values are also for the ground vibrational level. The reactions with N_2, H_2, and CH_4 have very small rate constants for the vibrational ground state of N_2 and are most probably resulting in the quenching of N_2 into its ground electronic state. When N_2 (A) is in an excited vibrational state, the rate constant is somewhat higher and corresponds to vibrational quenching. On the contrary, the reactions with unsaturated hydrocarbons, C_2H_2 and C_2H_4, have large rate constants and lead to dissociation of the target molecule with the release of H atoms. The rate constant dependence with vibrational energy of N_2 (A) is rather weak for these two reactions. The reactions of N_2 ($A\,^3\Sigma_u^+$) with the C_2H_6 and C_3H_8 saturated hydrocarbons are intermediate cases between reactions with N_2, H_2, and CH_4 on one side, and C_2H_2 and C_2H_4 on the other side.

2.3.1. Reaction N_2 ($A\,^3\Sigma_u^+$) + N_2

Kinetics:
Recommended value at 300 K: $k \leqslant 3 \times 10^{-18}$ cm^3 s^{-1}
The different rate constant data for the N_2 ($A\,^3\Sigma_u^+$) + N_2 reaction can be found in Table 3, which summarizes all published rate constant data for N_2 ($A\,^3\Sigma_u^+$) and N (^2D, ^2P) reactions. The second and fourth columns indicate the temperature and the experimental method used, respectively.

There is a considerable scattering of the measured rate constants, due to the experimental challenge of measuring such a slow reaction. Dreyer & Perner (1973), as well as Levron & Phelps (1978) also measured the rate constant for $v = 1$, but it remains very small. Herron (1999) recommended an upper limit of 3×10^{-18} cm^3 s^{-1}, disregarding the values which are above 10^{-17} cm^3 s^{-1}, as Vidaud et al. (1976) used a discharge flow system which does not produce only the N_2 ($A\,^3\Sigma_u^+$) state and Suzuki et al. (1997) corrected later their first measurement (Suzuki et al. 1993a). This very small rate constant demonstrates that the quenching of this excited state by collision with N_2 is not efficient.

2.3.2. Reaction N_2 ($A\,^3\Sigma_u^+$) + H_2

Kinetics:
Recommended value at 300 K: $k = 3.5 \times 10^{-15}$ cm^3 s^{-1} ($\pm 60\%$)
The reaction of N_2 ($A\,^3\Sigma_u^+$) with molecular hydrogen has been studied by many groups (see Table 3), but there is no recent study. The rate constant values are in relatively good agreement and the recommended value is the same as the one proposed by Herron (1999), who eliminated the three oldest values. Slanger et al. (1973) measured the temperature dependence of the rate constant as $k = 2.2 \times 10^{-10}$ exp $(-3500/T)$ cm^3 s^{-1} over the 240–370 K temperature range. However for the excited

vibrational levels, there are large discrepancies between the measurements made by Hack et al. (1988) and Bohmer & Hack (1989) who observe a level-off of the rate constant value at $v = 1$ and higher vibrational levels, and measurements of Golde et al. (Golde et al. 1989) who observe a continuous increase of the rate constant from $v = 2$ and higher vibrational levels. This discrepancy could be due to experimental uncertainties. Bohmer & Hack (1989) observed H atom release, but did not quantify it. It seems likely that the reaction is mainly quenching of the nitrogen excited state, due to the low value of the rate constant, but also produces some dissociation of H_2. This is confirmed by quasi-classical trajectory calculations (Sperlein & Golde 1989), showing that this reaction leads to electronic quenching and vibrational relaxation, but also to dissociative energy transfer with branching ratios which vary with the vibrational level of N_2 (A).

2.3.3. Reaction N_2 ($A\,^3\Sigma_u^+$) + CH_4

Kinetics:
Recommended value at 300 K: $k = 3.0 \times 10^{-15}$ cm^3 s^{-1} ($\pm 60\%$)
Our recommended rate constant value is the same one recommended by Herron (1999) which is based on the measurements of Slanger et al. (1973). Slanger et al. (1973) measured the temperature dependence of the rate constant as $k = 1.3 \times 10^{-10}$ exp $(-3170/T)$ cm^3 s^{-1} over the 300–360 K temperature range. Several authors measured the rate constant as a function of the vibrational level of N_2 ($A\,^3\Sigma_u^+$) (Clark & Setser 1980; Golde et al. 1989; Piper et al. 1985; Thomas et al. 1983), which can be higher than for $v = 0$ by a factor of 100 and can be interpreted as vibrational quenching into the vibrational ground state. For $v = 0$, the products have not been measured. Golde et al. (1989) detected H atom products, but could not quantify this reaction channel.

2.3.4. Reaction N_2 ($A\,^3\Sigma_u^+$) + C_2H_2

Kinetics:
Recommended values at 300 K: $k = 1.40 \times 10^{-10}$ cm^3 s^{-1} ($\pm 60\%$) for C_2H_2
$k = 1.45 \times 10^{-10}$ cm^3 s^{-1} ($\pm 60\%$) for C_2D_2.
This reaction has a high rate constant and the different measurements are in rather good agreement (see Table 3). We recommend the most recent rate constant value measured by Umemoto (2007), with an uncertainty that takes into account the scattering of the rate constants measured by other authors. Umemoto also studied the reaction with C_2D_2 which has almost the same rate constant as for C_2H_2. Bohmer & Heck (1991) did not observe any dependence of the rate constant with the vibrational energy of N_2 (A). Both the high rate constant and the absence of vibrational dependence are explained by the fact that, as opposed to reactions with N_2, H_2, and CH_4, this reaction is not mainly quenching of N_2 (A) but produces the dissociation of C_2H_2, as shown by Umemoto et al. (Umemoto 2007).
Products:
Recommended yields: (N_2 + C_2H + H)/(N_2 + C_2 + H_2), 0.52/0.48 for the reaction with C_2H_2
(N_2 + C_2D + D)/(N_2 + C_2 + D_2), 0.33/0.67 for the reaction with C_2D_2.
Umemoto (2007) measured the H atom yield and D atom yield to be equal to 0.52 and 0.33, for the reactions with C_2H_2 and C_2D_2, respectively. They conclude that the presence of an

Table 3
Rate Constant Measurements for the Neutral N_2 (A $^3\Sigma_u^+$) and N (^2D, ^2P) Reactions

Reaction	T (K)	k (cm^3 s^{-1})	Method	Reference
N_2 (A $^3\Sigma_u^+$) + N_2	298	$\leqslant 10 \times 10^{-18}$	FP-CL	(Callear & Wood 1971)
N_2 (A $^3\Sigma_u^+$) + N_2	298	$\leqslant 3.7 \times 10^{-16}$	PR-RA	(Dreyer & Perner 1973)
N_2 (A $^3\Sigma_u^+$) + N_2	298	4.5×10^{-17}	DF	(Vidaud et al. 1976)
N_2 (A $^3\Sigma_u^+$) + N_2	298	2.6×10^{-18}	PD-ES	(Levron & Phelps 1978)
N_2 (A $^3\Sigma_u^+$) + N_2	298	3.7×10^{-17}	PD	(Suzuki et al. 1993a)
N_2 (A $^3\Sigma_u^+$) + N_2	298	1.8×10^{-18}	PD	(Suzuki et al. 1997)
N_2 (A $^3\Sigma_u^+$) + N_2	298	$\leqslant 3 \times 10^{-18}$	Compilation	(Herron 1999)
N_2 (A $^3\Sigma_u^+$) + H_2	298	3×10^{-15}	FP-CL	(Black et al. 1969)
N_2 (A $^3\Sigma_u^+$) + H_2	298	$\leqslant 7 \times 10^{-15}$	P-CL	(Young et al. 1969)
N_2 (A $^3\Sigma_u^+$) + H_2	298	3×10^{-15}	FP-CL	(Callear & Wood 1971)
N_2 (A $^3\Sigma_u^+$) + H_2	240–370	1.9×10^{-15} [a]	FP-CL	(Slanger et al. 1973)
N_2 (A $^3\Sigma_u^+$) + H_2	298	2.4×10^{-15}	PD-ES	(Levron & Phelps 1978)
N_2 (A $^3\Sigma_u^+$) + H_2	298	3.8×10^{-15}	DF-LIF	(Hack et al. 1988)
N_2 (A $^3\Sigma_u^+$) + H_2	298	5.8×10^{-15}	DF-LIF	(Bohmer & Hack 1989)
N_2 (A $^3\Sigma_u^+$) + H_2	298	3.5×10^{-15}	Compilation	(Herron 1999)
N_2 (A $^3\Sigma_u^+$) + CH_4	298	3×10^{-15}	FP-CL	(Black et al. 1969)
N_2 (A $^3\Sigma_u^+$) + CH_4	298	$\leqslant 7 \times 10^{-15}$	P-CL	(Young et al. 1969)
N_2 (A $^3\Sigma_u^+$) + CH_4	298	$\leqslant 2 \times 10^{-14}$	DF-CL	(Meyer et al. 1971)
N_2 (A $^3\Sigma_u^+$) + CH_4	298	$\leqslant 1.7 \times 10^{-15}$	FP-CL	(Callear & Wood 1971)
N_2 (A $^3\Sigma_u^+$) + CH_4	300–360	3.2×10^{-15} [a]	FP-CL	(Slanger et al. 1973)
N_2 (A $^3\Sigma_u^+$) + CH_4	298	$\leqslant 1 \times 10^{-14}$	DF-ES	(Clark & Setser 1980)
N_2 (A $^3\Sigma_u^+$) + CH_4	298	3.0×10^{-15}	Compilation	(Herron 1999)
N_2 (A $^3\Sigma_u^+$) + C_2H_2	298	1.6×10^{-10}	P-CL	(Young et al. 1969)
N_2 (A $^3\Sigma_u^+$) + C_2H_2	298	1.6×10^{-10}	FP-CL	(Callear & Wood 1971)
N_2 (A $^3\Sigma_u^+$) + C_2H_2	298	2.5×10^{-10}	DF-CL	(Meyer et al. 1971)
N_2 (A $^3\Sigma_u^+$) + C_2H_2	298	2.0×10^{-10}	DF-LIF	(Bohmer & Hack 1991)
N_2 (A $^3\Sigma_u^+$) + C_2H_2	298	2.0×10^{-10}	Compilation	(Herron 1999)
N_2 (A $^3\Sigma_u^+$) + C_2H_2	298	$(1.40 \pm 0.02) \times 10^{-10}$ for C_2H_2 $(1.45 \pm 0.03) \times 10^{-10}$ for C_2D_2	LP-LIF	(Umemoto 2007)
N_2 (A $^3\Sigma_u^+$) + C_2H_4	298	1.2×10^{-10}	FP-CL	(Black et al. 1969)
N_2 (A $^3\Sigma_u^+$) + C_2H_4	298	1.5×10^{-10}	P-CL	(Young et al. 1969)
N_2 (A $^3\Sigma_u^+$) + C_2H_4	298	1.1×10^{-10}	FP-CL	(Callear & Wood 1971)
N_2 (A $^3\Sigma_u^+$) + C_2H_4	298	1.6×10^{-10}	DF-CL	(Meyer et al. 1971)
N_2 (A $^3\Sigma_u^+$) + C_2H_4	298	0.64×10^{-10}	DF-LIF	(Dreyer & Perner 1973)
N_2 (A $^3\Sigma_u^+$) + C_2H_4	298	1.2×10^{-10}	DF-ES	(Clark & Setser 1980)
N_2 (A $^3\Sigma_u^+$) + C_2H_4	298	1.2×10^{-10}	DF-CL	(Cao & Setser 1985)
N_2 (A $^3\Sigma_u^+$) + C_2H_4	298	1.0×10^{-10}	DF-LIF	(Thomas et al. 1987)
N_2 (A $^3\Sigma_u^+$) + C_2H_4	298	1.2×10^{-10}	DF-ES	(Ho & Golde 1991)
N_2 (A $^3\Sigma_u^+$) + C_2H_4	298	1.1×10^{-10}	Compilation	(Herron 1999)
N_2 (A $^3\Sigma_u^+$) + C_2H_4	298	$(0.97 \pm 0.04) \times 10^{-10}$ for C_2H_4 $(0.93 \pm 0.04) \times 10^{-10}$ for C_2D_4	LP-LIF	(Umemoto 2007)
N_2 (A $^3\Sigma_u^+$) + C_2H_6	298	$\leqslant 5 \times 10^{-15}$	P-CL	(Young et al. 1969)
N_2 (A $^3\Sigma_u^+$) + C_2H_6	298	3.6×10^{-13}	FP-CL	(Callear & Wood 1971)
N_2 (A $^3\Sigma_u^+$) + C_2H_6	298	$\leqslant 2 \times 10^{-14}$	DF-CL	(Meyer et al. 1971)
N_2 (A $^3\Sigma_u^+$) + C_2H_6	298	2.9×10^{-13}	PR-AS	(Dreyer & Perner 1973)
N_2 (A $^3\Sigma_u^+$) + C_2H_6	300–370	2.2×10^{-13} [a]	FP-CL	(Slanger et al. 1973)
N_2 (A $^3\Sigma_u^+$) + C_2H_6	298	2.3×10^{-13}	Compilation	(Herron 1999)

Table 3
(Continued)

Reaction	T (K)	k (cm^3 s^{-1})	Method	Reference
N$_2$ (A $^3\Sigma_u^+$) + C$_3$H$_8$	298	1.3×10^{-12}	FP-ES	(Callear & Wood 1971)
N$_2$ (A $^3\Sigma_u^+$) + C$_3$H$_8$	298	1.3×10^{-12}	Compilation	(Herron 1999)
N (^2D) + N$_2$	298	$\leqslant 6 \times 10^{-15}$	FP-CL	(Black et al. 1969)
N (^2D) + N$_2$	298	1.6×10^{-14}	DF-RA	(Lin & Kaufman 1971)
N (^2D) + N$_2$	298	2.3×10^{-14}	FP-RA	(Husain et al. 1972)
N (^2D) + N$_2$	298	1.5×10^{-14}	FP-RA	(Husain et al. 1974)
N (^2D) + N$_2$	298	$\leqslant 1.8 \times 10^{-14}$	FP-CL	(Black et al. 1969)
N (^2D) + N$_2$	198–372	1.8×10^{-14}[a]	FP-CL	(Slanger & Black 1976)
N (^2D) + N$_2$	298	$(1.3 \pm 0.2) \times 10^{-14}$	PR-RA	(Sugawara et al. 1980)
N (^2D) + N$_2$	213–294	2.4×10^{-14}[a]	PR-RA	(Suzuki et al. 1993b)
N (^2D) + N$_2$	298	1.7×10^{-14}	Compilation	(Herron 1999)
N (^2P) + N$_2$	400	6×10^{-14}	DF-RA	(Lin & Kaufman 1971)
N (^2P) + N$_2$	298	$\leqslant 3 \times 10^{-16}$	DF-RA	(Husain et al. 1972)
N (^2P) + N$_2$	298	1.0×10^{-16}	FP-RA	(Husain et al. 1974)
N (^2P) + N$_2$	298	$(3.3 \pm 0.3) \times 10^{-17}$	PR-RA	(Sugawara et al. 1980)
N (^2P) + N$_2$	298	$\leqslant 4 \times 10^{-16}$	PR-RA	(Umemoto et al. 1985)
N (^2P) + N$_2$	298	3.3×10^{-17}	Compilation	(Herron 1999)
N (^2D) + H$_2$	298	5×10^{-12}	FP-CL	(Black et al. 1969)
N (^2D) + H$_2$	298	1.7×10^{-12}	FP-RA	(Husain et al. 1972)
N (^2D) + H$_2$	298	2.1×10^{-12}	FP-RS	(Husain et al. 1974)
N (^2D) + H$_2$	298	2.7×10^{-12}	FP-CL	(Black et al. 1975)
N (^2D) + H$_2$	298	3.5×10^{-12}	DF-ESR	(Fell et al. 1981)
N (^2D) + H$_2$	298	2.3×10^{-12}	DF-RF	(Piper et al. 1987)
N (^2D) + H$_2$	298	1.8×10^{-12}	DF-RA	(Whitefield & Hovis 1987)
N (^2D) + H$_2$	213–300	2.4×10^{-12}[a]	PR-RA	(Suzuki et al. 1993b)
N (^2D) + H$_2$	298	2.3×10^{-12}	LP-LIF	(Umemoto et al. 1998a)
N (^2D) + H$_2$	298	2.2×10^{-12}	Compilation	(Herron 1999)
N (^2P) + H$_2$	298	3.0×10^{-15}	FP-RA	(Husain et al. 1972)
N (^2P) + H$_2$	298	1.9×10^{-15}	FP-RA	(Husain et al. 1974)
N (^2P) + H$_2$	298	$\leqslant 8 \times 10^{-16}$	DF-ES	(Young & Dunn 1975)
N (^2P) + H$_2$	298	1.4×10^{-14}	PR-RA	(Umemoto et al. 1985)
N (^2P) + H$_2$	213–300	1.4×10^{-14}[a]	PR-RA	(Suzuki et al. 1993b)
N (^2P) + H$_2$	298	1.9×10^{-15}	Compilation	(Herron 1999)
N (^2D) + CH$_4$	298	3×10^{-12}	FP-CL	(Black et al. 1969)
N (^2D) + CH$_4$	298	4.6×10^{-12}	DF-ESR	(Fell et al. 1981)
N (^2D) + CH$_4$	298	3.3×10^{-12} for CH$_4$ 2.0×10^{-12} for CD$_4$	LP-LIF	(Umemoto et al. 1998b)
N (^2D) + CH$_4$	223–292	5.4×10^{-12} for CH$_4$[a] 3.2×10^{-12} for CD$_4$[a]	PR-RA	(Takayanagi et al. 1999)
N (^2D) + CH$_4$	298	4.0×10^{-12}	Compilation	(Herron 1999)
N (^2P) + CH$_4$	298	7.8×10^{-14}	PR-RA	(Umemoto et al. 1985)
N (^2P) + CH$_4$	223–292	9.3×10^{-14} for CH$_4$[b] 6.0×10^{-14} for CD$_4$[b]	PR-RA	(Takayanagi et al. 1999)
N (^2P) + CH$_4$	298	8.55×10^{-14}	Compilation	(Herron 1999)
N (^2D) + C$_2$H$_2$	298	1.1×10^{-10}	DR-ESR	(Fell et al. 1981)
N (^2D) + C$_2$H$_2$	223–293	6.5×10^{-11} for C$_2$H$_2$[c] 6.25×10^{-11} for C$_2$D$_2$[c]	PR-RA	(Takayanagi et al. 1998b)
N (^2D) + C$_2$H$_2$	298	6.5×10^{-11}	Compilation	(Herron 1999)

<div align="center">**Table 3**</div>
<div align="center">(Continued)</div>

Reaction	T (K)	k (cm^3 s^{-1})	Method	Reference
N (^2P) + C$_2$H$_2$	295	3.2×10^{-11}	PR-RA	(Umemoto et al. 1985)
N (^2P) + C$_2$H$_2$	223–293	2.3×10^{-11} for C$_2$H$_2$[c] 2.0×10^{-11} for C$_2$D$_2$[c]	FP-RA	(Takayanagi et al. 1998b)
N (^2P) + C$_2$H$_2$	298	2.3×10^{-11}	Compilation	(Herron 1999)
N (^2D) + C$_2$H$_4$	298	1.2×10^{-10}	FP-CL	(Black et al. 1969)
N (^2D) + C$_2$H$_4$	298	3.7×10^{-11}	PR-RA	(Sugawara et al. 1980)
N (^2D) + C$_2$H$_4$	298	8.3×10^{-11}	DR-ESR	(Fell et al. 1981)
N (^2D) + C$_2$H$_4$	298	4.3×10^{-11}	Compilation	(Herron 1999)
N (^2D) + C$_2$H$_4$	230–292	4.3×10^{-11} for C$_2$H$_4$[c] 3.8×10^{-11} for C$_2$D$_4$[c]	PR-RA	(Sato et al. 1999)
N (^2P) + C$_2$H$_4$	298	2.8×10^{-11}	PR-RA	(Sugawara et al. 1980)
N (^2P) + C$_2$H$_4$	298	3.2×10^{-11}	PR-RA	(Umemoto et al. 1985)
N (^2P) + C$_2$H$_4$	230–292	3.0×10^{-11} ($\pm10\%$) for C$_2$H$_4$[c] 3.0×10^{-11} ($\pm10\%$) for C$_2$D$_4$[c]	PR-RA	(Sato et al. 1999)
N (^2P) + C$_2$H$_4$	298	3.0×10^{-11}	Compilation	(Herron 1999)
N (^2D) + C$_2$H$_6$	298	2.7×10^{-11}	DF-ESR	(Fell et al. 1981)
N (^2D) + C$_2$H$_6$	298	2.1×10^{-11}	LP-LIF	(Umemoto et al. 1998b)
N (^2D) + C$_2$H$_6$	298	1.9×10^{-11}	Compilation	(Herron 1999)
N (^2P) + C$_2$H$_6$	298	5.4×10^{-13}	FP-CL	(Umemoto et al. 1985)
N (^2D) + C$_3$H$_8$	298	4.6×10^{-11}	DF-ESR	(Fell et al. 1981)
N (^2D) + C$_3$H$_8$	298	3.1×10^{-11}	LP-LIF	(Umemoto et al. 1998b)
N (^2D) + C$_3$H$_8$	298	2.9×10^{-11}	Compilation	(Herron 1999)
N (^2P) + C$_3$H$_8$	298	1.9×10^{-12}	FP-CL	(Umemoto et al. 1985)

Notes.
[a] Rate constant value at 300 K.
[b] Rate constant value at 292 K.
[c] Rate constant value at 298 K.

isotope effect in the H/D atom yield suggests that the H/D release competes with the H$_2$/D$_2$ molecule release, the latter being favored in the case of C$_2$D$_2$. As the rate constant has a high value, the quenching is most probably a negligible channel, compared to the collision-induced C$_2$H$_2$ dissociation.

2.3.5. Reaction N$_2$ (A $^3\Sigma_u^+$) + C$_2$H$_4$

Kinetics:
Recommended values at 300 K: $k = 9.7 \times 10^{-11}$ cm^3 s^1 ($\pm60\%$) for C$_2$H$_4$
$k = 9.3 \times 10^{-11}$ cm^3 s^{-1} ($\pm20\%$) for C$_2$D$_4$.
As for acetylene, this reaction has a high rate constant and the different measurements are in rather good agreement (see Table 3). We recommend the rate constant value of the most recent work by Umemoto (2007), with an uncertainty which takes into account the scattering of the rate constants measured by other authors. Umemoto also studied the reaction with C$_2$D$_4$ which has almost the same rate constant as the reaction with C$_2$H$_4$. Dreyer & Perner (1973) and Thomas et al. (1987) measured a weak dependence of the rate constant with the vibrational energy of N$_2$ (A). Similarly to the case of acetylene, both the high rate constant and the quasi-absence of vibrational dependence are explained by the fact that this reaction produces the dissociation of C$_2$H$_4$, as shown by Umemoto (2007).

Products:
Recommended yields: (N$_2$ + C$_2$H$_3$ + H)/(N$_2$ + C$_2$H$_2$ + H$_2$), 0.30/0.70 for the reaction with C$_2$H$_4$
(N$_2$ + C$_2$D$_3$ + D)/(N$_2$ + C$_2$D$_2$ + D$_2$), 0.13/0.87 for the reaction with C$_2$D$_4$.
Umemoto (2007) measured the H and D atom yields to be equal to 0.30 and 0.13, respectively. Umemoto also concluded that this isotope effect in the H/D atom yield suggests that the H/D release competes with the H$_2$/D$_2$ release, the latter being favored in the case of C$_2$D$_4$.

2.3.6. Reaction N$_2$ (A $^3\Sigma_u^+$) + C$_2$H$_6$

Kinetics:
Recommended value at 300 K: $k = 2.3 \times 10^{-13}$ cm^3 s^{-1} ($\pm60\%$)
Our recommended rate constant value is the same as the one recommended by Herron (1999) which is based on the measurements of Slanger et al. (1973), slightly adjusted. It is higher by two orders of magnitude than that for the reaction with methane. Slanger et al. (1973) measured the temperature dependence of the rate constant as $k = 1.6 \times 10^{-10}$ exp $(-1980/T)$ cm^3 s^{-1} over the 300–370 K temperature range. The products are not known, but the value of the rate constant suggests that dissociation of the target molecule is a possible

reaction channel in addition to quenching. Several authors (Clark & Setser 1980; Dreyer & Perner 1973) measured the rate constant as a function of the vibrational level of N_2 ($A\ ^3\Sigma_u^+$), which can be higher than for $v = 0$ by a factor of 100 and can be interpreted as vibrational quenching into the vibrational ground state.

2.3.7. Reaction N_2 ($A\ ^3\Sigma_u^+$) + C_3H_8

Kinetics:

Recommended value at 300 K: $k = 1.3 \times 10^{-12}$ cm^3 s^{-1} ($\pm 60\%$).

The only existing data obtained by Callear & Wood (1971) give a rate constant 1.3×10^{-12} cm^3 s^{-1}. The uncertainty can be estimated to be about the same as for the reaction of N_2 (A) with C_2H_4 which is of the same order of magnitude. As for C_2H_6, the products are not known, but the value of the rate constant suggests that, in addition to quenching, the dissociation of the target molecule is a more important channel than in the case of the reaction with C_2H_6.

3. NITROGEN ATOMS IN THE N (^4S), N (^2D), AND N (^2P) STATES

N_2 dissociation produces N atoms. As discussed in detail below, the atom yields comprise about 50% N (^4S) ground-state atoms and about 50% long-lived N (^2D) and N (^2P) metastable state atoms. The energies of the long-lived N (^2D) and N (^2P) metastable states lie 2.38 eV and 3.57 eV above the N (^4S) ground state, respectively. The N (^4S) ground state is almost non-reactive (see below), as opposed to the N (^2D) and N (^2P) metastable states, which are reactive with stable molecules. There are many more experimental and theoretical studies concerning the N (^2D) state than the N (^2P) state. Generally, the N (^2P) state is much less reactive than the N (^2D) state, with rate constants lower than for the N (^2D) by several orders of magnitude. Therefore, according to most authors, the main reaction channel of N (^2P) reactions is quenching into the N (^2D) state (or maybe also N (^4S)), as opposed to the N (^2D) metastable state which is very reactive.

3.1. Production of N Atoms

Atomic nitrogen can be produced by N_2 dissociation induced by vacuum ultraviolet (VUV) photolysis, electron impact, dissociative photoionization, and N_2^+ dissociative recombination.
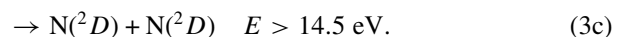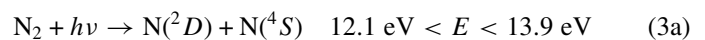
3.1.1. N Atom Production by UV Photodissociation of N_2

The dissociation processes of molecular nitrogen are not very well known. The absorption of VUV photons by the N_2 molecule induces dipole-allowed excitation from the ground *gerade* state to several singlet *ungerade* states with high energy content. These high-energy states are strongly bound, but can undergo predissociation through the crossing with dissociative triplet states. The photoabsorption spectrum of N_2 consists of very highly structured bands and as the solar spectrum is also highly structured in this spectral region, the correct calculation of atmospheric penetration requires a very high spectral resolution. The first band system of N_2 (Lyman–Birge–Hopfield bands from the ground $^1\Sigma_g^+$ to the excited $^1\Pi_g$ state) is in the region between 8.26 and 12.4 eV, but this transition is forbidden by electric dipole selection rules and the absorption cross sections are very small. Let us note that those bands are nevertheless observed in the airglow emission spectra of Titan (Ajello et al. 2008). The dissociation energy of N_2 is 9.76 eV. In principle,

therefore, the forbidden transitions to vibrationally excited levels of the $a\ ^1\Pi_g$ state can provide enough energy to dissociate the molecule. However, the $a\ ^1\Pi_g$ state does not correlate with N (^4S) + N (^4S) and predissociation via spin–orbit coupling to the ground state of N_2 molecules has never been observed. Absorption of UV light becomes significant only near 12.4 eV and the N_2 spectrum shows a strong banded structure between 12.4 and 18.8 eV and a continuum above 18.8 eV. The first electric dipole allowed and intense transition is toward the $b\ ^1\Pi_u$ valence state ($E < 12.5$ eV). This state correlates with N (^2D) + N (^2D) but the energy necessary to reach the dissociation limit is 14.5 eV. Nonetheless, the $b\ ^1\Pi_u$ state can undergo predissociation at lower energies via intersystem crossing to the C $^3\Pi_u$ and C $'^3\Pi_u$ states, producing N (^4S) + N (^2D) above 12.1 eV (Lewis et al. 2005). Predissociation competes with spontaneous emission, which is indeed observed for most vibrational levels of the $b\ ^1\Pi_u$ state (Itikawa 2006). Sprengers et al. (2004) measured a predissociation yield of only $\sim$28% for the $v = 1$ level of the N_2 $b\ ^1\Pi_u$ state. Higher valence singlet states populated by allowed transition at higher energy can also undergo predissociation through intersystem crossing (spin–orbit coupling) and can lead to atomic nitrogen in the second electronically excited state ^2P above 13.3 eV.

Because of the different reactivity of ground ^4S and excited ^2D and ^2P atomic nitrogen and the long radiative lifetime of the ^2D and ^2P states, it would be quite important to characterize the N_2 predissociation/dissociation yield to quantify the relative concentration of the three states and their role in the atmospheric chemistry of Titan. Unfortunately, the N (^2P), N (^2D), and N (^4S) production yields have been measured only for a few specific rovibrational of several electronic states of N_2 by Helm & Cosby (1989) and Walter et al. (1993), not including the $b\ ^1\Pi_u$ state (the first state accessible by an allowed transition). The observations are sparse and do not allow the derivation of a general model that can describe quantitatively the predissociation/dissociation products of N_2. Nevertheless, some observations of the authors can help in drawing more general conclusions. They have observed that the predissociation of the above-mentioned levels always produces one ground state atom and one excited atom, either in the ^2D or ^2P states, the energetic limit of the N (^2D) + N (^2D) channel (14.5 eV) being too high to be reached in their experiments. Remarkably, no dissociation was observed to the ground state N (^4S) + N (^4S).

Bakalian (2006) proposed in 2006 a simplified scheme of the N_2 dissociation for modeling the production of hot nitrogen atoms in the Martian thermosphere. More recently, Lavvas et al. (2011), in a work concerning the energy deposition in the upper atmosphere of Titan, summarized most of the recent information on the electronic transitions of N_2. This paper includes detailed calculations of high-resolution photoabsorption and photodissociation cross sections computed using a coupled-channel Schrödinger equation quantum-mechanical model. These authors suggest the following scheme for the N_2 photodissociation:

$$N_2 + h\nu \rightarrow N(^2D) + N(^4S) \quad 12.1\ \text{eV} < E < 13.9\ \text{eV} \quad (3a)$$

$$\rightarrow N(^2P) + N(^4S) \quad 13.9\ \text{eV} < E < 14.5\ \text{eV} \quad (3b)$$

$$\rightarrow N(^2D) + N(^2D) \quad E > 14.5\ \text{eV}. \quad (3c)$$

The choices of energy threshold were dictated by the fact that $E = 12.1$ eV corresponds to the asymptotic energy of

the channel (3a), $E = 14.5$ eV corresponds to the asymptotic energy of channel (3c), while $E = 13.9$ eV corresponds to the energy derived by Walter et al. (1993) above which the fragmentation into channel (3b) dominates over that into channel (3a). Nevertheless, this observation was related to the excited states populated in the experiment by Walter et al. (1993) and not the most intense transition to $b\ ^1\Pi_u$. Therefore, this scheme might be oversimplified and supplementary high-resolution absolute experimental cross sections complemented by dissociation branching ratios are highly desirable.

In conclusion, it is difficult to recommend a general N_2 photodissociation scheme for the modeling of the atmosphere of Titan because of the fragmentation of the available information, both regarding the predissociation probabilities for all the involved molecular electronic states and their product branching ratios. We suggest using the scheme of Lavvas et al. (2011), until further experimental and theoretical work emerges.

3.1.2 N Atom Production by Electron Impact Dissociation of N_2

In the upper atmosphere of Titan, N_2 molecules are subject to a significant bombardment by energetic (200 eV) magnetospheric electrons (Strobel & Shemansky 1982) and by lower energy electrons produced both by photoionization processes and by magnetospheric electrons impact creating secondary electrons. Electron impact can induce ionization, dissociative ionization, excitation, and dissociation. A comprehensive review on the processes that follow electron collision with N_2 (including elastic scattering, rotational and vibrational excitation, electronic excitation, dissociation and ionization) is given, and the dependence on the electron energy examined, in (Itikawa 2006). Since there are no selection rules, the collision of N_2 molecules with electrons can populate a plethora of N_2 states, including low-energy triplet states. One important effect is the observation of emission from many excited N_2 states, as well as from its neutral and ion fragments in highly excited atomic levels. The fluorescence yield from the various states depends on the electron energy. The electron-induced dissociation cross section reaches a maximum of 1.2×10^{-16} cm^2 at 40–100 eV and, at these energies, is comparable to the ionization cross section.

With the present knowledge, it is reasonable to assume that the N_2 dissociation processes by electron impact produce as many N atoms in the ^4S ground state as in the two ^2D and ^2P metastable states, with a much higher yield of ^2D state compared to ^2P state.

3.1.3. N Atom Production by Other Processes

N atoms are also formed by dissociative ionization of N_2 by photons or electrons (see Section 5.1 below). The excited electronic states of N_2^+, at energies higher than 26.3 eV, dissociate mainly into $N^+\ (^3P) + N\ (^2D)$ and somewhat into other dissociation channels (Aoto et al. 2006; Nicolas et al. 2003a). So globally it can be estimated that N atoms coming from the N_2 dissociative ionization are mainly in the ^4S ground state, with less than 10% being in the $N\ (^2D)$ excited state. Nitrogen atoms in the ^2D state were also observed following electron impact dissociative ionization when using high electron energies (Van Brunt & Kieffer 1975).

Finally, electron–ion recombination of N_2^+ produces fast N atoms in the ground and metastable states, with a branching ratio which can be estimated to 0.7/0.05/0.25 for $N(^2D)/N$ $(^2P)/N(^4S)$ (see Section 4.3.8 below).

3.2. Lifetime and Quenching

The radiative lifetime of the $N\ (^2D)$ metastable state is quite long (13.6 and 36.7 hr, for the two sub-states $^2D_{3/2}$ and $^2D_{5/2}$, respectively; Ralchenko et al. 2011), because this transition is strongly forbidden. In addition, collisional deactivation of N (^2D) by N_2 is a slow process (see below) and therefore the main fate of $N\ (^2D)$ above 800 km is chemical reaction with other constituents of Titan's atmosphere.

The radiative lifetime of the $N\ (^2P)$ metastable state is also long (11.1 and 10.5 s, for the two sub-states $^2P_{1/2}$ and $^2P_{3/2}$, respectively; Ralchenko et al. 2011), compared to the collision frequency in Titan's atmosphere conditions. Quenching by reaction with N_2 is a rather slow process (see below) and it is not clear whether this quenching produces $N\ (^4S)$ or $N\ (^2D)$, see the review by Herron (1999).

3.3. N Atom Chemical Reactions

Until the late 1970s, N atoms in their (^4S) ground state were believed to induce reactions with hydrocarbons (Herron 1966; Herron & Huie 1968; Sato et al. 1979), the reaction with H_2 being endothermic. However, it was later demonstrated that the weak reactivity with acetylene and ethylene, observed at temperatures from about 320 K and above, were not due to this species, but either to excited states still present in the experiments or to reactions with free radicals created together with N atoms (Michael 1979, 1980; Michael & Lee 1977; Umemoto et al. 1986). It is now admitted that $N\ (^4S)$ atoms are neither reactive with hydrocarbon molecules (Sato et al. 1999), nor with N_2 and H_2 and these reactions are therefore not considered in this review paper. However, $N\ (^4S)$ atoms are reactive with hydrocarbon radicals, in particular with CH_3, this reaction being the main loss channel of $N\ (^4S)$ in Titan's atmosphere (Yelle et al. 2010). We will therefore review the reactions of $N\ (^4S)$ atoms with some important radicals from Titan's atmosphere: CH_2, CH_3, C_2H_3, and C_2H_5. We will also discuss the reaction of $N\ (^4S)$ with H atoms.

Laboratory experiments on $N\ (^2D)$ and $N\ (^2P)$ reactions have been rather sparse; remarkably, reliable kinetic data on the reactions of $N\ (^2D)$ with the hydrocarbons present in the atmosphere of Titan became available only in the late 1990s. This lack of data arises because, in general, experimental studies of these reactive systems are problematic due to the difficulty in producing a sufficiently large amount of the electronically excited atoms without other interfering states or species. In his review, Herron (1999) reported a comprehensive compilation of the data on $N\ (^2D)$ and $N\ (^2P)$ reactions. Most of the evaluations performed in this review paper are still valid, especially as far as the kinetic data are concerned. However, a survey of the more recent literature reveals that significant improvements have been made regarding the identification of the reaction mechanisms and products for some of these reactions; these new data arising from studies of the reaction dynamics. In this context, starting from the evaluation of Herron (1999), we will compile together previous and more recent data exclusively for the $N\ (^2D)$ and $N\ (^2P)$ reactions with the main constituents of Titan's atmosphere.

3.3.1. Reactions of N (^4S) Ground State with Radicals

3.3.1.1. Reaction N (^4S) + H

Kinetics:
Estimated value at 150 K: k $= 1.0 \times 10^{-19}$ cm^3 s^{-1}
This reaction can produce NH by radiative association or three body collisions. The rate constant for three body collisions

has been measured by Brown ([1973](#)) giving a value of 4.8×10^{-32} cm^6 s^{-1} ($\pm 35\%$). However, this reaction will not occur under Titan's atmospheric conditions as, at the altitudes where N atoms are formed (>1000 km), the pressure is not sufficient to allow triple collisions. The radiative association rate constant can be estimated from theoretical calculations for the analogous reaction of Li with H giving LiH (Gianturco & Giorgi [1997](#)). It gives an estimated value of about 1.0×10^{-19} cm^3 s^{-1} at 150 K, with a large uncertainty. This value is very low, so this reaction is very unlikely to occur in Titan's atmosphere.

3.3.1.2. Reaction N (^4S) + CH$_2$

Kinetics:

Estimated value at 300 K: $k = 8.0 \times 10^{-11}$ cm^3 s^{-1}

The reaction of N (^4S) with CH$_2$ has two exothermic channels:

N (^4S) + CH$_2$ → HCN + H − 5.29 eV

→ HNC + H − 4.72 eV.
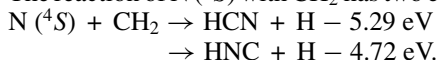
This reaction has not been studied experimentally. However, there is no barrier for this reaction, according to the ab initio calculations of Herbst et al. ([2000](#)), so it should be efficient. The N (^4S) + CH$_2$ ($^3B_1$) entrance channel correlates adiabatically to potential surfaces of sextet, quadruplet, and doublet spin multiplicity and products correlate only to doublet potential surfaces. So this leads to a reduction of the calculated capture rate constant by a factor equal to $1/6$. In these conditions, Herbst et al. calculated the rate constant with its temperature variation to be $8.0 \times 10^{-11} \times (T/300)^{0.17}$ cm^3 s^{-1} (Herbst et al. [2000](#)).

Products:

Estimated yields: (HCN + H)/(HNC + H), 0.50/0.50

The main products from the ab initio calculations of Herbst et al. (Herbst et al. [2000](#)) are HCN + H. The isomerization energy of HCN into HNC is 1.93 eV (DePrince & Mazziotti [2008](#)). There is so much excess energy available in the title reaction (5.29 eV) that the HCN product is able to undergo efficient isomerization after production. It leads to a near equal branching ratio between the two reaction channels (HNC + H) and (HCN + H), according to Herbst et al. ([2000](#)).
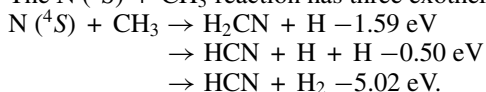
3.3.1.3. Reaction N (^4S) + CH$_3$

Kinetics:

Recommended value at 300 K: $k = 8.5 \times 10^{-11}$ cm^3 s^{-1} ($\pm 25\%$)

The N (^4S) + CH$_3$ reaction has been studied experimentally over the temperature range 200–423 K by Marston et al. ([1989a](#)). These authors measured a rate constant equal to $(8.5 \pm 2.0) \times 10^{-11}$ cm^3 s^{-1} at 298 K, with a strong and complex negative temperature dependence, which seems to deviate from the Arrhenius law. The authors propose two different expressions for the global rate constant: an Arrhenius law, $k\,(T) = 4.3 \times 10^{-10} \exp(-420/T)$ cm^3 s^{-1} or a more complex expression, $k\,(T) = 6.2 \times 10^{-11} + 2.2 \times 10^{-9} \exp(-1250/T)$ cm^3 s^{-1}. Their results suggest that the rate constant in the 150–170 K range will not be substantially lower than the value measured at 200 K, which is $(6.4 \pm 2.1) \times 10^{-11}$ cm^3 s^{-1}. So we recommend the use of a constant value of 6.2×10^{-11} cm^3 molecule^{-1} s^{-1} between 150 K and 200 K.

Products:

Recommended yields: (H$_2$CN + H)/(HCN + H + H), 0.90/0.10.

The N (^4S) + CH$_3$ reaction has three exothermic channels:

N (^4S) + CH$_3$ → H$_2$CN + H − 1.59 eV

→ HCN + H + H − 0.50 eV

→ HCN + H$_2$ − 5.02 eV.

Product branching ratios have been obtained for the N(^4S) + CH$_3$ and N(^4S) + CD$_3$ reactions (Marston et al. [1989b](#)), leading to H$_2$CN + H (85%–100%) with some HCN production (0–15%). The authors suggest that HCN formation is associated with H$_2$. However, the (HCN + H$_2$) production is spin-forbidden and needs an intersystem crossing process to occur. Additionally, recent ab initio calculations (Cimas & Largo [2006](#)) found almost 100% of H$_2$CN production, in good agreement with previous calculations (Nguyen et al. [1996](#)). As H$_2$CN may have enough internal energy to overcome the dissociation barrier for C–H dissociation, some (HCN + H + H) may be produced (Nguyen et al. [1996](#)). Moreover, as Marston et al. ([1989b](#)) used an excess of nitrogen atoms, some HCN molecules may come either from the reaction H$_2$CN + N → HCN + NH or more likely from the reaction H$_2$CN + N → CH$_2$ + N$_2$ followed by N + CH$_2$ → HCN + H. Taking in account the various uncertainties, we choose to recommend a branching ratio equal to 90% for H$_2$CN + H formation and 10% for HCN + H + H. As Marston et al. ([1989b](#)) observed no isotopic effect, we recommend to take the same branching ratio for the reaction with CD$_3$.

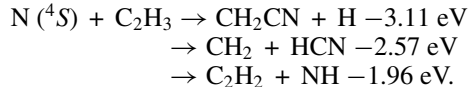### 3.3.1.4. Reaction N (^4S) + C$_2$H$_3$

Kinetics:

Recommended value at 300 K: $k = 7.7 \times 10^{-11}$ cm^3 s^{-1} ($\pm 40\%$)

Payne et al. ([1996](#)) studied this reaction at 298 K, measuring the rate constant to be equal to $(7.7 \pm 2.9) \times 10^{-11}$ cm^3 s^{-1}.

Products:

Recommended yields: (CH$_2$CN + H)/(C$_2$H$_2$ + NH), 0.83/0.17.

This reaction has three exothermic channels:

N (^4S) + C$_2$H$_3$ → CH$_2$CN + H − 3.11 eV

→ CH$_2$ + HCN − 2.57 eV

→ C$_2$H$_2$ + NH − 1.96 eV.

Payne et al. ([1996](#)) measured the branching ratio of this reaction at 298 K to be (CH$_2$CN + H)/(C$_2$H$_2$ + NH) equal to 0.83/0.17. They did not observe the (CH$_2$ + HCN) channel. Theoretical calculations of Sun et al. ([2004](#)) are in relatively good agreement, predicting (CH$_2$CN + H) to be the main exit channel. However, these calculations show the possible (CH$_2$ + HCN) contribution and the existence of a barrier in the entrance channel for the direct H atom abstraction. We recommend the values of the experimental branching ratios, hoping that further experimental work could check the predicted formation of the (CH$_2$ + HCN) channel.

3.3.1.5. Reaction N (^4S) + C$_2$H$_5$

Kinetics:

Recommended value at 300 K: $k = 1.1 \times 10^{-10}$ cm^3 s^{-1} ($\pm 25\%$)

The rate constant for this reaction has been measured at 298 K by Stief et al. ([1995](#)) to be equal to $(1.1 \pm 0.3)\,10^{-10}$ cm^3 s^{-1}. Based on the comparison with the N (^4S) + CH$_3$ reaction, these authors suppose that the temperature dependence of the rate constant down to 200 K would be small or negligible.

Products:

Recommended yields: (C$_2$H$_4$ + NH)/(H$_2$CN + CH$_3$), 0.65/0.35

The main exothermic channels of the reaction N (^4S) + C$_2$H$_5$ are

N (^4S) + C$_2$H$_5$ → H$_2$CN + CH$_3$ − 2.07 eV

→ C$_2$H$_4$ + NH − 1.93 eV

→ CH$_3$CHN + H − 1.83 eV.
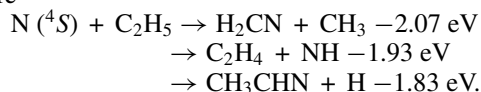
Stief et al. (Stief et al. 1995) measured the branching ratio of the reaction of N (^4S) with deuterated C_2D_5. They observed two reactive channels, (C_2D_4 + ND) being the major channel, with a branching ratio (C_2D_4 + ND)/(D_2CN + CD_3) equal to 0.65/0.35. No uncertainties are given for the branching ratio. These authors consider implicitly that the branching ratio should be the same for the reaction with C_2H_5. They did not observe the (CH_3CHN + H) products, which could also be formed according to the theoretical calculations by Yang et al. (2005). Stief et al. (1995) estimate the branching ratio by measuring the C_2H_4/C_2H_5 ratio by comparison with a known C_2H_4 concentration, the C_2H_5 being estimated from initial F atom concentration (F + C_2H_6 → C_2H_5 + HF) and also from the C_2H_5 decay. Their branching ratio measurements are very sensitive to uncertainty in the initial C_2H_5 concentration. The C_2H_4 + NH production might be overestimated, particularly at low temperatures, as this channel is calculated to involve a barrier in the entrance reactive channel for the direct H atom abstraction or to have a much higher transition state than the H_2CN + CH_3 exit channel (Yang et al. 2005).

3.3.2. Reactions of N (^2D) and N (^2P) Metastable States with Molecules

3.3.2.1. Reaction N (^2D) + N_2

Kinetics:
Recommended value at 300 K: $k = 1.7 \times 10^{-14}$ cm^3 s^{-1} ($\pm 40\%$)

N_2 being the most abundant component in the atmosphere of Titan, the role of the physical quenching of N (^2D) by its parent molecule needs to be assessed. Herron has suggested 1.7×10^{-14} cm^3 s^{-1} as the recommended room temperature rate constant, which is an average value of the most accurate available data (Husain et al. 1974; Lin & Kaufman 1971; Slanger & Black 1976; Sugawara et al. 1980; Suzuki et al. 1993b) (see Table 3). Such a low value was explained by the inefficiency of crossing between doublet and quartet N_3 potential energy surfaces (Donovan & Husain 1970). Interestingly, both Suzuki et al. (1993b) and Slanger & Black (1976) investigated the temperature dependence of this rate constant over the range 213–294 and 198–372 K, respectively. The temperature dependence obtained in the two experiments is, however, quite different being $k = 5.4 \times 10^{-11}$ exp $(-1620/T)$ cm^3 s^{-1} for Suzuki et al. (1993b) and $k = 1.0 \times 10^{-13}$ exp $(-(510 \pm 156)/T)$ cm^3 s^{-1} for Slanger & Black (1976). Notwithstanding the disagreement in the rate expression, it is relevant to note that the rate constant decreases with decreasing temperature in both cases. It seems to us reasonable to recommend to use the temperature dependence measured by Slanger & Black (1976) in the 198–372 K range, to extrapolate the rate constant at Titan's atmospheric temperatures.

3.3.2.2. Reaction N (^2P) + N_2

Kinetics:
Recommended value at 300 K: $k = 3.3 \times 10^{-17}$ cm^3 s^{-1} ($\pm 60\%$)

The recommended value for the rate constant is the one from Sugarawa et al. (1980), as proposed by Herron (1999) and is lower than the rate constant of the N (^2D) state by several orders of magnitude. According to Suzuki et al. (1993b), the main reaction channel of N (^2P) with N_2 involves quenching of the metastable state, but it most probably produces N (^2D) atoms, as the quenching into N (^4S) + N_2 is spin forbidden.

3.3.2.3. Reaction N (^2D) + H_2

Kinetics:
Recommended value at 300 K: $k = 2.2 \times 10^{-12}$ cm^3 s^{-1} ($\pm 25\%$)

This reaction is the best investigated reaction involving the ^2D state of atomic nitrogen, so far. The room temperature rate constant recommended by Herron is the average value of the most reliable available data (see Table 3). The rate expression as a function of the temperature has been determined by Suzuki et al. (1993b) in the 213–300 K range and the reported expression is $k = 4.6 \times 10^{-11}$ exp $(-880/T)$ cm^3 s^{-1}.

Products: NH (X $^3\Sigma^-$) + H.

The reaction dynamics has been extensively investigated and it is actually one of the few insertion reactions for which a comparison between state-of-the-art quantum-dynamical calculations and detailed experimental data has been possible (Balucani et al. 2002, 2006). This work has allowed a complete characterization of the reaction mechanism. The only exothermic reactive channel is the one leading to NH in its X $^3\Sigma^-$ electronic ground state and atomic hydrogen. Of potential relevance for the atmosphere of Titan is the product energy partitioning, that has been determined in the studies of Umemoto et al. (2000) and Balucani et al. (2006), which show that NH vibrational states are populated up to $v = 3$ (Umemoto et al. 2000). Let us note that the vibrational excitation of NH can significantly change its capability to undergo subsequent reactions. The determination of the product energy release can also provide important information to establish whether H atoms are formed with enough translational energy to escape the atmosphere of the satellite.

3.3.2.4. Reaction N (^2P) + H_2

Kinetics:
Recommended value at 300 K: $k = 1.9 \times 10^{-15}$ cm^3 s^{-1} ($\pm 60\%$)

No new study has been performed since 1999, so the recommended value for the rate constant is the same as the one proposed by Herron (1999; see Table 3). It is much lower than for the N (^2D) state and the outcome of the reaction is probably not the production of NH, but quenching giving N (^2D) (or eventually N(^4S) atoms), as for the reaction with N_2. Suzuki et al. (1993b) measured the temperature dependence of the rate constant as 3.5×10^{-13} exp$(-950/T)$ cm^3 s^{-1} over the 213–300 K temperature range.

3.3.2.5. Reaction N (^2D) + CH_4

Kinetics:
Recommended values at 300 K: $k = 4.0 \times 10^{-12}$ cm^3 s^{-1} ($\pm 40\%$) for CH_4
$k = 2.6 \times 10^{-12}$ cm^3 s^{-1} ($\pm 40\%$) for CD_4.

Since the collisional deactivation of N (^2D) by N_2 is a slow process, the reaction of N (^2D) with methane has been soon recognized as an important pathway. The rate constant at 298 K recommended by Herron (4.0×10^{-12} cm^3 s^{-1}) is the average of the values determined by Fell et al. (1981), Umemoto et al. (1998b) and Takayanagi et al. (1999) (see Table 3). The data by Black et al. (1969) were disregarded as they differ too much with respect to the other measurements. Umemoto et al. (1998b) and Takayanagi et al. (1999) also studied the reaction with CD_4, measuring at 298 K slightly lower rate constants for CD_4 than for CH_4. Takayanagi et al. (1999) also measured the temperature dependence of the rate constant over the range 223–292 K as
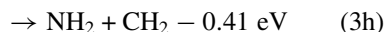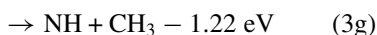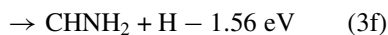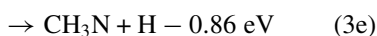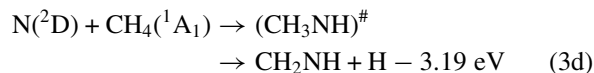
$k = 7.1 \times 10^{-11} \exp(-750/T)$ cm^3 s^{-1} and $3.3 \times 10^{-11} \exp(-700/T)$ for the reactions with CH$_4$ and CD$_4$, respectively.

Products:

Recommended yields: (CH$_2$NH and/or CH$_3$N + H)/ (NH + CH$_3$), (0.8 ± 0.2/(0.2 ± 0.1) for CH$_4$

(CD$_2$ND and/or CD$_3$N + D)/(ND + CD$_3$), (0.8 ± 0.2/ (0.2 ± 0.1) for CD$_4$.

In addition to kinetic data, much work has been done on this system at the level of reaction dynamics experiments and theoretical calculations in recent years. The first hint of the reaction mechanism and primary products came from the ab initio calculations by Kurosaki et al. (1998) of the relevant potential energy surface. According to those calculations, the exothermic channels are:

$$N(^2D) + CH_4(^1A_1) \rightarrow (CH_3NH)^{\#}$$

$$\rightarrow CH_2NH + H - 3.19 \text{ eV} \qquad (3d)$$

$$\rightarrow CH_3N + H - 0.86 \text{ eV} \qquad (3e)$$

$$\rightarrow CHNH_2 + H - 1.56 \text{ eV} \qquad (3f)$$

$$\rightarrow NH + CH_3 - 1.22 \text{ eV} \qquad (3g)$$

$$\rightarrow NH_2 + CH_2 - 0.41 \text{ eV} \qquad (3h)$$

All of these products can be formed after N (^2D) has inserted into one of the C-H bonds of methane forming a first intermediate, CH$_3$NH, which is bound by about 4.43 eV, with respect to the reactants. The insertion mechanism, through a small barrier, has been confirmed by recent ab initio calculations (Ouk et al. 2011). The CH$_3$NH intermediate can directly dissociate into the products CH$_2$NH + H (3d), CH$_3$N + H (3e), and NH + CH$_3$ (3f), or can rearrange to the isomeric form CH$_2$NH$_2$, which is the global minimum of the PES (4.68 eV lower in energy with respect to the reactants). CH$_2$NH$_2$ can also fragment and the possible products are essentially CHNH$_2$ + H (3f), and again CH$_2$NH + H. A first spectroscopic dynamical study by Umemoto et al. (1997) identified NH (from channel (3g)) and H (from channels (3d–f)) as primary reaction products with an absolute yield of 0.2 ± 0.1 and 0.8 ± 0.2, respectively. Later these authors measured the vibrational population of NH produced in this reaction by a laser induced fluorescence technique. The vibrational distribution was determined to be 10.0 ($v = 0$); 8.0 ± 1.0 ($v = 1$); 5.0 ± 0.7 ($v = 2$); 2.5 ± 0.5 ($v = 3$), in very good agreement with the theoretical calculations of Pederson et al. (1999) and Honvault & Launay (1999). Casavecchia et al. (Balucani et al. 2009; Casavecchia et al. 2001) have used the crossed molecular beam technique with mass spectrometric detection to investigate which of the three possible CH$_3$N isomers (CH$_2$NH, CHNH$_2$ and CH$_3$N) is actually produced in conjunction with H. According to the experimental results obtained in a wide range of E_{CM} collision energies (from about 0.21 to 0.62 eV, it was established that two isomers are actually formed: methylene-imine (CH$_2$NH) and methyl-nitrene (CH$_3$N). Notably, the relative branching ratio for the formation of CH$_2$NH with respect to CH$_3$N isomers was found to change considerably with E_{CM}, from 0.6 at $E_{CM} \sim 0.21$ to 0.04 at ~0.62 eV.

So the assumption that only NH + CH$_3$ would be the products of the N (^2D) + CH$_4$ reaction is not correct. This reactive channel accounts only for about 20% of the products in the room temperature laboratory experiment and we can assume that the product branching ratios are about the same for the reaction with CD$_4$. By analyzing the trend of the branching ratio as a function of the available energy (Balucani et al. 2009), we can presume that the yield of NH + CH$_3$ will be even smaller under the low temperature conditions of Titan's atmosphere. Therefore, the nitrogen chemistry that relies on the dominance of the CH$_3$ + NH channel in the photochemical models of the atmosphere of Titan should be reconsidered. Furthermore, the crossed molecular beam results suggest that the reaction of N (^2D) with CH$_4$ is an active route for formation of methylene-imine (CH$_2$NH), a closed-shell molecule containing a new unsaturated CN bond. This reaction demonstrates that C-N bonds can be generated directly by a reaction involving an active form of N$_2$. An indirect identification of CH$_2$NH in the atmosphere of Titan has indeed been reported by Vuitton et al. (2006, 2007) and Yelle et al. (2010).

3.3.2.6. Reaction N (^2P) + CH$_4$

Kinetics:

Recommended values at 300 K: k = 8.5 × 10^{-14} cm^3 s^{-1} (±25%) for CH$_4$

k = 6.0 × 10^{-14} cm^3 s^{-1} (±25%) for CD$_4$

No new studies have been performed since 1999, so the recommended value for the rate constant is the same as the one proposed by Herron (1999; see Table 3). As for N(^2D) reaction, Takayanagi et al. (1999) measured a rate constant for the reaction with CD$_4$, which was found to be slightly lower than for CH$_4$. Both Umemoto et al. (1985) and Takayanagi et al. (1999) suppose that the main reaction channel is quenching of N (^2P), most probably into N (^2D) state. Takayanagi et al. (1999) also measured the temperature dependence of the rate constant over the range 223–292 K as $k = 5.0 \times 10^{-13} \exp(-490/T)$ cm^3 s^{-1} and $3.1 \times 10^{-13} \exp(-480/T)$ for the reactions with CH$_4$ and CD$_4$, respectively.

3.3.2.7. Reaction N (^2D) + C$_2$H$_2$

Kinetics:

Recommended values at 300 K: $k = 6.5 \times 10^{-11}$ cm^3 s^{-1} (±25%) for C$_2$H$_2$

$k = 6.25 \times 10^{-11}$ cm^3 s^{-1} (±25%) for C$_2$D$_2$.

The rate constant has been measured by two groups (Fell et al. 1981; Takayanagi et al. 1998b; see Table 3) measured the rate constants over the temperature range 223–293 K and reported values of $k = 1.6 \times 10^{-10} \exp(-270/T)$ cm^3 s^{-1} and $1.4 \times 10^{-10} \exp(-240/T)$ for C$_2$H$_2$ and C$_2$D$_2$, respectively. So the H/D isotope effect was found to be very small. The recommended rate constant value of 6.5×10^{-11} cm^3 s^{-1} for C$_2$H$_2$ is the same as the one proposed by Herron (1999), based on the results from Takayanagi et al. (1998b). It is quite significantly larger than the value postulated by Yung (1987).

Products:

Recommended yields at 300 K (and at 150 K): (HCCN + H)/(cyclic-HCCN + H), (0.9 ± 0.1)/(0.1 ± 0.05)

Ab initio calculations of the potential energy surface have been reported (Balucani et al. 2000a), according to which the initial approach is N (^2D) addition to the unsaturated π-system of C$_2$H$_2$, which leads to the formation of a three-member cyclic HC(N)CH intermediate. HC(N)CH can then either decompose to cyclic-HC(N)C + H or isomerize to HCCNH and/or H$_2$CCN (cyanomethyl). Both HCCNH and H$_2$CCN can dissociate into

HCCN + H. Crossed beam experiments have been performed by Balucani et al. (2000a) and the results are consistent with both HCCN + H and cyclic-HC(N)C + H formation. Unfortunately, the difference in the energetics of the two channels does not allow a clear discrimination between these products, but some arguments are in favor of HCCN formation. RRKM estimates (Balucani et al. 2000a) based on the ab initio potential energy surface calculations confirmed that the channels leading to HCCN + H and cyclic-HCCN + H are the main pathways, with branching ratios σ(HCCN + H)/σ (cyclic-HCCN + H) estimated to be 86:14 and 77:23 at $E_{CM} = 0.135$ and 0.42 eV, respectively. By extrapolating this variation, we thus recommend a branching ratio of $(0.9 \pm 0.1)/(0.1 \pm 0.05)$ at 300 K, as well as at 150 K.

3.3.2.8. Reaction N (^2P) + C_2H_2

Kinetics:
Recommended values at 300 K: $k = 2.3 \times 10^{-11}$ cm^3 s^{-1} ($\pm40\%$) for C_2H_2
$k = 2.0 \times 10^{-11}$ cm^3 s^{-1} ($\pm40\%$) for C_2D_2.

No new measurement has been performed since 1999, so the recommended rate constant value is the same as the one proposed by Herron (1999; see Table 3). Takayanagi et al. (1998b) measured the rate constants over the temperature range 223–293 K and reported values of $k = 1.0 \times 10^{-10}$ exp $(-440/T)$ cm^3 s^{-1} and 7.1×10^{-11} exp $(-380/T)$ for C_2H_2 and C_2D_2, respectively. The products of this reaction have not been measured, but the measured rate constant, which is much larger than for the reactions of N (^2P) with H_2 or CH_4, suggests that the main process is chemical reaction and not N (^2P) quenching. However, the products are hard to predict without an experimental or theoretical study.

3.3.2.9. Reaction N (^2D) + C_2H_4

Kinetics:
Recommended values at 300 K: $k = 4.3 \times 10^{-11}$ cm^3 s^{-1} ($\pm25\%$) for C_2H_4
$k = 3.8 \times 10^{-11}$ cm^3 s^{-1} ($\pm25\%$) for C_2D_4.

The room temperature rate constant recommended by Herron is 4.3×10^{-11} cm^3 s^{-1}, in excellent agreement with the more recent determination of Sato et al. (1999) who reported a value of 4.1×10^{-11} cm^3 s^{-1} at $T = 292$ K (see Table 3). Sato et al. (1999) also measured the temperature dependence of the rate constants over the 230–292 K temperature range, as $k = (2.3 \pm 0.3) \times 10^{-10}$ exp $(-500 \pm 50/T)$ cm^3 s^{-1} and $(2.4 \pm 0.5) \times 10^{-10}$ exp $(-550 \pm 50/T)$ for C_2H_4 and C_2D_4, respectively.
Products:
Recommended yields:
(CH_2NCH + H)/(c-CH_2(N)CH + H)/(CH_2CNH + H)/ (HCN/HNC + CH_3)/(CH_3CN/CH_3NC + H)/(CH_2NC/ CHNCH + H_2)/(CH_2N/CHNH + CH_2), 0.67/0.23/0.05/ 0.02/0.01/0.01/0.01

Table 4 summarizes the product branching ratios of the N (^2D) + C_2H_4 reaction.

According to early ab initio calculations of the relevant potential energy surface (Takayanagi et al. 1998a), the initial step is the addition of N (^2D) to the π bond of the C_2H_4 molecule with formation of cyclic H_2C(N)CH_2 which can either decompose directly to 2H-azirine (cyclic-CH_2(N)CH) and H (^2S) or isomerize (via H-migration) to HC(NH)CH_2. The latter intermediate can decompose to 1H-azirine or 2H-azirine and H (^2S), or isomerize to CH_2-CHNH (^2A) which can, in turn, isomer-

ize to CH_3CNH ($^2A'$) or decompose to ketene-imine, CH_2CNH ($^1A'$), and H (^2S). CH_3CNH ($^2A'$) is the only intermediate which correlates with the CH_3CN + H products. RRKM calculations can help us to understand, which are the major channels among the above possibilities. According to the estimates at 0 K made by Takayanagi et al. (1998a), the channel leading to (2H-azirine (cyclic-CH_2(N)CH) + H) is by far the most dominant, accounting for 84.8% of the total reaction, followed by the channel leading to (ketene-imine (CH_2CNH) + H) (13.2%), CH_3 + HNC (1.2%) and CH_3CN + H (0.8%). The yields of the other energetically allowed reaction channels were found to be negligible. Balucani et al. (2000b) have performed a series of crossed beam experiments at $E_{CM} = 0.345$ eV. The experimental data are consistent with the formation of both 2H-azirine, as well as other isomers. In that paper, it was pointed out that a large fraction of 2H-azirine is formed with enough internal energy to spontaneously tautomerize to the most stable isomer acetonitrile, CH_3CN, even in a collision-free environment. A more recent crossed beam study (Lee et al. 2011), associated with a more complex determination of the potential energy surface, has pointed out that the radical CH_2NCH is also formed, as well as the CH_2CN radical. In general, the channels corresponding to one H-loss made a contribution 5.7 times smaller than the channels corresponding to the loss of two hydrogen atoms. RRKM calculations on the new potential energy surface, however, kept on predicting the dominance of 2H-azirine over the other products (87%; Lee et al. 2011). Finally, a very recent work has led to the construction of a different and more accurate potential energy surface (Rosi et al. 2012) where a larger basis set was used. RRKM calculations have been conducted at 170 K, typical temperature of Titan's atmosphere, by using the new electronic structure calculations (Balucani et al. 2012). These new results are different from those of Takayanagi et al. (1998a) and Lee et al. (2011), possibly because of the incompleteness of the previous potential energy surfaces (see Table 4). Only the channels with a significant yield have been reported in Table 4. The possibility that the primary products 2H-azirine or CH_2NCH isomerize to acetonitrile (CH_3CN) has been considered within the RRKM estimates. Differently from what was previously supposed, neither 2H-azirine (cyclic-CH_2(N)CH) nor the CH_2NCH radicals can significantly rearrange into acetonitrile at 170 K (Balucani et al. 2012). Therefore, the reaction N (^2D) + C_2H_4 cannot be a formation route of acetonitrile (CH_3CN), as previously suggested and our recommended product yields for this reaction are those calculated by Balucani et al. (2012) at 170 K. Collision-induced isomerization of 2H-azirine and CH_2NCH radical into CH_3CN is, therefore, only possible in dense high-temperature environments.

The most probable fate in Titan's atmosphere of the highly strained cyclic molecule 2H-azirine, as well as of the CH_2NCH radical, is further reaction with other molecular species present in the upper atmosphere of Titan. These molecular species could then contribute to the formation of N-rich organic macro-molecules of Titan's atmosphere.

3.3.2.10. Reaction N (^2P) + C_2H_4

Kinetics:
Recommended values at 300 K: $k = 3.0 \times 10^{-11}$ cm^3 s^{-1} ($\pm25\%$) for C_2H_4
$k = 3.0 \times 10^{-11}$ cm^3 s^{-1} ($\pm25\%$) for C_2D_4.

Since the review of Herron (1999), Sato et al. (1999) published an experimental study of this reaction with both C_2H_4 and C_2D_4, showing no isotope effect (see Table 3). These

Table 4
Product Branching Ratios of the N (^2D) + C_2H_4 Reaction

$CH_2NCH + H$	$c\text{-}CH_2(N)CH + H$	$CH_2CNH + H$	$HNC/HCN + CH_3$	$CH_3NC/CH_3CN + H$	$CH_2NC/CH_2CN/CHNCH + H_2$	$CH_2N/CHNH + CH_2$	References
. . .	0.848	0.132	0.012/. . .	. . ./0.008	. . ./$\sim$0/. . .	$\sim$0/. . .	Takayanagi et al. 1998b[a]
0.0440	0.8691	0.0228	0.0009/0.0039	0.0418/0.0003	0.0021/$\sim$0/0.0117	0.0034/. . .	Lee et al. 2011[b]
0.675	0.230	0.052	0.0118/0.0022	0.0111/0.0006	0.008/$\sim$0/. . .	0.0049/0.0017	Balucani et al. 2012[c]

Notes.
[a] Calculated yields at 0 K.
[b] Calculated yields at 0.22 eV collision energy (equivalent to 2500 K).
[c] Calculated yields at 170 K.

Table 5
Product Branching Ratios of the N (^2D) + C_2H_6 Reaction

Products	Branching ratio
CH_2=NH + CH_3	0.79
CH_3CH=NH + H	0.12
NH + C_2H_5	0.06
CH_2=CHNH$_2$ + H	0.02
$^3CH_2$=NH* + CH_3	0.01

authors measured the rate constant as a function of temperature in the 230–292 K range reporting the following temperature dependence: $k = (1.4 \pm 0.5) \times 10^{-10} \exp(-455 \pm 90/T)$ cm^3 s^{-1} and $(1.3 \pm 0.2) \times 10^{-10} \exp(-435 \pm 50/T)$ for C_2H_4 and C_2D_4, respectively. Their value at 292 K is in good agreement with previous data, so the recommended rate constant value is the same as the one proposed by Herron (1999). The reaction products have not been identified, but the value of the rate constant suggests that chemical reaction is the dominant channel versus N (^2P) quenching (Sato et al. 1999), as for the N (^2P) + C_2H_2 reaction.

3.3.2.11. Reaction N (^2D) + C_2H_6

Kinetics:
Recommended value at 300 K: $k = 1.9 \times 10^{-11}$ cm^3 s^{-1} ($\pm$25%)

The kinetic of the N (^2D) + C_2H_6 reaction has been investigated by two groups (Fell et al. 1981; Umemoto et al. 1998b) and the room temperature value recommended by Herron is 1.9×10^{-11} cm^3 s^{-1} (see Table 3). Considering the rate constant value at room temperature and by comparison with the reactions with other hydrocarbons, there is almost no doubt that this reaction has a small barrier (few hundreds of Kelvin). This implies that the rate constant value will be smaller at the temperatures of Titan's atmosphere.

Products:
Recommended yields:
(CH_2=NH + CH_3)/(CH_3CH=NH + H)/(NH + C_2H_5)/ (CH_2=CHNH$_2$ + H)/($^3CH_2$=NH* + CH_3), 0.79/0.12/0.06/ 0.02/0.01

Table 5 summarizes the product branching ratios of the N (^2D) + C_2H_6 reaction.

Balucani et al. (2010) have studied the reaction of N (^2D) with ethane, both experimentally at two different collision energies and theoretically by calculating the statistical product branching ratios, at temperatures relevant to Titan's conditions. The main reaction channels involve the C–C bond breaking giving CH_2NH + CH_3 and H atom transfer giving NH + C_2H_5. At all energies, the dominant channel is dissociation into CH_2NH + CH_3 and its branching ratio only varies from 0.79 at the lowest energy ($E_{CM} = 0.008$ eV) to 0.74 at the highest one ($E_{CM} = 0.325$ eV). The recommended yields are the values calculated at a collision energy of $E_{CM} = 0.015$ eV, corresponding to a temperature of 175 K, which is characteristic for Titan's strastosphere.

3.3.2.12. Reaction N (^2P) + C_2H_6

Kinetics:
Recommended value at 300 K: $k = 5.4 \times 10^{-13}$ cm^3 s^{-1} ($\pm$25%)

The only experimental study of this reaction was performed by Umemoto et al. (1985) who measured a small rate constant of 5.4×10^{-13} cm^3 s^{-1}, suggesting that the main channel is

quenching of N (^2P) and not any reactive process, as for the reaction with methane. So N (^2P) seems to be mainly quenched in collisions with saturated hydrocarbons, whereas the reaction of N (^2P) with unsaturated hydrocarbons, such as C_2H_2 and C_2H_4, leads to chemical reactions.

3.3.2.13. Reaction N (^2D) + C_3H_8

Kinetics:
Recommended value at 300 K: $k = 2.9 \times 10^{-11}$ cm^3 s^{-1} ($\pm$25%)

The kinetics of the N (^2D) + C_3H_8 reaction has been investigated by the same two groups mentioned for the reaction with C_2H_6 (Fell et al. 1981; Umemoto et al. 1998b; see Table 3). The room temperature value recommended by Herron is 2.9×10^{-11} cm^3 s^{-1}. Considering the rate constant value at room temperature and by comparison with the reactions with other hydrocarbons, there is almost no doubt that this reaction has a small barrier (a few hundreds of Kelvin). This implies that the rate constant value will be smaller at the temperatures of Titan's atmosphere.

No information is available on the nature of the products and we can expect that the favored mechanism will proceed through N (^2D) insertion into one of the C–H bonds, maybe giving CH_2NH + C_2H_5 or CH_3CHNH + CH_3, by analogy with the N insertion into C_2H_6. It could also produce NH associated with C_3H_7 or C_2H_5CHNH + H. But it would be too speculative to propose branching ratio values without theoretical calculations.

3.3.2.14. Reaction N (^2P) + C_3H_8

Kinetics:
Recommended value at 300 K: $k = 1.9 \times 10^{-12}$ cm^3 s^{-1} ($\pm$25%)

The only experimental study of this reaction was done by Umemoto et al. (1985) who measured a rate constant equal to 1.9×10^{-12} cm^3 s^{-1}. There is no information about the products. The measured rate constant is higher than for the other CH_4 and C_2H_6 saturated hydrocarbons, but lower than those for the unsaturated C_2H_2 and C_2H_4 hydrocarbons. Hence, it is hard to deduce for sure whether this reaction proceeds via quenching of the N (^2P) state or by chemical reaction, but quenching is more likely, as for the reactions of N (^2P) with the other saturated hydrocarbons, CH_4 and C_2H_6.

4. N_2^+ SINGLY CHARGED IONS

4.1. Production

Ionization of N_2 by photons or electrons produces N_2^+ ions in the ground state $X\,^2\Sigma_g^+$, as well as in the $A\,^2\Pi_u$, $B\,^2\Sigma_u^+$, and $C\,^2\Sigma_u^+$ valence electronic excited states. For most reactions, only N_2^+ (X, v) ground-state molecular ions will be considered in this review. The photoionization cross section of N_2 has been measured from threshold up to 107 eV by Samson et al. (1987) and partial ionization cross sections into electronic and vibrational states have been measured by Woodruff & Marr (1977). The ionization threshold of N_2 is at 15.58 eV, but above this energy, the absorbed photon energy does not only result in the ionization of N_2, but also can induce the formation of dissociative neutral Rydberg states. Shaw (1992) measured the absolute absorption cross section and the photoionization quantum efficiency from threshold

up to 25.6 eV. The N_2^+ formation cross section by electron impact has been measured by Tian & Vidal (1998), from threshold up to 600 eV (see the comment of Stebbings & Lindsay (2001) on the accuracy of these cross sections). The N_2^+ formation cross section is a maximum ($\sim 1.85 \times 10^{-16}$ cm^2) for an electron energy of 80–100 eV (Itikawa 2006). We note that the N_2^+ quartet state ($^4\Sigma_u^+$) can also be produced by electron impact, whereas this process is forbidden by photoionization. Ionization of N_2 molecules produces N_2^+ in different vibrational levels. The N_2^+ ($X\,^2\Sigma_g^+$) state is produced mainly in the ground vibrational level by direct ionization (Potts & Williams 1974). But vibrationally excited N_2^+ (X, $v = 1$–4) states are also populated, both by autoionization in the case of photoionization and by radiative cascades from excited electronic states. Their relative population is difficult to estimate because it strongly depends on the photon or electron energy. Partial cross sections into individual vibrational levels of the N_2^+ ground state have been measured by Woodruff & Marr (1977) for photon energies between 16 and 40 eV.

4.2. Lifetimes and Quenching

The $A\,^2\Pi_u$ and $B\,^2\Sigma_u^+$ excited electronic states of N_2^+ decay by radiative emission to the ground state. The $A\,^2\Pi_u$ state has a lifetime which decreases from 13.9 μs to 7.3 μs when its vibrational energy increases (Peterson & Moseley 1973) and the lifetime of the $B\,^2\Sigma_u^+$ state is equal to 67 ns (Wuerker et al. 1988). In Titan's ionosphere, these two states have a lifetime which is too short compared to the time between collisions (~ 1 s at the peak of the ionosphere) for their reactivity to be significant. The N_2 dissociative ionization threshold is at 24.3 eV, in the N_2^+ ($C\,^2\Sigma_u^+$) state region for vibrational levels $v \geqslant 3$. The radiative lifetime of N_2^+ ($C\,^2\Sigma_u^+$, $v \leqslant 2$) levels is equal to 0.09 μs and about 5×10^{-9} s for predissociated vibrational levels $v \geqslant 4$ (Fournier et al. 1971). N_2^+ ions in the ($C\,^2\Sigma_u$, $v \geqslant 3$) states and in the higher inner valence states dissociate into $N^+ + N$. Thus relevant reactions in Titan's atmosphere are only due to N_2^+ ions in their ($X\,^2\Sigma_g^+$) ground state. The excited vibrational states of N_2^+ (X, $v = 1$–4) can only relax by collisional quenching. Böhringer et al. (1983) predict that vibrational quenching in planetary atmospheres will generally be efficient, $k > 1 \times 10^{-12}$ cm^3 s^{-1} for almost all ions and neutral gases.

4.3. Reactions

Anicich & McEwan made several compilations of all ion–molecule reactions which may play a role in Titan's atmospheric chemistry (Anicich 1993; Anicich & McEwan 1997; McEwan & Anicich 2007; McEwan et al. 1998). They give the reaction rate constants at 300 K, and most of these reactions have only been studied at room temperature. In this review, we have updated the most recent of those compilations (McEwan & Anicich 2007) for N_2^+ reactions with the main neutral constituents of Titan's atmosphere, adding a discussion of the reaction mechanisms, as well as information about isotope effects and their dependence with collision and internal energy.

4.3.1. Reaction $N_2^+ + N_2$

Kinetics
Recommended value at 300 K: $k = 5.0 \times 10^{-10}$ cm^3 s^{-1} ($\pm 25\%$)

The different rate constant data for the $N_2^+ + N_2$ reaction can be found in Table 6, which summarizes all published rate constant data for N_2^+, N^+ (^3P, ^1D) and N^{++} reactions. The second

and fourth columns indicate the temperature or collision energy and the experimental method used, respectively.

Collisions of N_2^+ ions ($v = 0$–4) with N_2 can lead to vibrational deactivation and charge transfer (CT) processes. The formation of N_3^+, which is endothermic by 4.97 eV, has been studied from thermal energies up to 25 eV energy by Tosi et al. (2001) and has been interpreted as resulting from reactions of the N_2^+ ($^4\Sigma_u^+$) quartet state. The symmetric charge transfer reaction has been studied using isotopic labeling, i.e., by measuring the $^{15}N_2^+$ ($v = 0$) + $^{14}N_2$ or the $^{14}N_2^+$ ($v = 0$) + $^{15}N_2$ reaction. This charge transfer is an efficient process with a rate constant equal to about half the Langevin rate constant (8.3×10^{-10} cm^3 s^{-1}). It is hard to predict the value at 150 K, so we recommend the same value as at 300 K with a 70% uncertainty in order to include the maximum Langevin rate value. The recommended rate constant value for N_2^+ (X, $v = 0$) at 300 K is 5.0×10^{-10} cm^3 s^{-1}, which is the mean value of the literature values (see Table 6). Frost et al. (1994) and Kato et al. (1998) measured the rate constant as a function of the vibrational energy of N_2^+. Kato et al. explain the observed increase of the rate constant with vibrational energy (about 6.0×10^{-10} ($\pm 30\%$) cm^3 s^{-1} for $v = 1$–4, instead of 4.0×10^{-10} ($\pm 20\%$) cm^3 s^{-1} for $v = 0$), as the result of vibrational relaxation in addition to symmetric charge transfer. Vibration and translation inter-conversion processes can occur coincidently with charge transfer during collisions between N_2^+ and N_2, and several vibrational quanta can efficiently be converted to product kinetic energy during exothermic charge transfer reactions (McAfee et al. 1981; Sohlberg 1999).

4.3.2. Reaction $N_2^+ + H_2$

Kinetics
Recommended values at 300 K: $k = 1.56 \times 10^{-9}$ cm^3 s^{-1} ($\pm 15\%$) for H$_2$ and 1.15×10^{-9} cm^3 s^{-1} ($\pm 20\%$) for D$_2$
Recommended values at 150 K: $k = 1.3 \times 10^{-9}$ cm^3 s^{-1} ($\pm 20\%$) for H$_2$ and 9.6×10^{-10} cm^3 s^{-1} ($\pm 20\%$) for D$_2$.

This reaction has been extensively studied over the years. All rate constant measurements at 300 K are in very good agreement (see Table 6) and give a value nearly equal to the Langevin rate (1.56×10^{-9} cm^3 s^{-1}), which is therefore our recommended value. Rowe et al. (1989) and Randeniya & Smith (1991) have measured the rate constant as a function of temperature below 300 K. When temperature decreases, the rate constant goes through a minimum and then increases to reach about 2×10^{-9} cm^3 s^{-1} at about 8 K (Randeniya & Smith 1991). At 150 K, it is about 1.3×10^{-9} cm^3 s^{-1}, which is our recommended value for Titan's ionosphere. Knott et al. (1995) measured the cross section as a function of collision energy and found two regimes: it follows an $E_{CM}^{-0.5}$ law for $E_{CM} = 8$–90 meV and an $E_{CM}^{-0.33}$ law for $E_{CM} = 90$ meV to 2 eV. These authors did not observe a variation of the rate constant with the vibrational level of N_2^+. Similar behavior is observed at higher collision energies (Henri et al. 1988; Koyano et al. 1987). Isotopic effects have been investigated in guided ion beam experiments (Schultz & Armentrout 1992). These authors found that there is no significant isotopic effect on the rate constant for the reactions of N_2^+ with H$_2$, HD, or D$_2$, which are equal to the Langevin rate within experimental errors. The rate constants decrease from H$_2$ to HD to D$_2$, but the ratio of the measured rate constant divided by the Langevin rate remains equal to about 1. In a selected ion flow drift tube (SIFDT) experiment, Schwarzer et al. (1991) observed the same trend in kinetics for the reactions of N_2^+ with H$_2$ and D$_2$. Given the above, the recommended rate constant values are the Langevin

Table 6
Rate Constant Measurements for the Ion N_2^+, $N^+(^3P, ^1S)$ and N^{++} Reactions

Reaction	T (K) or E_{CM}(eV)	k (cm^3 s^{-1})	Method	Reference
$N_2^+ + N_2$	300 K	6.6×10^{-10} ($\pm 8\%$)	ICR	(McMahon et al. 1976)
$N_2^+ + N_2$	300 K	5.0×10^{-10} ($\pm 25\%$)	SIFT	(Adams & Smith 1981)
$N_2^+ + N_2$	300 K	4.24×10^{-10} ($\pm 20\%$) for $v = 0$ 5.32×10^{-10} ($\pm 20\%$) for $v = 1$ 5.13×10^{-10} ($\pm 20\%$) for $v = 2$	SIFT	(Frost et al. 1994)
$N_2^+ + N_2$	300 K	4.0×10^{-10} ($\pm 20\%$) for $v = 0$ 6.3×10^{-10} ($\pm 30\%$) for $v = 1$ 5.8×10^{-10} ($\pm 30\%$) for $v = 2$ 6.4×10^{-10} ($\pm 30\%$) for $v = 3$ 5.5×10^{-10} ($\pm 30\%$) for $v = 4$	SIFT	(Kato et al. 1998)
$N_2^+ + N_2$	300 K	5.80×10^{-10} ($\pm 25\%$)	Compilation	(Anicich & McEwan 1997)
$N_2^+ + H_2$	300 K	1.8×10^{-9} ($\pm 30\%$)	SIFT	(Tichy et al. 1979)
$N_2^+ + H_2$	300 K	2.1×10^{-9} ($\pm 20\%$)	SIFT	(Smith et al. 1978)
$N_2^+ + H_2$	< 200 K	1–1.2×10^{-9}	CRESU	(Rowe et al. 1989)
$N_2^+ + H_2$	< 15 K	0.8–2.0×10^{-9}	FJFR	(Randeniya & Smith 1991b)
$N_2^+ + H_2$	300 K	2.0×10^{-9} for H_2 1.5×10^{-9} for D_2	SIFDT	(Schwarzer et al. 1991)
$N_2^+ + H_2$	300 K	1.7×10^{-9} ($\pm 30\%$)[a]	GIB	(Tosi et al. 1992)
$N_2^+ + H_2$	300 K	1.72×10^{-9} ($\pm 30\%$) for H_2 1.27×10^{-9} ($\pm 30\%$) for HD 1.15×10^{-9} ($\pm 30\%$) for D_2	GIB	(Schultz & Armentrout 1992)
$N_2^+ + H_2$	300 K	1.71×10^{-9} ($\pm 5\%$) for (X, $v = 0$) 1.69×10^{-9} ($\pm 3\%$) for (X, $v = 1$) 1.80×10^{-9} ($\pm 6\%$) for (X, $v = 2$) 1.68×10^{-9} ($\pm 3\%$) for (X, $v = 3$) 1.47×10^{-9} ($\pm 5\%$) for (X, $v = 4$)	SIFT-LIF	(de Gouw et al. 1995)
$N_2^+ + H_2$	300 K	1.1×10^{-9} ($\pm 20\%$) for (X, $v = 0$–4, $J = 2$)[a]	GIB	(Knott et al. 1995)
$N_2^+ + H_2$	300 K	2.00×10^{-9} ($\pm 15\%$) for H_2 1.25×10^{-9} ($\pm 20\%$) for D_2	Compilation	(McEwan & Anicich 2007)
$N_2^+ + CH_4$	300 K	1.01×10^{-9} ($\pm 17\%$)	Opt	(Herod et al. 1971)
$N_2^+ + CH_4$	300 K	1.28×10^{-9}	PIMS	(Warneck 1972)
$N_2^+ + CH_4$	300 K	1.06×10^{-9} ($\pm 5\%$)	IonTrap	(Li & Harrison 1978)
$N_2^+ + CH_4$	300 K	1.30×10^{-9} ($\pm 30\%$)	SIFT	(Tichy et al. 1979)
$N_2^+ + CH_4$	298 K	9.80×10^{-10} ($\pm 10\%$)	ICR	(Huntress et al. 1980)
$N_2^+ + CH_4$	300 K	1.00×10^{-9} ($\pm 20\%$)	SIFT	(Smith et al. 1978)
$N_2^+ + CH_4$	70 K	1.20×10^{-9} ($\pm 30\%$)	CRESU	(Rowe et al. 1989)
$N_2^+ + CH_4$	8–15 K	1.90×10^{-9} ($\pm 50\%$)	FJFR	(Randeniya & Smith 1991a)
$N_2^+ + CH_4$	0.36 eV	1.15×10^{-9} ($\pm 20\%$)[a]	GIB	(Nicolas 2002)
$N_2^+ + CH_4$	0.1–3 eV	1.53–2.83×10^{-9}($\pm 20\%$)[a]	GIB	(Nicolas et al. 2003b)
$N_2^+ + CH_4$	298 K	1.00×10^{-9}	SIFT	(Anicich et al. 2004)
$N_2^+ + CH_4$	300 K	1.14×10^{-9} ($\pm 15\%$)	Compilation	(McEwan & Anicich 2007)
$N_2^+ + C_2H_2$	300 K	8.80×10^{-10} ($\pm 11\%$)	Opt	(Dreyer & Perner 1971)
$N_2^+ + C_2H_2$	300 K	4.30×10^{-10}	PIMS	(Warneck 1972)
$N_2^+ + C_2H_2$	298 K	4.00×10^{-10} ($\pm 15\%$)	ICR	(McEwan et al. 1998)
$N_2^+ + C_2H_2$	0.08 eV	1.7×10^{-10} ($\pm 20\%$)[a]	GIB	(Nicolas 2002)
$N_2^+ + C_2H_2$	298 K	5.50×10^{-10}	SIFT	(Anicich et al. 2004)
$N_2^+ + C_2H_2$	300 K	4.0×10^{-10}($\pm 15\%$)	Compilation	(McEwan & Anicich 2007)
$N_2^+ + C_2H_4$	298 K	7.10×10^{-10}	SIFT	(Anicich et al. 2004)
$N_2^+ + C_2H_4$	298 K	1.30×10^{-9} ($\pm 15\%$)	ICR	(McEwan et al. 1998)
$N_2^+ + C_2H_4$	298 K	1.30×10^{-9} ($\pm 15\%$)	Compilation	(McEwan & Anicich 2007)

Table 6
(Continued)

Reaction	T (K) or E_{CM}(eV)	k (cm^3 s^{-1})	Method	Reference
$N_2^+ + C_2H_6$	298 K	1.44×10^{-9} ($\pm$30%)	SIFDT	(Praxmarer et al. 1998)
$N_2^+ + C_2H_6$	298 K	$\sim 1.30 \times 10^{-9}$($\pm$30%)	ICR	(McEwan et al. 1998)
$N_2^+ + C_2H_6$	0.1 eV	7.4×10^{-10} ($\pm$20%)[a] for C_2D_6	GIB	(Nicolas 2002)
$N_2^+ + C_2H_6$	298 K	1.44×10^{-9} ($\pm$30%)	ICR	(McEwan & Anicich 2007)
$N_2^+ + C_3H_8$	298 K	1.30×10^{-9} ($\pm$30%)	SIFDT	(Praxmarer et al. 1998)
$N^+ + N_2$	300 K	1.8×10^{-10}($\pm$ 40%)[b]	FA	(Fehsenfeld et al. 1974)
$N^+ + N_2$	300 K	3.3×10^{-10} ($\pm$25%)[b]	ICR	(Anicich et al. 1977)
$N^+ + N_2$	300 K	1.6×10^{-10} ($\pm$20%)[b,c]	GIB	(Freysinger et al. 1994)
$N^+ + N_2$	300 K	1.9×10^{-10}($\pm$ 20%)[b,c]	GIB-TOF	(Glosik et al. 2000)
$N^+ + H_2$	300 K	5.6×10^{-10}($\pm$ 30%)	FA	(Fehsenfeld et al. 1967)
$N^+ + H_2$	298 K	4.8×10^{-10}($\pm$ 10%)	ICR	(Kim et al. 1975)
$N^+ + H_2$	300 K	6.4×10^{-10}($\pm$ 20%)	SIFT	(Adams & Smith 1976)
$N^+ + H_2$	300 K	6.2×10^{-10}($\pm$ 30%)	SIFT	(Tichy et al. 1979)
$N^+ + H_2$	300 K	4.8×10^{-10}($\pm$ 20%)	SIFT	(Smith et al. 1978)
$N^+ + H_2$	300 K	3.7×10^{-10} ($\pm$20%) for H_2 3.5×10^{-10} ($\pm$20%) for HD 1.3×10^{-10} ($\pm$20%) for D_2	SIFT	(Adams & Smith 1985)
$N^+ + H_2$	67 K	2.3×10^{-10} ($\pm$30%)	CRESU	(Marquette et al. 1985)
$N^+ + H_2$	11–20 K	0.3–4×10^{-12} ($\pm$40%)	Ion Trap	(Luine & Dunn 1985)
$N^+ + H_2$	300 K	3.9×10^{-10} ($\pm$20%) for H_2 2.7×10^{-10} ($\pm$20%) for HD 1.7×10^{-10} ($\pm$20%) for D_2	GIB	(Ervin & Armentrout 1987)
$N^+ + H_2$	163 K	3.0×10^{-10} ($\pm$30%) for p-H_2	CRESU	(Marquette et al. 1988)
$N^+ + H_2$	300 K	3.73×10^{-10} for H_2 1.2×10^{-10} for D_2	Calculations	(Gerlich 1989)
$N^+ + H_2$	15–100 K	0.2–4×10^{-10} for nH_2[d]	GIB	(Gerlich 1993)
$N^+ + H_2$	300 K	4.16×10^{-10}	Calculations	(Ge et al. 2006)
$N^+ + H_2$	300 K	5.0×10^{-10} ($\pm$20%) for H_2 3.1×10^{-10} ($\pm$20%) for HD 1.5×10^{-10} ($\pm$20%) for D_2	Compilation	(McEwan & Anicich 2007)
$N^+ (^3P) + CH_4$	298 K	1.35×10^{-9} ($\pm$10%)	ICR	(Anicich et al. 1977)
$N^+ (^3P) + CH_4$	300 K	1.1×10^{-9} ($\pm$30%)	SIFT	(Tichy et al. 1979)
$N^+ (^3P) + CH_4$	300 K	9.4×10^{-10} ($\pm$20%)	SIFT	(Adams et al. 1980)
$N^+ (^3P) + CH_4$	300 K	1.20×10^{-9} ($\pm$10%)	DT	(Dheandhanoo et al. 1984)
$N^+ (^3P) + CH_4$	8 K	8.2×10^{-10} ($\pm$35%)	CRESU	(Rowe et al. 1985)
$N^+ (^3P) + CH_4$	300 K	1.15×10^{-9} ($\pm$15%)	Compilation	(Anicich 1993)
$N^+ (^3P) + CH_4$	298 K	1.1×10^{-9}($\pm$ 20%)	SIFT	(Anicich et al. 2004)
$N^+ (^3P) + CH_4$	0.2–2 eV	1.5×10^{-9} ($\pm$25%)[a] for the $^{15}N^+ + CD_4$ reaction	GIB	(Alcaraz et al. 2004)
$N^+ (^3P) + CH_4$	300 K	1.15×10^{-9} ($\pm$15%)	Compilation	(McEwan & Anicich 2007)
$N^+ (^1D) + CH_4$	300 K	1.1×10^{-9} ($\pm$15%)[e]	SIFT	(Tichy et al. 1979)
$N^+ (^1D) + CH_4$	0.2–2 eV	1.5×10^{-9} ($\pm$25%)[a] for the $^{15}N^+ + CD_4$ reaction	TPEPICO	(Alcaraz et al. 2004)
$N^+ (^3P) + C_2H_2$	298 K	1.50×10^{-9} ($\pm$15%)	ICR	(McEwan et al. 1998)
$N^+ (^3P) + C_2H_2$	298 K	1.30×10^{-9} ($\pm$20%)	SIFT	(Anicich et al. 2004)
$N^+ (^3P) + C_2H_2$	298 K	1.50×10^{-9} ($\pm$15%)	compilation	(McEwan & Anicich 2007)
$N^+ (^3P) + C_2H_4$	300 K	1.54×10^{-9} ($\pm$20%)	SIFT	(Rakshit 1980)
$N^+ (^3P) + C_2H_4$	300 K	1.60×10^{-9} ($\pm$20%) for C_2H_4 1.50×10^{-9} ($\pm$20%) for C_2D_4	SIFT	(Smith & Adams 1980)

Table 6
(Continued)

Reaction	T (K) or E_{CM}(eV)	k (cm^3 s^{-1})	Method	Reference
N$^+$ (^3P) + C$_2$H$_4$	298 K	1.30×10^{-9} ($\pm$15%)	ICR	(McEwan et al. 1998)
N$^+$ (^3P) + C$_2$H$_4$	298 K	1.10×10^{-9} ($\pm$20%)	SIFT	(Anicich et al. 2004)
N$^+$ (^3P) + C$_2$H$_4$	298 K	1.3×10^{-9} ($\pm$15%)	Compilation	(McEwan & Anicich 2007)
N$^+$ (^1D) + C$_2$H$_4$	300 K	3.80×10^{-9} ($\pm$30%)	SIFT	(Rakshit 1980)
N$^+$ (^1D) + C$_2$H$_4$	0.2 eV	1.7×10^{-9} ($\pm$30%)[a] for the ^{15}N$^+$+ C$_2$D$_4$ reaction	GIB	(Alcaraz et al., unpublished)
N^{++}+ N$_2$	300 K	2.8×10^{-9} ($\pm$20%)	Penning trap	(Church & Holzscheiter 1980)
N^{++}+ N$_2$	1.8 eV	2.1×10^{-9} ($\pm$10%)	rf ion trap	(Fang & Kwong 1997)
N^{++}+ H$_2$	0.34 eV	3.38×10^{-11} ($\pm$10%)	rf ion trap	(Fang & Kwong 1997)

Notes.
[a] Converted from cross sections by using the expression $k = \sigma \langle v \rangle$.
[b] Rate constants related to the isotope exchange channel measured with isotopically labelled reactants ^{15}N$^+$+^{14}N$_2$ or ^{14}N$^+$+^{15}N$_2$.
[c] Extrapolated to 300 K and converted from cross sections by using the expression $k = \sigma \langle v \rangle$.
[d] The range of the rate constant values are given here for normal H$_2$, but there are also values for para-H$_2$ with different ortho-H$_2$ admixtures in the paper of Gerlich(Gerlich 1993).
[e] This rate constant corresponds to both the reactivity of the excited state and its quenching.

rate constants at 300 K for both reactions with H$_2$ and D$_2$. At 150 K, the recommended rate constant values are lower. For the reaction with H$_2$, it is the one measured by Randeniya & Smith (1991) and for the reaction with D$_2$, it is a value calculated from the one at 300 K, decreased in the same proportion.

Products
Recommended yields at 300 K: (N$_2$H$^+$ + H)/(H$_2^+$ + N$_2$), 0.99/0.01.

Reactive collisions between N$_2^+$ and H$_2$ result either in hydrogen transfer to give N$_2$H$^+$ + H or in charge transfer to give H$_2^+$ + N$_2$, the former channel being strongly favored at 300 K. The hydrogen transfer giving N$_2$H$^+$ + H products has been the subject of extensive experimental investigations. Three of the most recent papers describe guided ion beam experiments (Knott et al. 1995; Schultz & Armentrout 1992; Tosi et al. 1992), while two other experiments focused on the dependence of the reactivity on the N$_2^+$ internal state (electronic and vibrational) (de Gouw et al. 1995; Uiterwaal et al. 1995). For ground-state reactants, the reaction proceeds at thermal energies with the rate predicted by the Langevin classical ion–molecule capture theory (1.56×10^{-9} cm^3 s^{-1}). Vibrational excitation of the N$_2^+$ appears to have only minor effects on the reaction rates (de Gouw et al. 1995; Knott et al. 1995). As far as the electronic excitation is concerned, the reaction rate for N$_2^+$ in the first electronically excited A $^2\Pi_u$ state is 50% lower with respect to the X state (Uiterwaal et al. 1995). This difference in rate is not relevant for Titan, as the A state has a lifetime which is much shorter than the average collision time in Titan's ionosphere. When HD is used as reactant, the production of N$_2$D$^+$ is slightly favored over N$_2$H$^+$, for collision energies below 0.1 eV cm. In particular, at thermal energies the branching ratio is N$_2$D$^+$:N$_2$H$^+$ = 0.52: 0.48 (Schultz & Armentrout 1992), while the formation of N$_2$H$^+$ is favored at energies above 0.1 eV.

The charge transfer process giving H$_2^+$ + N$_2$ products is only a minor product channel (Schultz & Armentrout 1992; Uiterwaal et al. 1995), and has been investigated as a function of the collision energy for ground-state reactants (Schultz & Armentrout 1992), and at thermal energies as a function of the internal state of N$_2^+$ (Uiterwaal et al. 1995). The charge transfer cross section is about two orders of magnitude lower than that

for the hydrogen abstraction reaction, according to Schultz et al. (Schultz & Armentrout 1992) and one order of magnitude lower, according to Uiterwaal et al. (1995). This small cross section has been explained by the absence of crossing between the potential energy surfaces (Schultz & Armentrout 1992).

4.3.3. Reaction N$_2^+$ + CH$_4$

Kinetics:
Recommended values at 300 K: $k = 1.18 \times 10^{-9}$ cm^3 s^{-1} ($\pm$15%) for CH$_4$
$k = 1.10 \times 10^{-9}$ cm^3 s^{-1} ($\pm$20%) for CD$_4$.

The kinetics of this reaction has been extensively studied (see Table 6). The latest determinations at 300 K are all in good agreement, and are satisfyingly represented by the value (1.14×10^{-9} cm^3 s^{-1} ($\pm$15%)) in the compilation of McEwan & Anicich (2007). Moreover, this value is very equal within experimental uncertainties to the Langevin rate (1.18×10^{-9} cm^3 s^{-1}), which is reasonable for such a reaction. It is thus our recommended value.

Rowe et al. (1989) and Randeniya & Smith (1991) studied this reaction at low temperatures, 70 and 8–15 K, respectively. In spite of a slight increase of the rate constant at low temperatures, 1.20×10^{-9} at 70 K and 1.90×10^{-9} at 8–15 K, the difference with the value of the rate constant at 300 K is not significant. The rate constant seems effectively unchanged over the temperature range 8–300 K, so the recommended value is the same at 300 K and 150 K. The study of Nicolas et al. (2003b) shows, however, a substantial increase of the rate constant with collision energy, and in the thesis report of Nicolas (2002), a variation of less than 20% in the rate constant is observed with vibrational energy ($v = 0$–4). A small isotopic effect has been observed by Nicolas et al. (2003b), who measured, in the 0.1–3 eV E_{CM} range, rate constants equal to (1.53–2.83) $\times$ 10^{-9} cm^3 s^{-1} and (1.43–1.64) $\times 10^{-9}$ for the reaction with CH$_4$ and CD$_4$, respectively, as expected for the Langevin rates, because the reaction relative mass and the polarization are not the same for CH$_4$ and CD$_4$. The Langevin rate for the reaction with CD$_4$ is 1.10×10^{-9} cm^3 s^{-1}, calculated with the polarization of CD$_4$ which is lower by 0.034 than the one from CH$_4$ according to Bell (1942) and Wong et al. (1991). So the recommended rate

Table 7
Product Branching Ratio Data for the N_2^+ + CH_4 Reaction

CH_3^+ + H + N_2	CH_2^+ + H_2 + N_2	N_2H^+ + CH_3	Reference
0.89	0.11	. . .	Tichy et al. 1979
0.92	0.08	. . .	Huntress et al. 1980
0.93	0.07	. . .	Smith et al. 1978
0.80	0.20	. . .	Randeniya & Smith 1991
0.91	0.09	. . .	Anicich 1993
0.80	0.05	0.15	McEwan et al. 1998
0.86 ($\pm$2%) for CH_4	0.09 ($\pm$2%) for CH_4	0.05 ($\pm$2%) for CH_4	Nicolas et al. 2003b[a]
0.88 ($\pm$2%) for CD_4	0.07 ($\pm$2%) for CD_4	0.05 ($\pm$2%) for CD_4	
0.88	0.12	. . .	Anicich et al. 2004
0.91	0.09	. . .	McEwan & Anicich 2007
0.84	0.09	0.07	C. Alcaraz et al., unpublished
0.83 $\pm$ 0.02	0.17 $\pm$ 0.02	. . .	Gichuhi & Suits 2011

Note. [a] Measured at E_{CM} = 0.1 eV.

constant values at 300 K and 150 K for the reaction with CD_4 are the Langevin rates, which are independent of temperature.

Products

Recommended yields at 300 K and 150 K:

$(CH_3^+ + H + N_2)/(CH_2^+ + H_2 + N_2)/(N_2H^+ + CH_3)$, **0.86/0.09/0.05 for CH_4**

$(CD_3^+ + D + N_2)/(CD_2^+ + D_2 + N_2)/(N_2D^+ + CD_3)$, **0.88/0.07/0.05 for CD_4.**

Table 7 summarizes the product branching ratio data for the N_2^+ + CH_4 reaction.

All studies are in agreement concerning the identity of the dissociative charge transfer products, CH_2^+ and CH_3^+, with CH_3^+ formation being the major channel. The nondissociative charge transfer product CH_4^+ is not observed (less than 0.2% in the study of Nicolas et al. (2003b) because a large amount of internal energy is transferred to the primary CH_4^+ product which then dissociates. However, there is an important disagreement concerning the production of N_2H^+. Only three studies relate its formation (McEwan et al. 1998; Nicolas et al. 2003b; C. Alcaraz et al., unpublished). Note that an older work of Harrison & Myher (Harrison & Myher 1967; Li & Harrison 1978) studied specifically this reaction channel. They found a partial rate constant of 2.3×10^{-10} cm^3 s^{-1} for the production of N_2D^+ in the reaction with CD_4, but underline it only represents 2% maximum of the products. Their results are not directly comparable with other values in the literature, but do confirm the production of this ion. The detection of N_2H^+ is difficult because there is a mass overlap with the secondary product $C_2H_5^+$ (from the reaction CH_3^+ + CH_4) and the natural isotope of N_2^+, $^{14}N^{15}N^+$. In their work, Nicolas et al. (2003b) studied very precisely, at collision energies between 0.1 and 3 eV, the production of N_2H^+ and N_2D^+ in the reactions of N_2^+ with CH_4 and CD_4, respectively. Their time of flight analysis allowed them to unambiguously distinguish between N_2H^+ and $C_2H_5^+$, and the uncertainty of their determination is very small. The measurements of Nicolas et al. (2003b) were confirmed in unpublished experiments of some of the authors of the present paper (C. Alcaraz et al., unpublished). The measured branching ratios are almost constant with collision energy. So it is reasonable to expect the same values at 300 K. C. Alcaraz et al. (unpublished) also studied the variation of the branching ratios with vibrational energy of N_2^+ ($X\ ^2\Sigma_g^+$, $v = 0, 4$). The effect is very weak, 2%–3% for the main product CH_3^+. Recently, Gichuhi et al. (Gichuhi & Suits 2011) measured the branching ratio of this reaction at 45 ± 5 K. Their mass resolution was not

sufficient to distinguish N_2H^+ from the intense N_2^+ parent ion peak. But for the two other products, their branching ratio is very close to the measurements made at 300 K, in good agreement with the previous measurements of Randeniya & Smith. (1991) at even lower temperatures (8–15 K). In conclusion, the product branching ratio of this reaction seems to be constant as a function of temperature and vibrational excitation of N_2^+ parent ions within experimental uncertainties. Our recommended yields are the values from Nicolas et al. (2003b).

4.3.4. Reaction N_2^+ + C_2H_2

Kinetics

Recommended value: $k = 4.15 \times 10^{-10}$ cm^3 s^{-1} ($\pm$25%)

All published rate constant data are shown in Table 6. The study of Dreyer et al. (Dreyer & Perner 1971) involves quite particular conditions, such as a high pressure of N_2 (about 40 Torr, and up to 160 Torr). The results of Anicich et al. (2004) have also been obtained at rather high pressure in order to detect the products of multiple successive reactions and not only the primary products. We thus recommend an average value ($k = 4.15 \times 10^{-10}$ cm^3 s^{-1}) for the two other experimental determinations at $\sim$300 K ($k = 4.15 \times 10^{-10}$ cm^3 s^{-1}). This value is significantly smaller than the Langevin rate (1.16×10^{-9} cm^3 s^{-1}). It can be explained by the fact that it is mainly a nonresonant charge transfer reaction (see below). Nicolas et al. (Nicolas 2002) measured a lower rate constant at $E_{CM} = 0.08$ eV (928 K), which indicates that most probably the rate constant decreases with temperature, as expected such a nonresonant charge transfer. This decrease is compatible with the typical variation of the cross section with collision energy for such reactions, i.e., proportional to $E_{CM}^{-1/2}$. Using this expression, the reaction cross section value extrapolated down to 150 K is 39.6 Å^2, giving a rate constant of 1.03×10^{-9} cm^3 s^{-1} at 150 K. This should be checked experimentally, but until then, we recommend a rate constant value of 1.0×10^{-9} cm^3 s^{-1} at 150 K, with an uncertainty of 50% which includes the value at 300 K.

Products

Recommended yields: $(C_2H_2^+ + N_2)/(N_2H^+ + C_2H)$, 0.94/0.06.

Table 8 summarizes the product branching ratio data of the N_2^+ + C_2H_2 reaction.

$C_2H_2^+$ is the only significant product observed by Nicolas (2002), which is in agreement with Anicich et al. (2004), Warneck (1972) and with the recent work at low temperature

Table 8
Product Branching Ratio Data for the $N_2^+ + C_2H_2$ Reaction

$C_2H_2^+ + N_2$	$HCN^+ + HCN$	$N_2H^+ + C_2H$	Reference
0.94	...	0.06	Nicolas 2002[a]
1	...	...	Anicich et al. 2004
0.37	0.03	0.60	McEwan et al. 1998
1	...	...	Warneck 1972
1	...	...	Gichuhi & Suits 2011[b]

Notes.
[a] Measured at $E_{CM} = 0.08$ eV.
[b] Measured at $T = 45 \pm 5$ K.

$(45 \pm 5$ K) of Gichuhi et al (Gichuhi & Suits 2011). The disagreement with the study of McEwan et al. (1998) is assumed by Anicich et al. (2004) to be due to the presence of impurities in the instrument, so these results are disregarded. The erroneous old branching values are still present in the compilation of McEwan & Anicich (2007), probably due to an error. The N_2H^+ product observed by Nicolas (2002) is a very minor product and was probably not detected in other studies, due to experimental difficulties. In conclusion, we recommend the branching ratios measured by Nicolas (2002). They should be nearly identical at 150 K.

4.3.5. Reaction $N_2^+ + C_2H_4$

Kinetics
Recommended value at 300 K: $k = 1.30 \times 10^{-9}$ cm^3 s^{-1} ($\pm 15\%$)
The disagreement between the determinations of Anicich et al. (2004, 7.10×10^{-10} cm^3 s^{-1}) and McEwan et al. (1998, 1.30×10^{-9} cm^3 s^{-1}) which are the only published rate constant data for this reaction, is not explained by the authors (see Table 6). However, the experimental conditions are substantially different, with a higher pressure in the case of Anicich et al. (2004) inducing secondary reactions. The inherent uncertainty in this higher pressure procedure being more significant, we recommend the rate constant determined by McEwan et al. (1998), as in the recent compilation of McEwan & Anicich (2007). This value is equal to the Langevin rate (1.29×10^{-9} cm^3 s^{-1}) within experimental errors. As the Langevin rate does not depend on temperature, the value will be the same at 150 K.

Products
Recommended yields: $(C_2H_3^+ + H + N_2)/(C_2H_2^+ + H_2 + N_2)/(N_2H^+ + C_2H_3)$, 0.67/0.23/0.10.
Table 9 summarizes the product branching ratio data for the $N_2^+ + C_2H_4$ reaction.
In the study of McEwan et al. (1998), C_2D_4 was used in addition to C_2H_4. They could conclude that the direct charge transfer product fragmented into $C_2H_3^+ + H$ and $C_2H_2^+ + H_2$, as for the study of Gichuhi et al. (Gichuhi & Suits 2011) at 45 ± 5 K. The chemical products $HCNH^+$ and HCN^+, observed by

McEwan et al. (1998), which would result from an N_2 triple bond breaking, are, however, very unlikely to be produced in this reaction, which is confirmed by the results of Anicich et al. (2004), who did not detected them. The production of N_2H^+, observed by McEwan et al. (1998) was not confirmed in the work of Anicich et al. (2004). Nevertheless, the production of this ion cannot be definitively excluded. That is, N_2H^+ signals could have been masked in the work of Anicich et al. (2004), as a mass overlap with $^{14}N^{15}N^+$ complicates this ion's detection. Gichuhi et al. (Gichuhi & Suits 2011) could also not have detected N_2H^+ product ions, due to a lack of mass resolution. We thus recommend the branching ratios measured at low temperature by Gichuhi et al. (Gichuhi & Suits 2011), normalized to 100%, after adding 10% of N_2H^+ ions, i.e., $C_2H_3^+/C_2H_2^+/N_2H^+$ yields being equal to 0.67/0.23/0.10.

4.3.6. Reaction $N_2^+ + C_2H_6$

Kinetics
Recommended value at 300 K: $k = 1.30 \times 10^{-9}$ cm^3 s^{-1} ($\pm 30\%$) with C_2H_6
$k = 1.25 \times 10^{-9}$ cm^3 s^{-1} ($\pm 30\%$) with C_2D_6.
The three different rate constant measurements made at 298 K for this reaction (see Table 6) are in good agreement and very close to the Langevin rate (1.30×10^{-9} cm^3 s^{-1}), so this is our recommended value. As the Langevin rate is independent of temperature, we recommend the same value at 150 K. Nicolas et al. (2002) measured a lower value at $E_{CM} = 0.1$ eV for the $N_2^+ + C_2D_6$ reaction. It seems to indicate a small isotope effect, as expected for the Langevin rate. So we recommend the Langevin rates for both reactions.

Products
Recommended yields: $C_2H_5^+/C_2H_4^+/C_2H_3^+/C_2H_2^+/CH_3^+/CH_4^+$, 0.14/0.27/0.32/0.18/0.08/0.01.
For clarity, the neutrals associated with the ions are not indicated in this paragraph due to a too high number of product channels. However, they are reported in Table 17 which summarizes our recommended values for all ion–molecule reactions. Table 10 summarizes the product branching ratio data for the $N_2^+ + C_2H_6$ reaction.
The results of Praxmarer et al. (1998) and those of Nicolas (Nicolas 2002) are in good agreement for the products $C_2H_5^+$, $C_2H_4^+$, and $C_2H_3^+$, even though the experiments of Nicolas were not performed at thermal energy (~ 0.04 eV), but at $E_{CM} = 0.1$ eV. CH_3^+ was not detected in the experiments of Praxmarer et al. (1998) because of their lower sensitivity, and $C_2H_2^+$ was not detected in those of Nicolas because of a mass overlap between $C_2D_2^+$ and N_2^+. So the main product ions are the result of dissociative charge transfer, as expected. Both experiments suggest that the branching ratios do not depend much on collision energy and are not sensitive to an isotope effect when using C_2H_2 or C_2D_2. The $HCNH^+$ product detected by McEwan et al. (1998) is very unlikely to be produced directly by the reaction as for the N_2^+ with C_2H_4 reaction.

Table 9
Product Branching Ratio Data for the $N_2^+ + C_2H_4$ Reaction

$C_2H_3^+ + H + N_2$	$C_2H_2^+ + H_2 + N_2$	$HNC^+ + ?$	$HCNH^+ + ?$	$N_2H^+ + C_2H_3$	Reference
0.50	0.20	0.10	0.10	0.10	McEwan et al. 1998
0.64	0.36	...	...	...	Anicich et al. 2004
0.74 ± 0.02	0.26 ± 0.02	...	...	...	Gichuhi & Suits 2011[a]

Note. [a] Measured at $T = 45 \pm 5$ K.

Table 10
Product Branching Ratio Data for the $N_2^+ + C_2H_6$ Reaction

$C_2H_6^+$	$C_2H_5^+$	$C_2H_4^+$	$C_2H_3^+$	$C_2H_2^+$	CH_3^+	CH_4^+	HCNH$^+$	Reference
. . .	0.15	0.30	0.35	0.20	. . .	. . .	. . .	Praxmarer et al. 1998
Detected	Detected	Detected	Detected	. . .	. . .	. . .	Detected	McEwan et al. 1998
. . .	0.17	0.35	0.37	. . .	0.10	0.01	. . .	Nicolas 2002[a]

Note. [a] Measured at $E_{CM} = 0.1$ eV for the $N_2^+ + C_2D_6$ reaction.

In conclusion, we recommend branching ratio values which combine the results from the studies of Praxmarer et al. (1998) and Nicolas (2002), i.e., 0.14/0.27/0.32/0.18/0.08/0.01 for $C_2H_5^+/C_2H_4^+/C_2H_3^+/C_2H_2^+/CH_3^+/CH_4^+$, as well as for the reaction with deuterated ethane. In the experimental study of Nicolas (2002), cross sections were observed to be almost constant with the variation of the photon energy which produces N_2^+ reactant ions. This indicates that the reaction does not depend much on the vibrational energy of N_2^+ ions.

4.3.7. Reaction $N_2^+ + C_3H_8$

Kinetics
Recommended value at 300 K: $k = 1.30 \times 10^{-9}$ cm^3 s^{-1} ($\pm 30\%$)
There is only one experimental study of this reaction (Praxmarer et al. 1998). This value is close to the Langevin rate (1.42×10^{-9} cm^3 s^{-1}), so it will be about the same value at 150 K.
Products
Recommended yields $C_3H_5^+/C_2H_5^+/C_2H_4^+/C_2H_3^+$, 0.13/0.30/0.17/0.40.
For clarity, the neutrals associated with the ions are not indicated in this paragraph due to a too high number of product channels. However, they are reported in Table 17 which summarizes our recommended values for all ion–molecule reactions. Products of this reaction have been measured by only one group (Praxmarer et al. 1998). They have observed only dissociative charge transfer products with branching ratios $C_3H_5^+/C_2H_5^+/C_2H_4^+/C_2H_3^+$ equal to 0.13/0.30/0.17/0.40.
Further studies would be required to confirm this experimental study.

4.3.8. Dissociative Recombination Reaction: $N_2^+ + e$

Kinetics
Recommended value: k (N_2^+, $v = 0$) $= 2.2 \times 10^{-7}$ ($T_e/300$)$^{-0.39}$ cm^3 s^{-1} ($\pm 25\%$).
The dissociative recombination of N_2^+ has been extensively studied, both experimentally (Canosa et al. 1991; Cunningham & Hobson 1972; Geoghegan et al. 1991; Kasner 1967; Kella et al. 1996; Mahdavi et al. 1971; Mehr & Biondi 1969; Mul & McGowan 1979; Noren et al. 1989; Oddone et al. 1997; Peterson et al. 1998; Queffelec et al. 1985; Sheehan & St. Maurice 2004; Zipf 1980) and theoretically (Guberman 1991, 2003, 2012; Guberman et al. 1993). The interest in the reaction arises because of its involvement in Earth's atmosphere photochemistry (Fox & Dalgarno 1985; Torr & Torr 1979), and more generally in the chemistry of terrestrial planet ionospheres (Fox 1992, 1993; Fox et al. 1993). All the previous studies on the N_2^+ recombination process are summarized in the review papers on ion dissociative recombination reactions by Florescu-Mitchell & Mitchell (Florescu-Mitchell & Mitchell 2006) and more recently by Johnsen (2011). This recombination process is usually

very exothermic and therefore tends to be an important source of kinetically and internally excited fragments which contribute to heating. Furthermore, the energetic nascent products may have enough energy to escape the atmosphere. As a consequence, the dissociative recombination of N_2^+ for example, may contribute to $^{15}N/^{14}N$ isotope enrichment at Titan (Lammer et al. 2000).

From an experimental point of view, two classes of studies have been carried out: those measuring directly the rate constant k (Canosa et al. 1991; Cunningham & Hobson 1972; Geoghegan et al. 1991; Kasner 1967; Mahdavi et al. 1971; Mehr & Biondi 1969; Zipf 1980) and those which determined cross sections as a function of the relative energy of the N_2^+ ions and electrons (Kella et al. 1996; Mul & McGowan 1979; Noren et al. 1989; Oddone et al. 1997; Peterson et al. 1998; Sheehan & St. Maurice 2004). The latter were then able to derive a rate constant by averaging the cross section over a Maxwellian energy distribution. Three main aspects had to be considered: the electron temperature (T_e) dependence of k, the role of the vibrational state of the ions and finally the state of the nitrogen atoms formed through this process.

Two extensive determinations of the direct electron temperature dependence of k are available in the literature. In 1969, Mehr & Biondi (1969) studied the dissociative recombination of N_2^+ ($v = 0$) within the temperature range 300 K $\leqslant T_e \leqslant$ 5000 K using an afterglow apparatus, then in 1972, Cunningham & Hobson (1972) studied this process in a reduced temperature range, 700–2700 K, using a shock tube experiment. Both experiments were in good agreement with each other and led to a temperature dependence of k (T_e) $\sim T_e^{-n}$ (with n = 0.39 or 0.37, respectively). All other rate constant determinations were carried out at $T_e = 300$ K (Canosa et al. 1991; Geoghegan et al. 1991; Mahdavi et al. 1971) or within a reduced temperature range (Kasner 1967). Interestingly, more recent studies from Peterson et al. (1998) and Sheehan & St. Maurice (2004) who measured cross sections using merged beam techniques led to the same electron temperature dependence of k ($k(T_e) \sim T_e^{-0.39}$) for $T_e < 1200$ K (Sheehan & St. Maurice 2004), but for a population of ions in several vibrational states among which the ground state accounted for about 50%. This observation suggests that the vibrational excitation of the ions has probably little influence on the electron temperature dependence below 1200 K. It is worth indicating however that recent merged beam experiments demonstrated that the electron temperature dependence may be non-monotonic. Thus, the authors proposed a power law such as k (T_e) $\sim T_e^{-0.56}$ for 1200 K $\leqslant T_e \leqslant$ 4000 K indicating that vibrationally excited ions present a steeper temperature dependence within the range 1200–4000 K, which is of interest for the ionosphere of Titan at altitudes greater than 1600 km (Keller et al. 1992; Wahlund et al. 2005). No uncertainty is given with respect to the power-law exponent, but an error of 20% seems reasonable. A theoretical work by Guberman (2003) concluded that the electron temperature dependence is slightly different

Table 11
Product Branching Ratio Data for the $N_2^+ + e$ Recombination Reaction

N (^4S) + N (^4S)	N (^2D) + N (^4S)	N (^2P) + N (^4S)	N (^2D) + N (^2D)	Reference
. . .	. . .	. . .	0.9^a	Queffelec et al. 1985
. . .	0.46 ± 0.06	0.08 ± 0.06	0.46 ± 0.06	Kella et al. 1996
. . .	0.37 ± 0.08	0.11 ± 0.06	0.52 ± 0.04	Peterson et al. 1998
. . .	0.7	0.03	0.27	Guberman 2003

Note. [a] 0.9 corresponds to the total N (^2D) yield, without distinguishing between the N (^2D) + N (^4S) and N (^2D) + N (^2D) channels.

according to the temperature range. For the ground state $v = 0$, he proposed three different power laws: $T_e^{-0.20}$ for 200 K $\leqslant T_e \leqslant$ 400 K; $T_e^{-0.35}$ for 700 K $\leqslant T_e \leqslant$ 900 K; and $T_e^{-0.50}$ for 1800 $\leqslant T_e \leqslant$ 2000 K (Guberman 2003; S. L. Guberman 2006, private communication). His set of results however is in good agreement with the global single temperature dependence $T_e^{-0.39}$ found experimentally and recommended by Sheehan & St. Maurice (2004) for the $v = 0$ state. Very recently, Guberman (2012) revisited this reaction including for the first time in calculations both major and minor dissociative routes for the $v = 0$ state. He was able to derive from his calculation a rate coefficient for the N_2^+ ground vibrational level in the temperature range 100–3000 K which was well fitted by the following expression: $(2.2\pm^{+0.2}_{-0.4}) \times 10^{-7} \times (T_e/300)^{-0.40}$ cm^3 s^{-1}, in perfect agreement with the previous recommendation for the temperature dependence. Guberman, however, points out in his paper that an improved representation of k (N_2^+, $v = 0$) can be obtained by separating the temperature range into two sub-ranges: k (N_2^+, $v = 0$) = 2.2×10^{-7} ($T_e/300)^{-0.22}$ cm^3 s^{-1} for 100 K $\leqslant T_e \leqslant$ 600 K and k (N_2^+, $v = 0$) = 1.1×10^{-7} ($T_e/1800)^{-0.51}$ cm^3 s^{-1} for 600 K $\leqslant T_e \leqslant$ 3000 K.

Considering now the absolute rate constant k, analysis of the literature shows that several experiments (Canosa et al. 1991; Cunningham & Hobson 1972; Geoghegan et al. 1991; Mehr & Biondi 1969) dealt with N_2^+ ($v = 0$) ions. At 300 K, a rate constant of 2.2×10^{-7} cm^3 s^{-1} matches all these studies (Sheehan & St. Maurice 2004) with a typical 25% uncertainty. Therefore, it seems reasonable to recommend the following expression for the rate constant for the dissociative recombination of the ground state:

$$k(N_2^+, v = 0) = (2.2 \pm 0.5) \times 10^{-7}(T_e/300)^{-(0.39\pm0.08)} \text{ cm}^3 \text{ s}^{-1}.$$

Finally, it is also worth mentioning that the dissociative recombination of $^{15}N^{14}N^+$ ($v = 0$) has been found to be rather similar to that of $^{14}N_2^+$ ($v = 0$). The only available work is a quantum-theoretical calculation from Guberman (2003) who indicated that at room temperature the rate constant is 2.6×10^{-7} cm^3 s^{-1} and at 1000 K 1.6×10^{-7} cm^3 s^{-1}.

For ions in vibrational excited states, however, there are no experiments that allow clear conclusions, because ions are formed in a mixture of different vibrational states (Peterson et al. 1998; Sheehan & St. Maurice 2004; Zipf 1980). In 1980, Zipf (1980) made a study in which he identified the $v = 0$, 1, and 2 levels by laser-induced fluorescence and reported rate constants at 300 K, which were increasing with the excitation level. However, it was recognised later that his experiment reflected the effective recombination for N_2^+ ions with a vibrational temperature near 1500 K. Reanalysis of this work by Bates & Mitchell (1991) led to the qualitative conclusion that, at 300 K, the rate constant for the dissociative recombination of N_2^+ ($v = 1$, 2) should be much smaller than for the ground state. From a theoretical point of view, work is presently in progress (Guberman
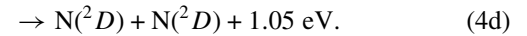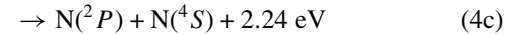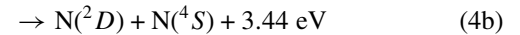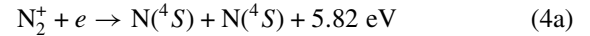
2012). It is worth mentioning however that in the ionosphere of Titan, vibrational excited N_2^+ ions should be quenched prior dissociative recombination by collisions with N_2. The rate constant for the N_2^+ (X, v) vibrational relaxation can be estimated to be efficient and equal to a few 10^{-10} cm^3 s^{-1} (see the above discussion about the N_2^+ reaction with N_2). Although it is about three orders of magnitude less than the dissociative recombination rate constant, the relative abundance of electrons with respect to N_2 in the ionosphere of Titan is too small ($\sim$1 ppm) to favor this latter process.

Products

Recommended yields: N (^4S)/N (^2D)/N (^2P), 0.25, 0.7, 0.05 ($\pm$25%.)

Table 11 summarizes the product branching ratio data for the $N_2^+ + e$ recombination reaction.

Determination of the products issued from the dissociative recombination of N_2^+ is also of great interest. Four channels are exothermically accessible:

$$N_2^+ + e \rightarrow N(^4S) + N(^4S) + 5.82 \text{ eV} \qquad (4a)$$

$$\rightarrow N(^2D) + N(^4S) + 3.44 \text{ eV} \qquad (4b)$$

$$\rightarrow N(^2P) + N(^4S) + 2.24 \text{ eV} \qquad (4c)$$

$$\rightarrow N(^2D) + N(^2D) + 1.05 \text{ eV}. \qquad (4d)$$

A fifth channel, namely N (^2D) + N (^2P) (endothermic by 0.13 eV), is only accessible for vibrational excited ions. From an experimental point of view, only three studies have been carried out (Kella et al. 1996; Peterson et al. 1998; Queffelec et al. 1985). The pioneering work by Queffelec et al. (1985) using a flowing afterglow apparatus with $T_e \sim$ 1000 K showed that the yield of N (^2D) was higher than 0.85 for $N_2^+(v = 0, 1)$ ions, whereas the yield of N (^4S) atoms was lower than 0.05, indicating that the main channel is clearly N (^2D) + N (^2D) ($\sim$0.90). More recent experiments using storage rings working at close to 0 eV relative collision energy confirmed that this channel was important but also indicated a significant branching ratio for the channel N (^4S) + N (^2D) which cannot be reconciled with the previous afterglow study. For ground state $^{15}N^{14}N^+$, Kella et al. (1996) found branching ratios of 0.46 ± 0.06, 0.08 ± 0.06, and 0.46 ± 0.06 for channels (4b), (4c), and (4d), respectively, whereas Peterson et al. (1998) indicated values of 0.37 ± 0.08, 0.11 ± 0.06, and 0.52 ± 0.04 for $^{14}N_2^+$ ions. In both experiments, channel (4a) was not observed in agreement with a previous theoretical work by Guberman (1991). However, the agreement between theory and experiments remains poor. The more recent study by Guberman (2003) indicated branching ratios of 0.7, 0.03, and 0.27 for channels (4b), (4c), and (4d), respectively. This topic deserves further study to resolve the present discrepancies. However,

experiments clearly indicate that channel leading to two N (^2D) atoms accounts for at least 50% of the whole process. With the current state of knowledge, we recommend the following percentages for the different electronic states of N atoms: 0.7/0.05/0.25 for N (^2D)/N (^2P)/N (^4S).

It is now interesting to compare the loss rate of N_2^+ arising from the dissociative recombination process with that from other possible destruction routes. Neutral molecular nitrogen, methane and to a less extent H_2, are obviously the main potential competitors because of their predominance in the ionosphere of Titan. However, the only possible loss of N_2^+ by the reaction with N_2 would be via an association reaction (Rowe et al. 1984) which will be much too slow considering the small nitrogen concentration ($\sim 10^9$ cm^{-3} at ~ 1200 km altitude; Waite et al. 2005). On the other hand, the reactions at room temperature of N_2^+ with CH_4 and H_2 have been found to be 1.14×10^{-9} and 1.7×10^{-9} cm^3 s^{-1}, respectively (see above). These values are close to the Langevin rate constant and therefore it is expected that they will not change significantly with temperature. Although being two orders of magnitude less efficient than the dissociative recombination of N_2^+, the concentrations of CH_4 and H_2 are much higher than the electron density. At ~ 1200 km for example the abundance of methane (Waite et al. 2005) is about 2×10^7 cm^{-3}, that of H_2 (Waite et al. 2005) is 4×10^6 cm^{-3}, whereas the electron density (Wahlund et al. 2005) is typically 2×10^3 cm^{-3}. Considering a rate constant k ($N_2^+ + e$) $= 1.4 \times 10^{-7}$ cm^3 s^{-1} at $T_e = 1000$ K corresponding to a typical electron temperature at this altitude, the loss rate for N_2^+ through the reaction with methane is about 70 times greater than through dissociative recombination process, and the one resulting from the reaction with H_2 is 30 times greater. As a conclusion, it appears that the dissociative recombination of N_2^+ is a minor destruction route for this ion, at the 10^{-2} level, although it cannot completely be disregarded.

5. N$^+$ SINGLY CHARGED IONS

5.1. Production

In ionospheres, N$^+$ ions are mainly produced by dissociative ionization of N_2. The N_2 dissociative ionization threshold is at 24.29 eV and the different dissociation onsets are given in the Table 1. The only long-lived metastable atomic ion state which has been observed to arise from photon or electron impact on N_2 is the N$^+$ (^1D) state, which lies in 1.9 eV above the N$^+$ (^3P) ground state (see Table 1).

Samson et al. (1987) measured the N$^+$ production cross section by photo-dissociative ionization of N_2, from threshold up to 107 eV photon energy. The maximum cross section is $\sim 3.3 \times 10^{-18}$ cm^2 at about 47 eV photon energy. Above the double ionization threshold at 42.88 eV, there is a small contribution from N_2^{++} doubly charged ions, which have the same mass-to-charge ratio (m/z) as N$^+$ fragment ions. Tian & Vidal (1998) measured the N_2 electron impact ionization cross sections to form N_2^+, N$^+$, and N_2^{++} ions from threshold up to 600 eV electron energy. They found that the N$^+$ production cross section reaches a maximum value of 6.6×10^{-17} cm^2 at 120 eV electron energy (see the review from Itikawa 2006). The N_2 dissociative ionization threshold is at 24.29 eV, in the N_2^+ (C $^2\Sigma_u^+$) inner valence state region. As dissociative ionization occurs only in the region of inner valence states (C, F, E, G, and H bands), it is not a very efficient process and it only represents less than 5% of the total ionization of N_2 for photon energies up to 30 eV. For photons energies higher than 44.5 eV, N$^+$ ions are also produced

by dissociation of N_2^{++} doubly charged ions. Above 80 eV photon energy, the contribution of multiple-ionization processes to the total ionization is about 4% (Wehlitz 2010). By electron impact, this contribution reaches a maximum of 6% for 150 eV electron energy (Tian & Vidal 1998).

Most N$^+$ ions produced by the N_2^+ dissociation are in the ^3P ground state. Detailed photoionization experiments showed that in a narrow N_2^+ internal energy range, 60% of N$^+$ ions are in the long-lived ^1D excited state. But under ionospheric conditions, it was estimated that globally about 15% of N$^+$ ions are in the ^1D state and 85% are in the ground ^3P state (Nicolas et al. 2003a). No other excited states have been observed so far to be populated by dissociative photoionization of N_2 (Nicolas et al. 2003a), but it cannot be totally excluded that some N$^+$ (^1S) metastable state is produced at high internal energy. Dissociative ionization of N_2 produces N$^+$ ions which have some kinetic energy. The $N_2^+ \rightarrow$ N$^+ +$ N process releases a mean value of about 1 eV (Nicolas et al. 2003a), i.e., N$^+$ ions with about 0.5 eV kinetic energy. The $N_2^{++} \rightarrow$ N$^+ +$ N$^+$ process releases much more kinetic energy: due to the Coulomb repulsion, the charge separation releases a large amount of kinetic energy, shared equally between the two N$^+$ partners. This kinetic energy is important as it can potentially modify some reaction rate constants, as well as participate in the process of atmospheric escape. The kinetic energy released in the dissociation has been measured by Brehm & De Frenes (1978) for electron impact and by Besnard et al. (Besnard et al. 1988) for photoionization. The distribution of kinetic energy released can be described by a broad Gaussian, centered at 8 eV, with FWHM of 6 eV. Thermodynamically, Besnard et al. (1988) showed that the dissociation leads systematically to atomic ions in their ground state, which puts a lower limit of 4.8 eV on the kinetic energy release.

5.2. Lifetimes and Quenching

Two excited states of N$^+$ ions are metastable, the N$^+(^1D)$ and N$^+(^1S)$ states, which have a lifetime of 258 s and 31.5 s, respectively (Wiese & Fuhr 2007). The quenching of N$^+$ (^1D) metastable states by collisions with N_2 is negligible due to its spin forbidden nature (Freysinger et al. 1994). So when N$^+$ (^1D) is formed in ionospheres, these species will relax by reactions with other gases.

The kinetic energy of N$^+$ ions produced by dissociative ionization of N_2 is efficiently relaxed by collisions with N_2 (Glosik et al. 2000). However, the efficiency decreases with the relative kinetic energy. From the work of Glosik et al. (2000), we can estimate the kinetic energy relaxation for the two populations of N$^+$ ions. For N$^+$ coming from N_2^+ dissociation (~ 0.5 eV kinetic energy), each collision leads to a loss of $50 \pm 10\%$ of their kinetic energy. For the more energetic N$^+$ ions coming from N_2^{++} dissociation, this loss is of $15 \pm 7\%$ of their kinetic energy. So, for example, at the peak of Titan's ionosphere, where there are about 50 collisions on average with N_2 before N$^+$ ions collide with another gas, the kinetic energy of the N$^+$ ions from single ionization will be relaxed when reacting with other gases but N_2. This relaxation will not be complete for N$^+$ ions coming from N_2^{++} dissociation, but these are minor ions compared to the N$^+$ ions coming from N_2^+ dissociation. It is therefore a rather good approximation to take rate constants at thermal energy in the models of Titan's ionosphere. However, a rigorous treatment should precisely take into account the relaxation of N$^+$ kinetic energy as a function of altitude for N$^+$ ions coming from both N_2^+ and N_2^{++} dissociation.

5.3. Reactions

Before reviewing the different reactions of N^+ atoms, let us note that experimental studies had to face the problem of contamination of the N^+ reactant ions by the presence of some N_2^{++} doubly charged molecular ions, which have the same m/z as the N^+ atomic ions and which are very reactive. So the results of many older studies had to be reviewed and corrected at a later date.

5.3.1. Reaction $N^+ + N_2$

Kinetics
Recommended value at 300 K: $k = 2.1 \times 10^{-10}$ cm^3 s^{-1} ($\pm 25\%$)
When working with isotopically labeled reagents the following three reactive channels can be distinguished in a mass spectrometer:

Isotope exchange reaction $^{15}N^+ + {}^{14}N_2 \rightarrow {}^{14}N^+$ (m/z 14) $+ {}^{15}N^{14}N$
Atom abstraction $^{15}N^+ + {}^{14}N_2 \rightarrow {}^{14}N + {}^{15}N^{14}N^+$ (m/z 29)
Electron transfer $^{15}N^+ + {}^{14}N_2 \rightarrow {}^{15}N + {}^{14}N_2^+$ (m/z 28).

All published rate constant data for this reaction are shown in Table 6. They correspond to the isotope exchange $N^+ + N_2$ reaction ($^{15}N^+ + {}^{14}N_2$ or $^{14}N^+ + {}^{15}N_2$ reaction giving $^{14}N^+ + {}^{15}N^{14}N$ or $^{15}N^+ + {}^{15}N^{14}N$ products, respectively). At thermal energies (300 K) the only energetically allowed reaction channel is the isotope exchange process producing $^{14}N^+$ because the atom abstraction and electron transfer channels, giving $^{15}N^{14}N^+$ and $^{14}N_2^+$, respectively, are endothermic by 1.043 eV. Therefore, the rate constant at 300 K only concerns the isotope exchange process. The recommended rate constant value is the mean value of the different measurements (2.1×10^{-10} cm^3 s^{-1}). It is significantly lower than the Langevin rate (1.02×10^{-9} cm^3 s^{-1}). In guided ion beam (GIB) experiments, Freysinger et al. (1994) and Glosik et al. (2000) measured the kinetic energy dependence of this cross section via experiments using isotopically labeled reactants.
Products at 300 K (and 150 K): $^{14}N^+ + {}^{14,15}N_2$ isotope exchange channel
Since the isotope exchange channel does not change the species involved in the reaction, one might argue that it does not eventually influence the ion composition. This is not the case as, reactive collision with molecular nitrogen may generate cold N^+ product ions, as it has been shown that most of the kinetic energy of the incoming $^{15}N^+$ is converted into internal excitation of the neutral N_2 product (Glosik et al. 2000). According to Freysinger et al. (1994), the rate constant of this reaction does not vary with temperature.
Products at $E_{CM} > 2.7$ eV: $N_2^+ + N$ Electron Transfer/ Atom Abstraction Channel
These products, which result from both an electron transfer process and an atom abstraction process, can be distinguished by using suitable isotopic labeling (Fehsenfeld et al. 1974; Freysinger et al. 1994; Maier & Murad 1971; Mark & Gerlich 1996). For the scope of the present review, we treat the overall N_2^+ production as a unique reaction. In the oldest studies (Maier & Murad 1971; Phelps 1991), there were contributions from N_2^{++} and N^+ metastable states in the N^+ reactant ions, so the apparent threshold was not due to N^+ (^3P) ground state ions. According to the N^+ production mode, Freysinger et al. (1994) and Mark & Gerlich (1996) could measure the reaction of pure

N^+ (^3P) state ions; details are discussed in these papers. GIB investigations have shown that the reaction has an apparent threshold of 2.7 ± 0.2 eV, well above the thermochemical onset of 1.043 eV (Freysinger et al. 1994; Mark & Gerlich 1996). Except very close to threshold, the cross section σ varies with collision energy according to the following law:

$$\sigma(\text{Å}^2) = 0.9(E - 3.1)^2/E,$$

where E is the collision energy in eV (Mark & Gerlich 1996).
According to Freysinger et al. (1994) and Mark & Gerlich (1996), this reaction produces mainly N_2^+ (X) + N (^2D) above 3.43 eV, the thermochemical onset for the production of the N (^2D) metastable state in this reaction. The effective threshold of the charge transfer reaction is probably too large to make this channel significant under the conditions of Titan's ionosphere. Let us note that this reaction is exothermic by 0.9 eV when N^+ reactant ions are in the N^+ (^1D) metastable state, but the first spin-allowed channel giving N (^2D) + N_2^+ (X) is endothermic by 1.53 eV.

5.3.2. Reaction $N^+ + H_2$

Kinetics
Recommended values at 300 K: $k = 3.8 \times 10^{-10}$ cm^3 s^{-1} ($\pm 20\%$) for H$_2$
$k = 3.1 \times 10^{-10}$ cm^3 s^{-1} ($\pm 20\%$) for HD
$k = 1.2 \times 10^{-10}$ cm^3 s^{-1} ($\pm 20\%$) for D$_2$.
This reaction has been extensively studied both experimentally (see Table 6) and theoretically. It is almost a case study, as its reactive channel giving $NH^+ + H$ is very slightly endothermic by 17 meV (Gerlich 1989; Tosi et al. 1994) and by 29 meV for the reaction of $N^+ + D_2$ giving $ND^+ + D$ (Tosi et al. 1994). As a consequence, this reaction is very sensitive to the temperature (or collision energy) and to the rotational temperature of H$_2$. This sensitivity is because the activation energy can be overcome at 300 K, but not at very low temperatures and for para-H$_2$; this last fact is important, for example, in some regions of the interstellar medium. However in the temperature range of Titan's ionosphere ($\sim$150–200 K), the reaction is still efficient (Marquette et al. 1988). The charge transfer channel producing $H_2^+ + N$ is endothermic by 0.89 eV and is only energetically possible for the reaction of N^+ (^1D) metastable state, which lies 1.9 eV above the ground state; however, the reaction is spin-forbidden and has never been unambiguously observed. Therefore, the rate constant values in Table 6, which summarizes the rate constant data for the $N^+ + H_2$ reaction, are for the H transfer reaction producing $NH^+ + H$.
The recommended values for the rate constant at 300 K have been estimated from the more recent experimental results (Adams & Smith 1985; Ervin & Armentrout 1987) for the reactions of N^+ with H$_2$, HD and D$_2$. Experimental values are in very good agreement with theoretical calculations (Ge et al. 2006; Gerlich 1989), within experimental uncertainties.
This reaction has been investigated by a variety of techniques. The most detailed measurements (Gerlich 1993; Marquette et al. 1988; Tosi et al. 1994) have shown that the reaction is strongly influenced by the internal energy of the reactants: kinetic and rotational energies are equivalent in promoting the reaction, while the fine structure energy seems inefficient for surmounting the reaction barrier. These findings explain why the interpretation of low energy measurements is quite difficult, without a full control of the internal states.

Several authors measured the rate constant at very low temperatures (see Gerlich 1993; Luine & Dunn 1985; Marquette et al. 1988 and references therein). In the 40–100 K range, Gerlich (1993) could fit the data with the expression $k = 2 \times 10^{-10} \exp(-41/T)$. Below 40 K, the variation becomes $k = 1.1 \times 10^{-10} \exp(-26/T)$. At 15 K and for para-$H_2$, when the available energy is not sufficient to overcome the reaction barrier, the rate constant decreases by several orders of magnitude, being equal to 5×10^{-13} cm^3 s^{-1} (Gerlich 1993). The reactions of N^+ with H_2, HD, and D_2 have been studied as a function of translational energy and hydrogen temperature in a guided ion beam mass spectrometer (Sunderlin & Armentrout 1994). These authors found that the cross sections depend significantly upon the rotational temperature of H_2 for collision energies below 0.3 e V. The branching ratio for formation of NH^+ and ND^+ in the reaction with HD at 0.02 eV is 1:3 at 305 K and 1:13 at 105 K. These effects are consistent with rotational energy driving the reaction. Effects due to the presence of the N^+ (^1D) metastable state have been observed in a previous experiment of the same group (Ervin & Armentrout 1987). However, since the experiment is not state selected, it was only possible to estimate qualitatively the variation of the rate constant, which might be 50% larger than for ground-state N^+ ions.

5.3.3. Reaction N^+ (^3P) + CH_4

For this reaction, we will review separately the reaction of N^+ (^3P) ground state and the reaction of N^+ (^1D) metastable state, which lies 1.9 eV above the ground state.

5.3.3.1. Reaction N^+ (^3P) + CH_4

Kinetics:
Recommended value at 300 K: $k = 1.15 \times 10^{-9}$ ($\pm 20\%$) cm^3 s^{-1}
We recommend for this reaction the mean value of the experimental values measured at 300 K, i.e., 1.15×10^{-9} cm^3 s^{-1} ($\pm 20\%$), as in the compilation of McEwan & Anicich (2007) (see Table 6). This value matches the Langevin rate (1.38×10^{-9} cm^3 s^{-1}) within experimental uncertainties. The rate constant for the reaction with CD_4 has been measured by Alcaraz et al. (2004) to be, within experimental uncertainties, equal to the Langevin rate (1.30×10^{-9} cm^3 s^{-1}, calculated with the polarization of CD_4 which is lower by 0.034 than the one from CH_4 according to Bell 1942 and Wong et al. 1991), so it is our recommended value.

Rowe et al. (1985) studied this reaction at a low temperature, 8 K, and found a value of the rate constant slightly lower than the value at 300 K. Similarly, Alcaraz et al. (2004) studied the reaction at collision energies higher than 0.2 eV (i.e., $T >$ 1500 K) and found a higher value for the rate constant. These studies seem to confirm an increase of the rate constant with temperature or with collision energy. So we recommend a rate constant value of 1.0×10^{-9} cm^3 s^{-1} at 150 K. In Titan's ionosphere, the N^+ ions are thermalized by collisions with N_2, so the value at 150 K should be used.
Products:
Recommended yields: (CH_3^+ + NH)/(CH_4^+ + N)/ ($HCNH^+$ + H_2)/(HCN^+ + H_2 + H), 0.50/0.05/0.35/0.10.
Table 12 summarizes the product branching ratio data for the N^+ (^3P) + CH_4 reaction.
The values of the branching ratios determined by McEwan et al. (1998) are in agreement with the previous studies. The measurements by Alcaraz et al. (2004), at higher collision energy ($E_{CM} = 0.36$ eV) and with isotopic labeling, give similar results,

except for slight differences for CH_4^+ and HCN^+. This study indicates that there is no major isotopic effect for this reaction, so the branching ratios are the same for the reactions with CH_4 and CD_4. A joint experimental and theoretical study showed, in the case of the reaction with CD_4, that both $DCND^+$ and CD_2N^+ isomers can be formed (Zabka et al. 2010). The most recent determination of reaction ion products by Anicich et al. (2004) gives different branching ratios, especially for CH_3^+. Note that their measurements were performed under higher pressure conditions in order to detect the products of multiple successive reactions and not only the primary products. The uncertainty on this procedure being more significant, these authors recommended later (McEwan & Anicich 2007) branching ratios close to those measured by McEwan et al. (1998) at low collision energy, i.e., CH_3^+/CH_4^+/$HCNH^+$/HCN^+, 0.50/0.05/0.36/0.10. These are also our recommended values, slightly adjusted to have a sum equal to 1.

At higher collision energy, it has been shown that the formation of the products CH_3^+ and CH_4^+ was substantially favored at $E_{CM} = 0.05$–0.53 eV (Dheandhanoo et al. 1984), and at $E_{CM} = 0.36$–2 eV (Alcaraz et al. 2004). At 2 eV, the branching ratios change to 0.76/0.18/0.06/0.0. This can easily be explained, as CH_3^+ and CH_4^+ products resulting from charge transfer should be favored when collision energy is increased, compared to the $HCNH^+$ and HCN^+ products resulting from a collision complex with rearrangement of the molecular bonding. In contrary, with thermalized N^+ ions at 150 K in Titan's ionosphere, one can expect, as suggested by Dheandhanoo et al. (1984), that the reaction N^+ + CH_4 would favor the products HCN^+ and $HCNH^+$. Up to now, no experiment at low temperature has been performed to confirm this tendency.

5.3.3.2. Reaction N^+ (^1D) + CH_4

Kinetics:
Recommended value at 300 K: $k = 1.15 \times 10^{-9}$ cm^3 s^{-1} ($\pm 20\%$)
Tichy et al. (1979) and Alcaraz et al. (2004) measured the rate constant of the N^+ (^1D) + CH_4 reaction (see Table 6). Both studies showed that the rate constant values are similar to their respective values found for the reaction of the N^+ (^3P) ground state and close to the Langevin rate within experimental uncertainties. So it seems that the rate constant for this reaction does not change with the electronic excitation of N^+ and we recommend the same rate constant value as for the N^+ (^3P) state. Note that in the study of Alcaraz et al. (2004), the metastable state of N^+ (^1D) is strictly controlled and corresponds to 100% of the N^+ reactant ions. In the case of Tichy et al. (1979), the quantity of this metastable state (about 30%) is not directly measured, but only deduced. Moreover, the metastable state is not clearly identified, Tichy et al. (1979) suggesting a possible contribution from N^+ (^1S).
Products:
Recommended yields: (CH_3^+ + NH)/(CH_4^+ + N)/ ($HCNH^+$ + H_2)/(HCN^+ + H_2 + H), 0.09/0.40/0.33/0.18.
As previously noted, a pure sample of the N^+(^1D) metastable state being generated and identified in the study of Alcaraz et al. (2004), we recommend the product branching ratios from that work (see Table 12).

In comparison with the reactivity of N^+ (^3P), the ratio (CD_3^+ + CD_4^+)/(DCN^+ + $DCND^+$) decreases from 0.62/0.38 to 0.49/0.51, corresponding to a slight increase in the yield of the nitrogen-containing compounds. The strongest effect is a complete inversion of the ratio CD_3^+/CD_4^+, from 4.4/1.0 to

Table 12
Product Branching Ratio Data for the N^+ (^3P) + CH_4 Reaction

Reaction	CH_3^+ + NH	CH_4^+ + N	$HCNH^+$ + H_2	HCN^+ + H_2 + H	Reference
N^+ (^3P) + CH_4	0.53	0.04	0.32	0.10	(Anicich et al. 1977)
N^+ (^3P) + CH_4	0.42	0.06	0.38	0.14	(Tichy et al. 1979)
N^+ (^3P) + CH_4	0.51	0.03	0.40	0.06	(Adams et al. 1980)
N^+ (^3P) + CH_4	0.52	0.06	0.33	0.09	(Dheandhanoo et al. 1984)
N^+ (^3P) + CH_4	0.50	0.05	0.36	0.10	(Anicich 1993) (compilation)
N^+ (^3P) + CH_4	0.53	0.05	0.32	0.10	(McEwan et al. 1998)
N^+ (^3P) + CH_4	0.38	0.03	0.44	0.15	(Anicich et al. 2004)
$^{15}N^+$ (^3P) + CD_4*	0.51	0.11	0.29	0.09	(Alcaraz et al. 2004)
N^+ (^3P) + CH_4	0.50	0.05	0.36	0.10	(McEwan & Anicich 2007) (compilation)
N^+ (^1D) + CH_4	0.20	0.10	0.40	0.30	(Tichy et al. 1979)
$^{15}N^+$ (^1D) + CD_4*	0.09	0.40	0.33	0.18	(Alcaraz et al. 2004)

Note. * Measured at E_{CM} = 0.36 eV.

1.0/4.7. The present Titan ionospheric models do not take into account the N^+ (^1D) metastable state. Such an inversion in the reaction branching ratios could affect some model predictions and it would be worthwhile to evaluate precisely this effect.

5.3.4. Reaction N^+ (^3P) + C_2H_2

Kinetics:
Recommended value at 300 K: $k = 1.42 \times 10^{-9}$ ($\pm 20\%$) cm^3 s^{-1}

This rate constant value measured in two different studies (Anicich et al. 2004; McEwan et al. 1998; see Table 6) is very close to the Langevin rate (1.42×10^{-9} cm^3 s^{-1}), as for the reaction of N^+ with methane, so the recommended value is the Langevin rate. By analogy with the reactions with methane and ethylene (see below), it is reasonable to estimate that the reaction of N^+ (^1D) occurs also at the Langevin rate and are the same at 300 K and 150 K.

Products:
Recommended yields: ($C_2H_2^+$ + N)/(CNC^+ + H_2)/ ($CHCN^+$ + H), 0.70/0.15/0.15.

Table 13 summarizes the product branching ratio data for the N^+ (^3P) + C_2H_2 reaction.

For this reaction, the same authors made measurements of the branching ratios using two different techniques, the Ion cyclotron resonance (ICR) technique (McEwan et al. 1998) and later the selected ion flow drift tube (SIFT) technique (Anicich et al. 2004). Anicich et al. (2004) identified a new product ion, $HCNH^+$, but with the high pressure conditions of this experiment, there are more secondary reactions and therefore larger uncertainties on the resulting experimental outputs. As for the reaction of N^+ with methane (see above), McEwan et al. (McEwan & Anicich 2007) recommended later their oldest product yields, which are also our recommended values. At 150 K, the yield of $C_2H_2^+$ ions coming from charge transfer might be a little smaller than for the other products coming from a chemical reaction which require a long-lived complex intermediate, but it should be checked. No study exists for the reaction of N^+ (^1D) metastable state with acetylene, but it is reasonable to estimate that the charge transfer products dominate, as for the reactions of N^+ (^1D) with methane and ethylene.

5.3.5. Reaction N^+ + C_2H_4

For this reaction, we will separately review the reaction of the N^+ (^3P) ground state and the reaction of the N^+ (^1D) metastable state.

5.3.5.1. Reaction N^+ (^3P) + C_2H_4

Kinetics:
Recommended values at 300 K: $k = 1.58 \times 10^{-9}$ cm^3 s^{-1} ($\pm 20\%$) for C_2H_4
$k = 1.55 \times 10^{-9}$ cm^3 s^{-1} ($\pm 20\%$) for C_2D_4.

The experimental determinations of Rakshit (1980), Smith & Adams (1980), and McEwan et al. (1998) are in relatively good agreement, given their uncertainties (see Table 6). The most recent determination of Anicich et al. (2004) suggests a lower value of the rate constant. This discrepancy with the previous works can be explained by the different experimental conditions used in this later study, as for the reactions of N^+ with methane and acetylene. This value of k is equal to the Langevin value (1.58×10^{-9} cm^3 s^{-1}) within uncertainties, therefore most probably independent of temperature as for the reactions of N^+ with methane and acetylene. Note that Smith & Adams (1980) did not observe any significant isotope effect for this reaction. So the recommended values are the Langevin rates for both reactions.

Products:
Recommended yields: $C_2H_2^+$/$C_2H_3^+$/$C_2H_4^+$/HCN^+/$HCNH^+$/ $CHCN^+$/CH_2CN^+, 0.12/0.32/0.38/0.02/0.10/0.01/0.05.

Table 14 summarizes the product branching ratio data for the N^+ + C_2H_4 reaction. For clarity, the neutrals associated with the ions are not indicated in Table 14 due to a too high number of product channels. However, they are reported in Table 17 which summarizes our recommended values for all ion–molecule reactions.

All studies give product branching ratios which are in fair agreement for the N^+ (^3P) + C_2H_4 reaction, except the study of Rakshit (1980), which is surprising. No details are given on the instrument mass resolution in this study and one might suspect that the $C_2H_4^+$ production seen by Rakshit (1980) is in fact the sum of the three species ($C_2H_4^+$, $C_2H_3^+$, and $C_2H_2^+$) observed by the other groups (sum about 70%–87% according to the above studies). Moreover, the adduct CH_3CNH^+ is

Table 13
Product Branching Ratio Data for the N^+ (^3P) + C_2H_2 Reaction

$C_2H_2^+$ + N	$HCNH^+$ + C	CNC^+ + H_2	$CHCN^+$ + H	Reference
0.70	. . .	0.15	0.15	McEwan et al. 1998
0.65	0.07	0.06	0.22	Anicich et al. 2004
0.70	. . .	0.15	0.15	McEwan & Ancich 2007 (compilation)

Table 14
Product Branching Ratio Data for the N^+ (^3P) + C_2H_4 Reaction

Reaction	$C_2H_2^+$	$C_2H_3^+$	$C_2H_4^+$	HCN^+	$HCNH^+$	$CHCN^+$	CH_2CN^+	CH_3CNH^+	Reference
N^+ (^3P) + C_2H_4	0.10	0.30	0.25	0.15	0.10		0.10	. . .	(Smith & Adams 1980)
N^+ (^3P) + C_2H_4	. . .	. . .	0.76	. . .	. . .	. . .	. . .	0.24	(Rakshit 1980)
N^+ (^3P) + C_2H_4	0.10	0.25	0.35	0.10	0.15	0.05	. . .	. . .	(McEwan et al. 1998)
N^+ (^3P) + C_2H_4	0.13	0.44	0.30	. . .	. . .	0.04	0.10	. . .	(Anicich et al. 2004)
N^+ (^3P) + C_2H_4	0.12	0.32	0.38	0.02	0.10	0.01	0.05	. . .	(Alcaraz et al., unpublished)*
N^+ (^3P) + C_2H_4	0.10	0.25	0.35	0.10	0.15	0.05	. . .	. . .	(McEwan & Anicich 2007) (compilation)
N^+ (^1D) + C_2H_4	. . .	. . .	0.76	. . .	. . .	. . .	. . .	0.24	(Rakshit 1980)
N^+ (^1D) + C_2H_4	0.26	0.22	0.46	. . .	0.06**	. . .	. . .	. . .	Alcaraz et al., unpublished)*

Notes.
* Extrapolation at low collision energy of cross section measurements for $^{15}N^+$+C_2D_4.
** Estimated yield for the sum of N-bearing products (HCN^+, $HCNH^+$, $CHCN^+$ and CH_2CN^+).

a priori unstable under single collision conditions. C. Alcaraz et al. (unpublished) used ^{15}N and D isotopic labeling in order to avoid mass overlap, as in the studies of McEwan et al. (1998) and of Smith & Adams (1980). The yields reported by Anicich et al. (2004) are questionable for the same reasons already mentioned above. The studies of McEwan et al. (1998) and of Smith & Adams (1980) deduced branching ratios by analyzing both reactions with C_2H_4 and C_2D_4, assuming no isotopic effect. Except from the study of Rakshit (1980), all studies are in good agreement for the branching ratios of the three main species $C_2H_2^+$, $C_2H_3^+$, and $C_2H_4^+$ within uncertainties. Disagreements are however observed for the N-bearing species HCN^+, $HCNH^+$, $CHCN^+$, and CH_2CN^+. HCN^+ and $HCNH^+$ are not observed in the study of Anicich et al. (2004), because of the mass overlap with the main products $C_2H_3^+$ and $C_2H_4^+$. McEwan et al. (1998) do not observe CH_2CN^+, whereas Anicich et al. (2004), Smith & Adams (1980), and C. Alcaraz et al. (unpublished) revealed branching ratios between 0.05 and 0.10 for this product. Alcaraz et al. only observed 1% of HCN^+ versus 10%–15% in the cases of Smith & Adams (1980) and of McEwan et al. (1998). These differences are significant and hard to explain. Only the work of C. Alcaraz et al. (unpublished) allows a direct measurement of the branching ratios, thanks to complete isotopic labeling. We therefore recommend this determination of the branching ratios for the N-bearing species. For the reaction with deuterated ethylene C_2D_4, it seems reasonable to estimate that the yields are the same as for the reaction with C_2H_4.

Other branching ratio values should however be employed if the N^+ ions pertain some kinetic energy. Indeed, C. Alcaraz et al. (unpublished) also measured the variation of the reaction cross sections with collision energy between 0.2 and 6.4 eV in the center-of-mass frame. The $HCNH^+$, $CHCN^+$, and CH_2CN^+ production cross sections strongly decrease with collision energy, and the $C_2H_2^+$ and $C_2H_4^+$ cross sections slightly increase. A complex evolution of the cross section for form-

ing the $C_2H_3^+$ product has been observed: an important decrease between 0.05 and 0.3 eV collision energy, followed by an increase, similar to the decrease of $C_2H_2^+$ and $C_2H_4^+$. These observations seem to confirm a charge transfer mechanism forming $C_2H_2^+$ and $C_2H_4^+$, and a long lifetime complex involved in the formation of $HCNH^+$, $CHCN^+$, and CH_2CN^+. The formation of $C_2H_3^+$ could be explained by the competition of two formation routes: the pathway $C_2H_3^+$ + NH at low collision energy, and the dissociative charge transfer $C_2H_3^+$ + H + N at high collision energy. The collision energy dependence of the cross section for forming HCN^+ presents a different pattern from the other N-bearing species: a very minor product at low collision energy, it becomes the most important N-bearing species at high energy. From the cross sections, one can deduce the corresponding branching ratios. C. Alcaraz et al. (unpublished) thus observed an evolution of the branching ratios with the collision energy: $C_2H_4^+/C_2H_3^+/C_2H_2^+/HCN^+/HCNH^+/CHCN^+/CH_2CN^+$ from 0.38/0.32/0.12/0.02/0.10/0.01/0.05 to 0.53/0.23/0.17/0.02/0.03/0.01/0.01 when the collision energy increases from 0.2 to 6.4 eV in the center-of-mass frame. The most noticeable effect concerns the relative increase of $C_2H_4^+$ production.

5.3.5.2. Reaction N^+ (^1D) + C_2H_4

Kinetics
Recommended value at 300 K: $k = 1.58 \times 10^{-9}$ cm^3 s^{-1} ($\pm$30%)

Rakshit (1980) studied the reactivity of a mixture of N^+ ground and metastable states (see Table 6). The measured value for the rate constant is very surprising (3.80×10^{-9} cm^3 s^{-1}), as it is about twice the Langevin value (1.58×10^{-9} cm^3 s^{-1}). C. Alcaraz et al. (unpublished) performed preliminary experiments for this reaction, generating reactant ions involving just the metastable N^+ (^1D) state. Their measured rate constant is equal to the Langevin rate within experimental uncertainties, as for

the N$^+$ (^3P) ground state reaction with ethylene. Therefore this is our recommended rate constant value.

Products

Recommended yields: C$_2$H$_2^+$/C$_2$H$_3^+$/C$_2$H$_4^+$/(HCN$^+$ + HCNH$^+$ + CHCN$^+$ + CH$_2$CN$^+$), 0.26/0.22/0.46/0.06.

Table 14 shows the product branching ratio data for the N$^+$ (^1D) + C$_2$H$_4$ reaction.

The branching ratios found by Rakshit (1980) are the same as for the ground-state reactivity and have to be considered with care for the same reason as described above. In contrast, the preliminary results of C. Alcaraz et al. (unpublished) show a strong variation of the product branching ratios between the N$^+$ (^3P) and N$^+$ (^1D) reactions. These experiments reveal a significantly higher yield of C$_2$H$_4^+$, C$_2$H$_3^+$, and C$_2$H$_2^+$ product ions, than for the N$^+$ (^3P) ground-state reaction (+20%, −30%, and +120%, respectively) and much weaker signals from N-bearing species. These observations indicate that the charge transfer process is most probably the dominant reaction mechanism for the N$^+$ (^1D) state reaction with C$_2$H$_4$. With the present knowledge, we recommend the product yields estimated from the measurements of Alcaraz et al., but further studies are necessary to precise these values.

5.3.6. Reaction N$^+$ (^3P) + C$_2$H$_6$

Kinetics

Estimated value at 300 K: $k = 1.60 \times 10^{-9}$ cm^3 s^{-1}

The kinetics of this reaction has never been measured, to our knowledge. However, the rate constants for the reactions of N$^+$ with methane, ethylene, and acetylene are all very close to the Langevin rate. By analogy, the rate constant value is therefore estimated to be equal to the Langevin rate, i.e., 1.60×10^{-9} cm^3 s^{-1}. By analogy with the reactions with methane and ethylene, it is also reasonable to estimate that the reaction of N$^+$ (^1D) occurs at the Langevin rate.

Products

Recommended yields: (C$_2$H$_5^+$ + NH)/(C$_2$H$_4^+$ + NH$_2$)/(C$_2$H$_3^+$ + NH$_3$)/(HCNH$^+$ + CH$_4$), 0.10/0.55/0.25/0.10

The ion products and their respective branching ratios have been identified and quantified by McEwan et al. (1998) so they are our recommended values. No study exists for the reaction of N$^+$ (^1D) metastable state with ethane.

5.3.7. Reaction N$^+$ (^3P) + C$_3$H$_8$

Kinetics

Estimated value at 300 K: $k = 1.8 \times 10^{-9}$ cm^3 s^{-1} ($\pm$20%)

The rate constant of this reaction, measured at 300 K by Dryahina et al. (2011) with the SIFT technique, was found to be equal to 2.0×10^{-9} cm^3 s^{-1} ($\pm$20%), very close to the Langevin rate (1.8×10^{-9} cm^3 s^{-1}), which is our recommended value. It is thus expected to be the same value at 150 K. By analogy with the reactions with methane and ethylene, it is also reasonable to estimate that the reaction of N$^+$ (^1D) occurs at the Langevin rate.

Products

Recommended yields: C$_2$H$_3^+$/C$_2$H$_4^+$/C$_2$H$_5^+$/C$_3$H$_5^+$/C$_3$H$_6^+$/C$_3$H$_7^+$/C$_3$H$_8^+$, 0.12/0.25/0.36/0.11/0.05/0.09/0.02.

The ion products of this reaction have been unambiguously identified by Dryahina et al. (2011) by using isotope labeling for both the reacting ion (^{14}N$^+$ or ^{15}N$^+$) and the propane target molecule (C$_3$H$_8$ or C$_3$D$_8$). Their measured product ion yields are our recommended values. No N-bearing ion products were found. The neutrals associated with the other product

channels are less clear and discussed in the paper from Dryahina et al. (2011). According to these authors, they can result from processes which are either dissociative charge transfer and/or hydride (H$^-$) transfer producing NH neutrals. The production of NH$_2$ and NH$_3$ associated with the measured hydrocarbon ions is also possible, based on exoergicity considerations. No study exists for the reaction of N$^+$ (^1D) metastable state with propane, but it is reasonable to estimate that the (dissociative) charge transfer products dominate, as for the reactions of N$^+$ (^1D) with methane and ethylene.

5.3.8. Radiative Electron Recombination Reaction: N$^+$ + e

Kinetics

Recommended value: $k = 3.5 \times 10^{-12}$ (T_e/300)$^{-0.7}$ cm^3 s^{-1}.

The radiative recombination rate of an electron with N$^+$ has never been measured to our knowledge. However, calculations have been made for the recombination rate constant as a function of electron energy and these theoretical studies are reviewed in a compilation report (Kato & Asano 1999). The calculated rate constant varies between 10^{-12} and 10^{-11} cm^3 s^{-1} in the 1–10 eV electron energy rang. Beyond 10 eV, it decreases linearly with electron energy as the electron energy increases. This study is consistent with the previous estimated value of 3.5×10^{-12} (T_e/300)$^{-0.7}$ cm^3 s^{-1} reported in the compilation of Schmidt et al. (1988). In conclusion, in ionospheric conditions, N$^+$ will be essentially quenched by reactions with molecules, rather than by radiative recombination with electrons.

6. N$_2^{++}$ DOUBLY CHARGED IONS

Ionization by solar UV photons, as well as by solar wind electrons, can produce N$_2^{++}$ doubly charged ions (dications). Double ionization processes can represent up to a few percent of the total ion yield (see below). Nevertheless, to date, dications have almost never been considered in ionospheric models. Most of the electronic states of molecular doubly charged ions are dissociative due to Coulomb explosion, but ground-state N$_2^{++}$ ions are stable under ionospheric conditions. They have not been detected in any ionosphere to date, even if they have been predicted for more than 35 years to be present in the ionosphere of the Earth (Avakyan 1979; Prasad & Furman 1975; Simon et al. 2005), and more recently in Titan (Lilensten et al. 2005) and Venus (Gronoff et al. 2007). N$_2^{++}$ densities have been calculated to be about 10^{-4} of the total ion density in the case of Titan. In this review paper, we present the production processes, the lifetime and the reactivity of N$_2^{++}$ ions: the latter is still less than adequately understood as there have been very few experimental studies to date. For more details, see the recent review article by Thissen et al. (2011) on doubly charged ions in planetary atmospheres.

6.1. Production

The double ionization threshold of molecular nitrogen, together with the spectroscopy of the states located up to 11 eV above threshold have been measured very accurately by Ahmad et al. (2006) using coincidence methods. The double-ionization threshold of 42.88 ± 0.01 eV is found to be in excellent agreement with previous experimental (Dawber et al. 1994; Hochlaf 1996) and theoretical (Senekowitsch et al. 1991) works. Ahmad et al. (2006) show that the double ionization at

threshold is nondissociative and becomes dissociative into $N^+ + N^+$ above 44.5eV, with a lifetime in the microsecond time range.

The cross sections for the production of N_2^{++} doubly charged molecular ions are very difficult to measure, due to the mass to charge overlap with the N^+ fragment. Moreover, it is essential to distinguish between double ionization producing mainly dissociative doubly charged ions and production of long-lived N_2^{++} ions.

The cross sections for the production of doubly charged N_2^{++} ions by photoionization have only very recently been measured experimentally (Wehlitz 2010), by selecting the thermal N_2^{++} ions among the N^+ energetic ions, and detailed results are not yet published. In order to predict the N_2^{++} density which could be expected in the ionospheres of Earth (Simon et al. 2005), Venus (Gronoff et al. 2007), or Titan (Lilensten et al. 2005), these authors have used an empirical method based on the observation of a proportionality between electron impact ionization (Bahati et al. 2001), and photoionization (Samson 1990), as Samson showed that the double-photoionization cross section is proportional to the electron-impact ionization of the monocation multiplied by the total photoabsorption of the neutral species. In these studies, it was proposed to use a proportionality constant of 0.133 in order to obtain the photoionization cross section (Gronoff et al. 2007). The measured cross sections by Wehlitz (2010) show that this estimate was excellent and that the double-ionization cross section increases from threshold up to 100 eV photon energy, where it represents about 4% of total ionization.

For electron impact double-ionization cross sections, Märk (1975) performed a study using a mass spectrometer with sufficient mass resolution and sensitivity in order to detect accurately the $^{14}N^{15}N^{++}$ doubly charged ions, which appear as a peak at a mass-to-charge ratio (m/z) of 14.5. Märk provides absolute cross sections for electron impact double ionization from threshold up to 170 eV electron energy. The maximum cross section is 1.3×10^{-18} cm^2 ($\pm 5\%$) at 125 eV electron energy. This result is in very good agreement with the previous results of Halas & Adamczyk (1972) which extend to 600 eV, but has been criticized by Straub et al. (1996) and Tian & Vidal (1998) at a later date. The latter authors showed that the measurements made by Märk (1975) were probably underestimated by 20%. However, there is an excellent agreement between the measurements of Märk (1975) and the very recent ones of Ferreira et al. (2012), who measured the ratio of the double- to single-ionization cross sections by electron impact up to 400 eV electron energy.

Here we should add a comment concerning the cross sections for molecular N_2^{++} production, and their application to ionospheric questions. Laboratory measurements are based on the detection of an ionic signature corresponding to the presence in the spectrometer, at a specific time, of doubly charged ions. However, molecular dications such as N_2^{++} are often metastable species toward direct dissociation into N^+ and N^+. Therefore, an instrument probing the ionic population at longer times will inevitably observe a smaller amount of dications, the measured cross section being dependent on the instrument. The instruments of Märk (1975) and Halas & Adamczyk (1972) were probing the dications at times in the range of 1–5 ms, which is orders of magnitude shorter than the usual chemical lifetime considered in ionospheres (in the range of 1 s). One should therefore try to assess the effect of these differences in timescale. The consequent effect of population reduction is difficult to quantify,

but fortunately, in the case of nitrogen, Lundqvist et al. (1996) measured specific lifetimes, which show that the transition between short lifetimes (nanosecond scale) and long lifetimes (beyond 3 ms scale) occurs abruptly between two vibrational states. As Mathur et al. (1995) have shown that N_2^{++} ions have no or very few states with a lifetime in the range of micro or milliseconds, we propose to consider that values of absolute cross sections recorded in the microsecond time range are still valid for the ionospheric time range.

Though the density of ions in ionospheres is insufficient to require consideration of the competitive production of molecular dications by ionization of monocations, let us mention that data exist for electron impact ionization of N_2^+ and have been recorded by Bahati et al. (2001). To our knowledge, there is only a very recent, not yet published, work (J. M. Bizau 2011, private communication) for the equivalent process induced by photons.

6.2. Lifetime and Quenching

The metastable lifetime of N_2^{++} toward its dissociation into $N^+ + N^+$ has been determined by Mathur et al. (1995) by monitoring the decay curves of N_2^{++} beams in a heavy-ion storage ring. The longest component of the lifetime is measured to be of the order of 3 s. Mathur et al. performed ab initio configuration interaction calculations of the potential energy curve for the lowest-energy state of N_2^{++} in order to compute tunneling times for each vibrational level. They find that lifetimes in the range of 3 s would correspond to $v = 10$ of the ground state, and therefore propose the association of the experimentally measured lifetime to the effect of interactions of N_2^{++} with the residual gas in the ring, and consider that lifetime of $v = 0$ is effectively infinite. Further experimental evidence of the long lifetime of lower excited states is provided by Ahmad et al. (2006) showing that a stable dication signature is still visible in the coincident mass spectra at $v = 7$ of the $A(^1\Pi_u)$ excited state of the dication, about 2.5 eV above the N_2^{++} ground state.

Higher excited states of N_2^{++} have short lifetimes (Ahmad et al. 2006) due to dissociation, but also resulting, for the D $^1\Sigma_u^+$ state, from fluorescence decay. Already identified in 1958 (Carroll 1958), these fluorescence bands have been assigned to the D $^1\Sigma_u^+$–X $^1\Sigma_g^+$ transition by Cossart et al., corresponding to the (0–0) band (Cossart et al. 1991) and to the (1–1) band (Cossart et al. 1985), respectively. The lifetime of the D $^1\Sigma_u^+$ state has been measured to be 6 ± 0.5 ns (Olsson & Larsson 1988). The cross section for the photo production of this emission has been determined by Ehresman et al. (2003) in the energy range from threshold (51eV) to 66 eV, where it peaks at a value of 1×10^{-20} cm^2. It is interesting to note that, as shown by Ahmad et al. (2006), the emission is associated with the production of the non-dissociative ground state of N_2^{++}. Therefore, in ionospheres, the formation of the D $^1\Sigma_u^+$ state results in the formation of stable N_2^{++} ions, which will decay by reactions with the neutral gases.

6.3. Reactions

The reactivity of molecular doubly charged ions is still poorly known, but from the existing experimental data for reactions with rare gas atoms, diatomic as well as polyatomic molecules, single charge transfer is usually the dominant product channel. However, surprisingly chemical reactions involving chemical bond rearrangement have been observed (see, for example, the

Table 15
Product Branching Ratios for the $N_2^{++} + H_2$ and $N_2^{++} + D_2$ Reactions (X is H or D)

Reaction	$N_2^+ + X_2^+$	$N^+ + X_2^+ + N$	$N_2^+ + X^+ + X$	$N^+ + X^+ + (N + X)$	$NX^+ + X^+ + N$	Reference
$N_2^{++} + H_2$	0.53	0.32	0.10	0.03	0.02	(Lockyear et al. 2011)*
$N_2^{++} + D_2$	0.61	0.24	0.12	0.02	0.01	(Lockyear et al. 2011)**

Notes.
* Values measured for the reaction of N_2^{++} with H_2 at 0.9 eV CM collision energy.
** Values measured for the reaction of N_2^{++} with D_2 at 1.8 eV CM collision energy.

review articles from Price (2003, 2007) and from Roithová & Schröder (2007a, 2007b).

6.3.1. Reaction $N_2^{++} + N_2$

Kinetics:
Recommended value at 300 K: $k = 1.7 \times 10^{-9}$ cm^3 s^{-1} ($\pm 25\%$)

For the reaction of N_2^{++} ions with N_2, only very partially published results (Lilensten et al. 2005; Thissen et al. 2004) obtained by some of the co-authors are available. These results have been measured in a guided ion beam (GIB) apparatus for collision energies between 0.2 and 20 eV (Thissen et al. 2004). In order to distinguish between N_2^{++} and N^+ reactions, kinetic energy discrimination against the fast N^+ ions has been used. The efficiency of this methodology has been checked by using $^{15}N^{14}N^{++}$ reactant ions, dications which can be unambiguously distinguished from singly charged atomic ions. The value for the rate constant at 300 K has been estimated from extrapolations of these data (Lilensten et al. 2005). It gives a value of 2.4×10^{-9} cm^3 s^{-1} ($\pm 25\%$). It is nearly equal to the Langevin rate (1.66×10^{-9} cm^3 s^{-1}) within experimental uncertainties, but slightly higher, which is impossible. So the recommended rate constant value is the Langevin rate at 300 K and 150 K.

Products:
Recommended yields: $(N_2^+ + N_2^+)/(N_2^+ + N^+ + N)$, 0.90/ 0.10

Isotopic labeling has been used to identify the reaction products. In the case of the $^{14}N_2^{++} + {}^{15}N_2$ reaction at $E_{CM} = 0.2$ eV, the charge transfer of one electron giving $^{14}N_2^+ + {}^{15}N_2^+$ is the main observed reaction channel (Thissen et al. 2004). But the reaction also produces some dissociative charge transfer of the target molecule giving $^{14}N_2^+ + {}^{15}N^+ + {}^{15}N$ products. Let us note that the eventual production of dissociation induced by collision giving $^{14}N^+$ ions could not have been detected, as it has the same m/z ratio as the parent ions $^{14}N_2^{++}$.

6.3.2. Reaction $N_2^{++} + H_2$

Recommended value at 300 K: $k = 3.1 \times 10^{-9}$ cm^3 s^{-1} ($\pm 25\%$) for H_2
Estimated value at 300 K: $k = 2.2 \times 10^{-9}$ cm^3 s^{-1} ($\pm 25\%$) for D_2.

The reactions of N_2^{++} with H_2/D_2 have recently been investigated (Lockyear et al. 2011). The rate constant is estimated to be equal to the Langevin rate and independent of temperature. This estimate is supported by the very good agreement with the absolute cross section measured for the $NH^+ + H^+ + N$ reaction channel, multiplied by the corresponding branching ratio and converted into a partial rate constant. The uncertainty on this value is hard to estimate, but it seems reasonable to evaluate it to be equal to about 25%. It is naturally assumed that the reaction with D_2 is also governed by the Langevin rate.

Products:
Recommended yields: $(N_2^+ + H_2^+)/(N^+ + H_2^+ + N)/(N_2^+ + H^+ + H)/(N^+ + H^+ + (N + H))/(NH^+ + H^+ + N)$, 0.53/0.32/ 0.10/0.03/0.02 for H_2
$(N_2^+ + D_2^+)/(N^+ + D_2^+ + N)/(N_2^+ + D^+ + D)/(N^+ + D^+ + (N + D))/(ND^+ + D^+ + N)$, 0.61/0.24/0.12/0.02/0.01 for D_2

Table 15 gives the product branching ratios for the $N_2^{++} + H_2$ and $N_2^{++} + H_2$ reactions.

The experiments of Lockyear et al. (2011) reveal that, at elevated collision energies ($\sim$1 eV CM), charge transfer to form $N_2^+ + H_2^+$, $N^+ + H_2^+$, and $N_2^+ + H^+ + H$ dominates the reactivity; a reactivity almost certainly dominated by the ground electronic state of N_2^{++} which is the major species in the reactant beam. However, the formation of NH^+ is also observed, a product which quantum-chemical investigations indicate must arise from the reaction of a triplet state of N_2^{++}. The formation of the NH^+ product is assigned to the long-lived, but low-lying, $^3\Sigma_u^+$ excited state of N_2^{++} reacting at close to the Langevin rate; this long-lived state of N_2^{++} is present as a minor species in the reactant ion beam. These observations indicate that for fully comprehensive modeling of the role of N_2^{++} in Titan's ionosphere, a consideration of the electronic state distribution of the dication may well be required. Again further experimental investigations of reaction of N_2^{++} with H_2 would be highly desirable.

6.3.3. Reaction $N_2^{++} + CH_4$

Kinetics:
Recommended value at 300 K: $k = 1.8 \times 10^{-9}$ cm^3 s^{-1} ($\pm 25\%$).

For the reaction of N_2^{++} ions with CH_4, the results of studies available in the literature (Lilensten et al. 2005; Thissen et al. 2004) are augmented by additional data presented for the first time in this review. These results have been measured in a GIB apparatus for collision energies between 0.2 and 16 eV for the reaction of $^{15}N_2^{++}$ with CD_4 (Thissen et al. 2004). The recommended value for the rate constant at 300 K has been estimated from extrapolations of these data (Lilensten et al. 2005). It is close to the Langevin rate (2.36×10^{-9} and 2.20×10^{-9} cm^3 s^{-1} for the reaction with CH_4 and CD_4, respectively) and the rate constant at 150 K is estimated to be the same.

Products:
Recommended yields: $(N_2^+ + CD_4^+)/(N_2^+ + CD_3^+ + D)/(N_2^+ + CD_2^+ + D_2)/(DCND^+ + ND^+ + D)/(DCN^+ + ND_2^+ + D)$, 0.22/ 0.54/0.15/0.06/0.03

Isotopic labeling has been used to identify the reaction products. For the reaction of $^{15}N_2^{++}$ with CD_4 at $E_{CM} = 0.2$ eV (Thissen et al. 2004), the charge transfer of one electron is dominant, giving $N_2^+ + CD_4^+$, but also CD_3^+ and CD_2^+ product ions resulting from dissociative charge transfer. In addition, minor reactive channels giving ND^+, ND_2^+, DCN^+, and $DCND^+$ have also been observed. Product branching ratios cannot be precisely

derived from these experiments, as the derivation of such ratios would have required coincidence measurements between singly charged product ions as in the studies from Lockyear et al. (2011) in the case of the reactions of N_2^{++} with H_2 and D_2. Ion pairs given in our recommended yields are the most reasonable estimated ones. These preliminary experiments reveal the need for further studies.

6.3.4. Reaction $N_2^{++} + C_2H_2$

Kinetics:
Estimated value at 300 K: $k = 2.3 \times 10^{-9}$ cm^3 s^{-1}.
This reaction has never been studied. By analogy with the reactions of N_2^{++} with N_2, H_2, CH_4, and C_2H_4 (see below for C_2H_4), it is reasonable to estimate the rate constant to be equal to the Langevin rate, at 300 K and at 150 K.
Products:
By analogy with the reactions of N_2^{++} with CH_4 and C_2H_4 (see below for C_2H_4), it is reasonable to estimate that the main products come from the single charge transfer giving $N_2^+ + C_2H_2^+$ and from the dissociative charge transfer giving $N_2^+ + C_2H^+ + H$ and $N_2^+ + C_2^+ + H_2$, which are the dissociative channels observed by Mackie et al. (2003) for the dissociative photoionization of acetylene. Minor products coming from chemical reactions, such as $HCNH^+$ and HCN^+, can also be expected, especially at low collision energy.

6.3.5. Reaction $N_2^{++} + C_2H_4$

Kinetics:
Recommended value at 300 K: $k = 2.2 \times 10^{-9}$ cm^3 s^{-1} ($\pm 25\%$)
The recommended value for the rate constant at 300 K has been estimated from extrapolations of the measurements made at collision energies between 0.2 and 20 eV for the reaction of $^{15}N_2^{++}$ with C_2D_4 (Thissen et al. 2004). It is equal to the Langevin rate (2.36×10^{-9} cm^3 s^{-1}) within experimental uncertainties, so the rate constant at 150 K is most probably the same.
Products:
Recommended yields: $(N_2^+ + C_2D_4^+)/(N_2^+ + C_2D_3^+ + D)/(N_2^+ + C_2D_2^+ + D_2)/(N_2^+ + C_2D^+ + D_2 + D)/(N_2^+ + CD_3^+ + CD)/(N_2^+ + CD_2^+ + CD_2)/(DCND^+ + ND^+ + CD)/(DCN^+ + ND_2^+ + CD)$, 0.26/0.41/0.18/0.01/0.03/0.06/0.02/0.03
Isotopic labeling has been used to identify the reaction products. For the reaction of $^{15}N_2^{++}$ with C_2D_4 at $E_{CM} = 0.2$ eV (Thissen et al. 2004) as for the reaction of N_2^{++} with methane, the main products come from single charge transfer, non-dissociative as well as dissociative, giving $N_2^+ + (C_2D_4^+, C_2D_3^+, C_2D_2^+, C_2D^+, CD_3^+,$ and $CD_2^+)$ ions. These are the same dissociation products as those observed for the dissociative photoionization of ethylene (Mackie et al. 2003), except H^+ (D^+) which could not have been detected in the experiments of Thissen et al. (2004). The same minor reactive channels as for the reaction with methane have been observed giving ND^+, ND_2^+, DCN^+, and $DCND^+$. Product branching ratios cannot be precisely derived from these experiments, as the derivation of such ratios would have required coincidence measurements between singly charged product ions as in the studies from Lockyear et al. (2011) in the case of the reactions of N_2^{++} with H_2 and D_2. Ion pairs given in our recommended yields are the most reasonable estimated ones. These preliminary experiments reveal the need for further studies.

6.3.6. Reaction $N_2^{++} + C_2H_6$

Kinetics:
Estimated value at 300 K: $k = 2.6 \times 10^{-9}$ cm^3 s^{-1} ($\pm 25\%$).
This reaction has never been studied. By analogy with the reactions of N_2^{++} with N_2, H_2, CH_4, and C_2H_4, it is reasonable to estimate the rate constant to be equal to the Langevin rate, independent of temperature.
Products:
By analogy with the reactions of N_2^{++} with CH_4 and C_2H_4, it is reasonable to estimate that the main products come from the nondissociative ($N_2^+ + C_2H_6^+$) and dissociative single charge transfer giving $N_2^+ + (C_2H_5^+ + H, C_2H_4^+ + H_2, C_2H_3^+ + H_2 + H, C_2H_2^+ + 2H_2,$ and $CH_3^+ + CH_3)$ products. The dissociation channels are supposed to be the same ones as those observed for the dissociative photoionization of ethane (Mackie et al. 2002; Stockbauer 1973). Minor products coming from chemical reactions, such as $HCNH^+$, HCN^+, NH^+, and NH_2^+, can also be expected.

6.3.7. Reaction $N_2^{++} + C_3H_8$

Kinetics:
Estimated value at 300 K: $k = 2.8 \times 10^{-9}$ cm^3 s^{-1} ($\pm 25\%$).
This reaction has never been studied. By analogy with the reactions of N_2^{++} with N_2, H_2, CH_4, and C_2H_4, it is reasonable to estimate the rate constant to be equal to the Langevin rate, independent of temperature.
Products:
By analogy with the reactions of N_2^{++} with CH_4 and C_2H_4, it is reasonable to estimate that the main products come from the nondissociative ($N_2^+ + C_3H_8^+$) and dissociative single charge transfer giving $N_2^+ + (C_3H_7^+ + H, C_3H_5^+ + H_2 + H, C_2H_5^+ + CH_3, C_2H_4^+ + CH_4,$ and $C_2H_3^+ + CH_3 + H_2)$ products. The dissociation channels are proposed to be the same ones as those observed for the dissociative photoionization of propane (Stockbauer & Inghram 1976). Minor products coming from chemical reactions, such as $HCNH^+$, HCN^+, NH^+ and NH_2^+, can also be expected.

6.3.8. Reactions with Electrons: Dissociative Recombination and Collision-induced Dissociation

$N_2^{++} + e \rightarrow N^+ + N$ dissociative recombination
$N_2^{++} + e \rightarrow N^{++} + N + e$. collision-induced dissociation
Kinetics:
Recommended value: $k = 5.8 \times 10^{-7} (T_e/300)^{-0.5}$ cm^3 s^{-1} ($\pm 25\%$) for electron recombination
Absolute cross section measurements have been carried out by Seiersen et al. (2003) using the heavy-ion storage ring ASTRID in the relative collision energy range 10^{-4} to 10 eV. They studied the recombination of $^{14}N^{15}N^{++}$ and deduced from their data analysis a rate constant of

$$k = (5.8 \pm 2.9) \times 10^{-7}(T_e/300)^{-0.5} \text{ cm}^3 \text{ s}^{-1},$$

which is about 2.5 times greater than the dissociative recombination of N_2^+ at room temperature. Seiersen et al. did not measure the rate constant for dissociation without capture, a competing process that could be induced by the interaction with electrons, but they show that the later process is probably negligible for molecular doubly charged ions. Beyond 10.9 eV collision energy, the asymmetric dissociation into $N^{++} + N$ seems to become the dominant process.

7. N^{++} DOUBLY CHARGED IONS

7.1. Production

In 1941, Hagstrum & Tate (1941) observed the formation of N^{++} doubly charged atomic ions in the dissociative ionization of N$_2$ by electron impact. Only a very minor fraction of the N$_2^{++}$ ions created by electron ionization dissociate to N^{++} ions and an associated neutral N fragment. The photon-induced process was studied by Franceschi et al. (2007). They showed that the N$_2^{++}$ asymmetric dissociation has a threshold at 59.9 ± 0.2 eV and exhibits a maximum cross section of 2×10^{-20} cm^2 at 85 eV. Crowe & McConkey (1973) measured the cross section for electron impact formation of N^{++} and showed that it peaks around 190 eV, with a cross section of 1.9×10^{-18} cm^2.

N^{++} ions could also be formed in planetary atmospheres by double ionization of N atoms or ionization of N$^+$ singly charged ions. The double ionization potential of an N atom is 44.135 eV (Ralchenko et al. 2011). The double photoionization cross section of N atoms has been measured by Samson et al. (Samson & Angel 1990; Samson et al. 1996). The N double photoionization cross section reaches a maximum of 2.1×10^{-19} cm^2 at 60 eV photon energy and the ratio of doubly charged to singly charged ions has been measured to be 6.6% at this energy (Samson & Angel 1990).

The cross section for the photoionization of N$^+$ ions to give N^{++} doubly charged ions has been measured by Kjeldsen et al. (2002). It rises sharply from the threshold at 29.60 eV and exhibits many resonances. The continuum cross-section value is 7.0×10^{-18} cm^2 at threshold and decreases slowly down to 3.6×10^{-18} and 1.1×10^{-18} cm^2 at 50 and 80 eV photon energies, respectively. The experimental cross section is in good agreement with previous theoretical calculations (Nahar & Pradhan 1997). Tawara & Kato (1999) made a review of all measurements of the cross section for ionization of N$^+$ by electron impact. As for the photoionization cross section of N$^+$, it has a sharp onset and then reaches a maximum of 0.5 to 1×10^{-16} cm^2, according to the different authors, at about 90 eV electron energy.

7.2. Lifetime and Quenching

The lowest metastable state of N^{++}, about 7 eV above the ^2P ground state, is the ^4P_J state with $J = 1/2$, 3/2, and 5/2 (Ralchenko et al. 2011). These J states have lifetimes of 0.98, 13.4, and 3.2 ms, respectively (Fang et al. 1993). It is short with respect to the time between collisions under ionospheric pressure conditions, so these states will be relaxed by radiative decay to the ground state, before they can react by collisions.

The N^{++} ions produced by double ionization of N$_2$ by 125 eV electron impact have a broad kinetic energy distribution of about 6 eV, centered around 4 eV, according to the old measurements of Kieffer & van Brunt (1967). It is thus likely that their kinetic energy is not, or only partially, relaxed by collisions prior to reaction.

7.3. Reactions

7.3.1. Reaction N^{++} + N$_2$

Recommended value: $k = 2.04 \times 10^{-9}$ cm^3 s^{-1} ($\pm 20\%$)

The rate constant of this reaction has been measured by two groups (Church & Holzscheiter 1980; Fang & Kwong 1997). Church & Holzscheiter (1980) measured it at 300 K and found a value of 2.8×10^{-9} cm^3 s^{-1} ($\pm 20\%$). The rate constant measured by Fang & Kwong (1997) at a laboratory energy of 2.7 eV (1.8 eV CM and an equivalent temperature calculated to be 1.3×10^4 K) is very close to the value at 300 K and equal to the Langevin rate within experimental uncertainties (2.04×10^{-9} cm^3 s^{-1}). So the Langevin rate is our recommended rate constant value. According to Church & Holzscheiter (1980), the product ions are N$^+$ ions with a mean kinetic energy of 2–3 eV, resulting from the dissociative single charge transfer giving N$^+$ + N$^+$ + N.

7.3.2. Reaction N^{++} + H$_2$

Recommended value: $k = 3.4 \times 10^{-11}$ ($\pm 10\%$) cm^3 s^{-1}

Fang & Kwong (1997) measured the rate constant of this reaction at a laboratory energy of 2.7 eV (0.34 eV cm) for which they calculate the equivalent temperature (2.9×10^3 K). This is the only experimental study for this reaction and the products are unknown. The measured rate constant (3.4×10^{-11} ($\pm 10\%$) cm^3 s^{-1}) is about two orders of magnitude lower than the reaction of N^{++} with N$_2$ (see above), much lower than the Langevin rate (3.2×10^{-9} cm^3 s^{-1}). Three reaction channels are energetically possible: the single charge transfer giving N$^+$ + H$_2^+$, the dissociative charge transfer giving N$^+$ + H$^+$ + H, and the double charge transfer giving N + H$^+$ + H$^+$.

7.3.3. Radiative electron recombination reaction N^{++} + e

The electron recombination reactions of atomic doubly charged ions can only involve radiative recombination processes. For such reactions, there are only theoretical calculations (Nahar & Pradhan 1997; see also the review report from Kato & Asano 1999), due to the enormous difficulty in measuring such rates experimentally. All calculations give very close rate constant values as a function of the electron temperature. A typical expression was given by Aldrovandi & Pequignot (1973) as

$$k = 2.2 \times 10^{-12}(T_e/10^4)^{-0.639} \text{cm}^3 \text{ s}^{-1},$$

where T_e is the electron temperature in K.

8. SUMMARY AND CONCLUSIONS

In this paper, we have presented a critical review of the reactions of all nitrogen species, atomic and molecular, neutral, singly charged and doubly charged ions, with main neutral constituents of Titan's atmosphere. All recommended and estimated values for the rate constants and product yields are gathered in Tables 16–18 for neutral, ion–molecule and ion–electron recombination reactions, respectively. In Table 16, recommended rate constant values of neutral reactions are given at 300 K, as well as their temperature dependence, specifying the temperature range of the associated studies. Products and their branching ratios at 300 K are indicated when they are reasonably known. In Table 17, recommended rate constant values for ion–molecule reactions are given at 300 K and 150 K. Products and their branching ratios are given at 300 K. In Table 18, rate constants of electron-ion recombination reactions are given as a function of electron temperature. Products are indicated together with recommended yields.

In Tables 16 and 17, we propose estimated values for rate constants and product yields, when no data are available and when we could reasonably make appropriate estimates, using our expertise for chemical reactions, as planetary scientists need them for their atmospheric chemical models. However we would like to underline the importance to check such estimates

Table 16
Summary for Reactions of Neutral Active Nitrogen Species

Reaction	Products	Branching[a] Ratio	k (cm^3 s^{-1}) at 300 K with Uncertainty	k Temperature Dependence (Temperature Range)
N_2 ($A\,^3\Sigma_u^+$) + N_2	N_2 ($X\,^1\Sigma_g^+$) + N_2	1	$\leqslant 3 \times 10^{-18}$	?
N_2 ($A\,^3\Sigma_u^+$) + H_2	N_2 ($X\,^1\Sigma_g^+$) + H_2	0.9	3.5×10^{-15} ($\pm 60\%$)	2.2×10^{-10} exp ($-3500/T$)
	N_2 ($X\,^1\Sigma_g^+$) + H + H	0.1		(240–370 K)
N_2 ($A\,^3\Sigma_u^+$) + CH_4	N_2 ($X\,^1\Sigma_g^+$) + CH_4	0.9	3.0×10^{-15} ($\pm 60\%$)	1.3×10^{-10} exp ($-3170/T$)
	N_2 ($X\,^1\Sigma_g^+$) + CH_3 + H	0.1		(300–360 K)
N_2 ($A\,^3\Sigma_u^+$) + C_2H_2	N_2 ($X\,^1\Sigma_g^+$) + C_2H + H	$0.52 \pm 5\%$	1.40×10^{-10} ($\pm 60\%$)	?
	N_2 ($X\,^1\Sigma_g^+$) + C_2 + H_2	$0.48 \pm 5\%$		
N_2 ($A\,^3\Sigma_u^+$) + C_2D_2	N_2 ($X\,^1\Sigma_g^+$) + C_2D + D	$0.33 \pm 5\%$	1.45×10^{-10} ($\pm 60\%$)	?
	N_2 ($X\,^1\Sigma_g^+$) + C_2 + D_2	$0.67 \pm 5\%$		
N_2 ($A\,^3\Sigma_u^+$) + C_2H_4	N_2 ($X\,^1\Sigma_g^+$) + C_2H_3 + H	$0.30 \pm 5\%$	9.7×10^{-11} ($\pm 60\%$)	?
	N_2 ($X\,^1\Sigma_g^+$) + C_2H_2 + H_2	$0.70 \pm 5\%$		
N_2 ($A\,^3\Sigma_u^+$) + C_2D_4	N_2 ($X\,^1\Sigma_g^+$) + C_2D_3 + D	$0.13 \pm 5\%$	9.3×10^{-11} ($\pm 60\%$)	?
	N_2 ($X\,^1\Sigma_g^+$) + C_2D_2 + D_2	$0.87 \pm 5\%$		
N_2 ($A\,^3\Sigma_u^+$) + C_2H_6	N_2 ($X\,^1\Sigma_g^+$) + C_2H_6	?	2.3×10^{-13} ($\pm 60\%$)	1.6×10^{-10} exp ($-1980/T$)
	N_2 ($X\,^1\Sigma_g^+$) + C_2H_5 + H	?		(300–370 K)
	N_2 ($X\,^1\Sigma_g^+$) + C_2H_4 + H_2	?		
N_2 ($A\,^3\Sigma_u^+$) + C_3H_8	N_2 ($X\,^1\Sigma_g^+$) + C_3H_8	?	1.3×10^{-12} ($\pm 60\%$)	?
	N_2 ($X\,^1\Sigma_g^+$) + C_3H_7 + H	?		
	N_2 ($X\,^1\Sigma_g^+$) + C_3H_6 + H_2	?		
N (^4S) + H	NH + $h\nu$	1	1.0×10^{-19}	
N (^4S) + CH_2	HCN + H	0.50	8.0×10^{-11}	
	HNC + H	0.50		
N (^4S) + CH_3	H_2CN + H	$0.90 \pm 10\%$	8.5×10^{-11} ($\pm 25\%$)	6.2×10^{-11}
	HCN + H + H	$0.10 \pm 50\%$		(150–200 K)
N (^4S) + CD_3	D_2CN + D	$0.90 \pm 10\%$	8.5×10^{-11}	
	DCN + D + D	$0.10 \pm 50\%$		
N (^4S) + C_2H_3	CH_2CN + H	$0.83 \pm 10\%$	7.7×10^{-11} ($\pm 40\%$)	
	C_2H_2 + NH	$0.17 \pm 50\%$		
N (^4S) + C_2H_5	C_2H_4 + NH	0.65	1.1×10^{-10} ($\pm 25\%$)	
	H_2CN + CH_3	0.35		
N (^4S) + C_2D_5	C_2D_4 + ND	$0.65 \pm 50\%$	1.1×10^{-10}	
	D_2CN + CD_3	$0.35 \pm 50\%$		
N (^2D) + N_2	N (^4S) + N_2	1	1.7×10^{-14} ($\pm 40\%$)	1.0×10^{-13} exp ($-510/T$)
				(198–372 K)
N (^2D) + H_2	NH + H	1	2.2×10^{-12} ($\pm 25\%$)	4.6×10^{-11} exp ($-880/T$)
				(213–300 K)
N (^2D) + CH_4	CH_2NH/CH_3N + H	$0.8 \pm 20\%$	4.0×10^{-12} ($\pm 40\%$)	7.1×10^{-11} exp ($-750/T$)
	NH + CH_3	$0.2 \pm 50\%$		(223–292 K)
N (^2D) + CD_4	CD_2ND/CD_3N + D	0.8	2.6×10^{-12} ($\pm 40\%$)	3.3×10^{-11} exp ($-700/T$)
	ND + CD_3	0.2		(223–292 K)
N (^2D) + C_2H_2	HCCN + H	$0.9 \pm 10\%$	6.5×10^{-11} ($\pm 25\%$)	1.6×10^{-10} exp ($-270/T$)
	cyclic-HCCN + H	$0.1 \pm 50\%$		(223–293 K)
N (^2D) + C_2D_2	DCCN + D	0.9	6.25×10^{-11} ($\pm 25\%$)	1.4×10^{-10} exp ($-240/T$)
	cyclic-DCCN + D	0.1		(223–293 K)
N (^2D) + C_2H_4	CH_2NCH + H	0.67	4.3×10^{-11} ($\pm 25\%$)	$(2.3 \pm 0.3) \times 10^{-10}$ exp ($-500 \pm 50/T$)
	cyclic-CH_2(N)CH + H	0.23		(230–292 K)
	CH_2CNH + H	0.05		
	HCN/HNC + CH_3	0.01		
	CH_3CN/CH_3NC + H	0.01		
	$CH_2NC/CHNCH$ + H_2	0.01		
	$CH_2N/CHNH$ + CH_2	0.01		
N (^2D) + C_2D_4	CD_2NCD + D	0.67	3.8×10^{-11} ($\pm 25\%$)	$(2.4 \pm 0.5) \times 10^{-10}$ exp ($-550 \pm 50/T$)
	cyclic-CD_2(N)CD + D	0.23		(230–292 K)
	CD_2CND + D	0.05		

Table 16
(Continued)

Reaction	Products	Branching[a] Ratio	k (cm^3 s^{-1}) at 300 K with Uncertainty	k Temperature Dependence (Temperature Range)
	DCN/DNC + CD$_3$	*0.01*		
	CD$_3$CN/CD$_3$NC + D	*0.01*		
	CD$_2$NC/CDNCD + D$_2$	*0.01*		
	CD$_2$N/CDND + CD$_2$	*0.01*		
N (^2D) + C$_2$H$_6$	CH$_2$=NH + CH$_3$	0.79 ± 10%	1.9 × 10^{-11} (±25%)	?
	CH$_3$CH=NH + H	0.12 ± 10%		
	NH + C$_2$H$_5$	0.06 ± 20%		
	CH$_2$=CHNH$_2$ + H	0.02 ± 20%		
	^{3}CH$_2$=NH + CH$_3$	0.01 ± 20%		
N (^2D) + C$_3$H$_8$	CH$_2$NH + C$_2$H$_5$	?	2.9 × 10^{-11} (±25%)	?
	CH$_3$CHNH + CH$_3$	?		
	NH + C$_3$H$_7$	?		
	C$_2$H$_5$CHNH + H	?		
N (^2P) + N$_2$	N (^2D) + N$_2$	1	3.3 × 10^{-17} (±60%)	?
N (^2P) + H$_2$	N (^2D) + H$_2$	1	1.9 × 10^{-15} (±60%)	3.5 × 10^{-13} exp (−950/T) (213–300 K)
N (^2P) + CH$_4$	N (^2D) + CH$_4$	1	8.5 × 10^{-14} (±25%)	5.0 × 10^{-13} exp (−490/T) (223–292 K)
N (^2P) + CD$_4$	N (^2D) + CD$_4$	1	6.0 × 10^{-14} (±25%)	3.1 × 10^{-13} exp (−480/T) (223–292 K)
N (^2P) + C$_2$H$_2$	. . .	. . .	2.3 × 10^{-11} (±40%)	1.0 × 10^{-10} exp (−440/T) (223–293 K)
N (^2P) + C$_2$D$_2$	. . .	. . .	2.0 × 10^{-11} (±40%)	7.1 × 10^{-11} exp (−380/T) (223–293 K)
N (^2P) + C$_2$H$_4$	. . .	. . .	3.0 × 10^{-11} (±25%)	(1.4 ± 0.5) × 10^{-10} exp (−455 ± 90/T) (230–292 K)
N (^2P) + C$_2$D$_4$	. . .	. . .	3.0 × 10^{-11} (±25%)	(1.3 ± 0.2) × 10^{-10} exp (−435 ± 50/T) (230–292 K)
N (^2P) + C$_2$H$_6$	N (^2D) + C$_2$H$_6$	1	5.4 × 10^{-13} (±25%)	?
N (^2P) + C$_3$H$_8$	Quenching or chemical reaction?	?	1.9 × 10^{-12} (±25%)	?

Note. [a] Estimated values are in italic characters.

by detailed experimental or theoretical work. These estimated values are given in italic characters in Tables 16–18 in order to clearly distinguish them from measured or calculated values. Uncertainties are given for all data (except calculated and some estimated ones). Most uncertainties are estimated based on our knowledge of the experimental techniques used. In the literature, uncertainties are often not given by the authors, or if they are, they are mostly estimated by the authors from experimental scatter, without taking into account any systematic errors, which are much more difficult to evaluate.

We also included in this paper a review of the main production processes, lifetimes, and quenching of the active nitrogen species. For all reactions, temperature and/or collision energy dependence of the rate constants are discussed in the light of the available information from the literature. However for many reactions, this information is still unavailable, in particular at low temperatures, where it is essential for the modeling of the chemistry of Titan's atmosphere. We also note that the variation of the reaction cross sections of N atoms and N$^+$ atomic ions with collision energy up to a few eV is very important for some applications, in particular for the studies of atmospheric escape.

For neutral reactions, in summary, the most reactive nitrogen species is the N (^2D) metastable state and all quenching reactions are slow. The reactions of the N$_2$ (A $^3\Sigma_u^+$) state with N$_2$, H$_2$

and CH$_4$ produce only or mainly the quenching into the N$_2$ (X) ground state, but with C$_2$H$_2$ and C$_2$H$_4$, they produce the dissociation of the target molecule. Quenching is the main channel for reactions of the N (^2P) higher metastable state with N$_2$, H$_2$ and saturated hydrocarbons. This quenching is predicted to produce the N (^2D) lower metastable state and not the N (^4S) ground state, but it would be important to check this assumption, by either experimental or theoretical work. If this assumption is not correct, it could have important consequences for Titan's atmospheric chemistry, as N (^2D) is very reactive and N (^4S) is not. With unsaturated hydrocarbons, N (^2P) gives chemical reactions, but the products are unknown. The reactions of the N (^2D) metastable state with hydrocarbons involve C–N bond formation, but product yields are not well known. The measurement of relevant rate constants at low temperatures still requires much more laboratory work. Let us note that caution should be exercised when extrapolating rate constants to temperatures outside the temperature range over which the temperature dependence was determined. When no experimental temperature dependence was measured, it is reasonable to predict that the rate constant in the 150–200 K range will have a lower value than at 300 K, when an energy barrier is supposed to be present for the reaction. But no precise estimate can be made without theoretical or experimental work.

Table 17
Summary for Reactions of Nitrogen Ions

Reaction	Products[a]	Branching Ratio[a]	k (cm^3 s^{-1})[a] at 300 K with Uncertainty[a]	k (cm^3 s^{-1})[a] at 150 K with Uncertainty
$N_2^+ + N_2$	$N_2 + N_2^+$	1	5.0×10^{-10} ($\pm25\%$)	5.0×10^{-10} ($\pm70\%$)
$N_2^+ + H_2$	$N_2H^+ + H$	$0.99 \pm 5\%$	1.56×10^{-9} ($\pm15\%$)	1.3×10^{-9} ($\pm20\%$)
	$H_2^+ + N_2$	$0.01 \pm 10\%$		
$N_2^+ + D_2$	$N_2D^+ + D$	$0.99 \pm 5\%$	1.15×10^{-9} ($\pm20\%$)	9.6×10^{-10} ($\pm20\%$)
	$D_2^+ + N_2$	$0.01 \pm 10\%$		
$N_2^+ + CH_4$	$CH_3^+ + H + N_2$	$0.86 \pm 5\%$	1.18×10^{-9} ($\pm15\%$)	1.18×10^{-9} ($\pm15\%$)
	$CH_2^+ + H_2 + N_2$	$0.09 \pm 5\%$		
	$N_2H^+ + CH_3$	$0.05 \pm 10\%$		
$N_2^+ + CD_4$	$CD_3^+ + D + N_2$	$0.88 \pm 5\%$	1.10×10^{-9} ($\pm20\%$)	1.10×10^{-9} ($\pm20\%$)
	$CD_2^+ + D_2 + N_2$	$0.07 \pm 5\%$		
	$N_2D^+ + CD_3$	$0.05 \pm 10\%$		
$N_2^+ + C_2H_2$	$C_2H_2^+ + N_2$	$0.94 \pm 5\%$	4.15×10^{-10} ($\pm25\%$)	1.0×10^{-9} ($\pm50\%$)
	$N_2H^+ + C_2H$	$0.06 \pm 10\%$		
$N_2^+ + C_2H_4$	$C_2H_3^+ + H + N_2$	$0.67 \pm 5\%$	1.29×10^{-9} ($\pm15\%$)	1.29×10^{-9} ($\pm20\%$)
	$C_2H_2^+ + H_2 + N_2$	$0.23 \pm 5\%$		
	$N_2H^+ + C_2H_3$	$0.10 \pm 10\%$		
$N_2^+ + C_2H_6$	$C_2H_5^+ + H + N_2$	$0.14 \pm 5\%$	1.30×10^{-9} ($\pm30\%$)	1.30×10^{-9} ($\pm30\%$)
	$C_2H_4^+ + H_2 + N_2$	$0.27 \pm 5\%$		
	$C_2H_3^+ + H_2 + H + N_2$	$0.32 \pm 5\%$		
	$C_2H_2^+ + 2H_2 + N_2$	$0.18 \pm 5\%$		
	$CH_3^+ + CH_3 + N_2$	$0.08 \pm 10\%$		
	$CH_4^+ + CH_2 + N_2$	$0.01 \pm 10\%$		
$N_2^+ + C_2D_6$	$C_2D_5^+ + D + N_2$	0.14	1.25×10^{-9} ($\pm30\%$)	1.25×10^{-9} ($\pm30\%$)
	$C_2D_4^+ + D_2 + N_2$	0.27		
	$C_2D_3^+ + D_2 + D + N_2$	0.32		
	$C_2D_2^+ + 2 D_2 + N_2$	0.18		
	$CD_3^+ + CD_3 + N_2$	0.08		
	$CD_4^+ + CD_2 + N_2$	0.01		
$N_2^+ + C_3H_8$	$C_3H_5^+ + H_2 + H + N_2$	$0.13 \pm 5\%$	1.30×10^{-9} ($\pm30\%$)	1.30×10^{-9} ($\pm30\%$)
	$C_2H_5^+ + CH_3 + N_2$	$0.30 \pm 5\%$		
	$C_2H_4^+ + CH_4 + N_2$	$0.17 \pm 5\%$		
	$C_2H_3^+ + CH_4 + H + N_2$	$0.40 \pm 5\%$		
$^{14}N^+ + {}^{15}N_2$ or $^{15}N^+ + {}^{14}N_2$	$^{15}N^+ + {}^{14}N^{15}N$	1	2.1×10^{-10} ($\pm25\%$)	2.1×10^{-10} ($\pm25\%$)
	$^{14}N^+ + {}^{14}N^{15}N$	1		
$N^+ + H_2$	$NH^+ + H$	1	3.8×10^{-10} ($\pm20\%$)	3.0×10^{-10} ($\pm30\%$)
$N^+ + HD$	$NH^+ + D$	$0.25 \pm 5\%$ (300 K)	3.1×10^{-10} ($\pm20\%$)	2.4×10^{-10} ($\pm30\%$)
		$0.07 \pm 10\%$ (105 K)		
	$ND^+ + H$	$0.75 \pm 5\%$ (300 K)		
		$0.93 \pm 5\%$ (105 K)		
$N^+ + D_2$	$ND^+ + D$	1	1.2×10^{-10} ($\pm20\%$)	9.5×10^{-11} ($\pm30\%$)
$N^+ (^3P) + CH_4$	$CH_3^+ + NH$	$0.5 \pm 5\%$	1.15×10^{-9} ($\pm20\%$)	1.0×10^{-9} ($\pm20\%$)
	$CH_4^+ + N$	$0.05 \pm 10\%$		
	$HCNH^+ + H_2$	$0.35 \pm 5\%$		
	$HCN^+ + H_2 + H$	$0.10 \pm 10\%$		
$N^+ (^1D) + CH_4$	$CH_3^+ + NH$	$0.09 \pm 10\%$	1.15×10^{-9} ($\pm20\%$)	1.0×10^{-9} ($\pm20\%$)
	$CH_4^+ + N$	$0.40 \pm 5\%$		
	$HCNH^+ + H_2$	$0.33 \pm 5\%$		
	$HCN^+ + H_2 + H$	$0.18 \pm 5\%$		
$N^+ (^3P) + C_2H_2$	$C_2H_2^+ + N$	$0.70 \pm 5\%$	1.42×10^{-9} ($\pm20\%$)	1.42×10^{-9} ($\pm20\%$)
	$CNC^+ + H_2$	$0.15 \pm 5\%$		
	$CHCN^+ + H$	$0.15 \pm 5\%$		
$N^+ (^1D) + C_2H_2$	$C_2H_2^+ + N$	0.90	1.42×10^{-9} ($\pm20\%$)	1.42×10^{-9} ($\pm20\%$)
	$CNC^+ + H_2$	0.05		
	$CHCN^+ + H$	0.05		
$N^+ (^3P) + C_2H_4$	$C_2H_2^+ + NH_2$	$0.12 \pm 5\%$	1.58×10^{-9} ($\pm20\%$)	1.58×10^{-9} ($\pm20\%$)
	$C_2H_3^+ + NH$	$0.32 \pm 5\%$		
	$C_2H_4^+ + N$	$0.38 \pm 5\%$		

Table 17
(Continued)

Reaction	Products[a]	Branching Ratio[a]	k (cm^3 s^{-1})[a] at 300 K with Uncertainty[a]	k (cm^3 s^{-1})[a] at 150 K with Uncertainty
	HCN$^+$ + CH$_3$	0.02 ± 10%		
	HCNH$^+$ + CH$_2$	0.10 ± 10%		
	CHCN$^+$ + H$_2$ + H	0.01 ± 10%		
	CH$_2$CN$^+$ + H$_2$	0.05 ± 10%		
N$^+$ (^3P) + C$_2$D$_4$	C$_2$D$_2^+$ + ND$_2$	0.12	1.55 × 10^{-9} (±20%)	1.55 × 10^{-9} (±20%)
	C$_2$D$_3^+$ + ND	0.32		
	C$_2$D$_4^+$ + N	0.38		
	DCN$^+$ + CD$_3$	0.02		
	DCND$^+$ + CD$_2$	0.10		
	CDCN$^+$ + D$_2$ + D	0.01		
	CD$_2$CN$^+$ + D$_2$	0.05		
N$^+$ (^1D) + C$_2$H$_4$	C$_2$H$_2^+$ + NH$_2$	0.26 ± 5%	1.58 × 10^{-9} (±30%)	1.58 × 10^{-9} (±30%)
	C$_2$H$_3^+$ + NH	0.22 ± 5%		
	C$_2$H$_4^+$ + N	0.46 ± 5%		
	HCN$^+$ + CH$_3$	(0.06 ± 10%		
	HCNH$^+$ + CH$_2$	for the sum of		
	CHCN$^+$ + H$_2$ + H	N bearing ions)		
	CH$_2$CN$^+$ + H$_2$			
N$^+$ (^3P) + C$_2$H$_6$	C$_2$H$_5^+$ + NH	0.10 ± 10%	1.6 × 10^{-9} (±20%)	1.6 × 10^{-9} (±20%)
	C$_2$H$_4^+$ + NH$_2$	0.55 ± 5%		
	C$_2$H$_3^+$ + NH$_3$	0.25 ± 5%		
	HCNH$^+$ + CH$_4$	0.10 ± 10%		
N$^+$ (^1D) + C$_2$H$_6$	C$_2$H$_5^+$ + NH	?	1.6 × 10^{-9} (±30%)	1.6 × 10^{-9} (±30%)
	C$_2$H$_4^+$ + NH$_2$	?		
	C$_2$H$_3^+$ + NH$_3$	?		
	HCNH$^+$ + CH$_4$	?		
N$^+$ (^3P) + C$_3$H$_8$	C$_2$H$_3^+$ + CH$_4$ + NH	0.12	1.8 × 10^{-9} ± 20%	1.8 × 10^{-9} ± 20%
	C$_2$H$_4^+$ + CH$_3$ + NH	0.25		
	C$_2$H$_5^+$ + CH$_2$ + NH	0.36		
	C$_3$H$_5^+$ + NH$_3$	0.11		
	C$_3$H$_6^+$ + NH$_2$	0.05		
	C$_3$H$_7^+$ + NH	0.09		
	C$_3$H$_8^+$ + N	0.02		
N$^+$ (^1D) + C$_3$H$_8$	C$_2$H$_3^+$ + CH$_4$ + NH	?	1.8 × 10^{-9} ± 20%	1.8 × 10^{-9} ± 20%
	C$_2$H$_4^+$ + CH$_3$ + NH	?		
	C$_2$H$_5^+$ + CH$_2$ + NH	?		
	C$_3$H$_5^+$ + NH$_3$	?		
	C$_3$H$_6^+$ + NH$_2$	?		
	C$_3$H$_7^+$ + NH	?		
	C$_3$H$_8^+$ + N	?		
^{14}N$_2^{++}$ + ^{15}N$_2$	^{14}N$_2^+$ + ^{15}N$_2^+$	0.9 ± 25%	1.7 × 10^{-9} (±25%)	1.7 × 10^{-9} (±25%)
	^{14}N$_2^+$ + ^{15}N$^+$ + ^{15}N	0.1 ± 25%		
N$_2^{++}$ + H$_2$	N$_2^+$ + H$_2^+$	0.53 ± 5%	3.1 × 10^{-9} (±25%)	3.1 × 10^{-9} (±25%)
	N$^+$ + H$_2^+$ + N	0.32 ± 5%		
	N$_2^+$ + H$^+$ + H	0.10 ± 5%		
	N$^+$ + H$^+$ + (N + H)	0.03 ± 10%		
	NH$^+$ + H$^+$ + N	0.02 ± 10%		
N$_2^{++}$ + D$_2$	N$_2^+$ + D$_2^+$	0.61 ± 5%	2.2 × 10^{-9} (±25%)	2.2 × 10^{-9} (±25%)
	N$^+$ + D$_2^+$ + N	0.24 ± 5%		
	N$_2^+$ + D$^+$ + D	0.12 ± 5%		
	N$^+$ + D$^+$ + (N + D)	0.02 ± 10%		
	ND$^+$ + D$^+$ + N	0.01 ± 10%		
N$_2^{++}$ + CH$_4$	N$_2^+$ + CH$_4^+$	0.22	1.8 × 10^{-9} (±25%)	1.8 × 10^{-9} (±25%)
	N$_2^+$ + CH$_3^+$ + H	0.54		
	N$_2^+$ + CH$_2^+$ + H$_2$	0.15		
	HCNH$^+$ + NH$^+$ + H	0.06		
	HCN$^+$ + NH$_2^+$ + H	0.03		

Table 17
(Continued)

Reaction	Products[a]	Branching Ratio[a]	k (cm^3 s^{-1})[a] at 300 K with Uncertainty[a]	k (cm^3 s^{-1})[a] at 150 K with Uncertainty
N_2^{++} + CD$_4$	N_2^+ + CD$_4^+$	0.22 ± 25%	1.8×10^{-9} (±25%)	1.8×10^{-9} (±25%)
	N_2^+ + CD$_3^+$ + D	0.54 ± 25%		
	N_2^+ + CD$_2^+$ + D$_2$	0.15 ± 25%		
	DCND$^+$ + ND$^+$ + D	0.06 ± 25%		
	DCN$^+$ + ND$_2^+$ + D	0.03 ± 25%		
N_2^{++} + C$_2$H$_2$	N_2^+ + C$_2$H$_2^+$	?	2.3×10^{-9}	2.3×10^{-9}
	N_2^+ + C$_2$H$^+$ + H	?		
	N_2^+ + C$_2^+$ + H$_2$	?		
	HCNH$^+$ + CN$^+$	?		
	HCN$^+$ + HCN$^+$	?		
N_2^{++} + C$_2$H$_4$	N_2^+ + C$_2$H$_4^+$	0.26	2.2×10^{-9}	2.2×10^{-9}
	N_2^+ + C$_2$H$_3^+$ + H	0.41		
	N_2^+ + C$_2$H$_2^+$ + H$_2$	0.18		
	N_2^+ + C$_2$H$^+$ + H$_2$ + H	0.01		
	N_2^+ + CH$_3^+$ + CH	0.03		
	N_2^+ + CH$_2^+$ + CH$_2$	0.06		
	HCNH$^+$ + NH$^+$ + CH	0.02		
	HCN$^+$ + NH$_2^+$ + CH	0.03		
N_2^{++} + C$_2$D$_4$	N_2^+ + C$_2$D$_4^+$	0.26 ± 25%	2.2×10^{-9} (±25%)	2.2×10^{-9} (±25%)
	N_2^+ + C$_2$D$_3^+$ + D	0.41 ± 25%		
	N_2^+ + C$_2$D$_2^+$ + D$_2$	0.18 ± 25%		
	N_2^+ + C$_2$D$^+$ + D$_2$ + D	0.01 ± 25%		
	N_2^+ + CD$_3^+$ + CD	0.03 ± 25%		
	N_2^+ + CD$_2^+$ + CD$_2$	0.06 ± 25%		
	DCND$^+$ + ND$^+$ + CD	0.02 ± 25%		
	DCN$^+$ + ND$_2^+$ + CD	0.03 ± 25%		
N_2^{++} + C$_2$H$_6$	N_2^+ + C$_2$H$_6^+$	?	2.6×10^{-9} (±25%)	2.6×10^{-9} (±25%)
	N_2^+ + C$_2$H$_5^+$ + H	?		
	N_2^+ + C$_2$H$_4^+$ + H$_2$	?		
	N_2^+ + C$_2$H$_3^+$ + H$_2$ + H	?		
	N_2^+ + C$_2$H$_2^+$ + 2H$_2$	?		
	N_2^+ + CH$_3^+$ + CH$_3$	?		
	HCNH$^+$ + NH$^+$ + CH$_3$	?		
	HCN$^+$ + NH$_2^+$ + CH$_3$	?		
N_2^{++} + C$_3$H$_8$	N_2^+ + C$_3$H$_8^+$	?	2.8×10^{-9} (±25%)	2.8×10^{-9} (±25%)
	N_2^+ + C$_3$H$_7^+$ + H	?		
	N_2^+ + C$_3$H$_5^+$ + H$_2$ + H	?		
	N_2^+ + C$_2$H$_5^+$ + CH$_3$	?		
	N_2^+ + C$_2$H$_4^+$ + CH$_4$	?		
	N_2^+ + C$_2$H$_3^+$ + CH$_3$ + H$_2$	?		
	HCNH$^+$ + NH$_2^+$ + C$_2$H$_4$	?		
	HCN$^+$ + NH$^+$ + C$_2$H$_6$	?		
N^{++} + N$_2$	N^+ + N$^+$ + N	1	2.04×10^{-9} (±20%)	2.04×10^{-9} (±20%)
N^{++} + H$_2$	N^+ + H$_2^+$	?	3.4×10^{-11} (±10%)	3.4×10^{-11} (±20%)
	N^+ + H$^+$ + H	?		
	N + H$^+$ + H$^+$	?		

Note. [a] Estimated products and estimated rate constant and branching ratio values are in italic characters.

Table 18
Summary for Electron–Ion Recombination Reactions of Nitrogen Ions

Reaction	Products	Recommended Yield	Rate Constant (cm^3 s^{-1})
N_2^+ + e	N (^4S)	0.25 ± 25%	2.2×10^{-7} $(T_e/300)^{-0.39}$ (±25%)
	N (^2D)	0.7 ± 25%	
	N (^2P)	0.05 ± 25%	
N^+ + e	N + hν	1	3.5×10^{-12} $(T_e/300)^{-0.7*}$
N_2^{++} + e	N^+ + N	1	5.8×10^{-7} $(T_e/300)^{-0.5}$ (±25%)
N^{++} + e	N^+ + hν	1	2.2×10^{-12} $(T_e/10000)^{-0.639*}$

Note. * Calculated value (see the text).

Much more critical is the situation with the products of the reactions of the neutrals of interest, as there are almost no complete measurements of reaction product branching ratios, even at 300 K. It is worth noting that for neutral–neutral reactions, experimental support is necessary for determining branching ratios, especially at low temperatures, as theoretical estimates can only be achieved using RRKM methods, when reactions behave statistically. Rate constants involving neutral species have been measured for a large number of reactions, but it is only in the past 15 years that the experimental and theoretical tools have become available to explore quantitatively the product branching ratios of reactions. The latest promising development is the use of the Advanced Light Source (ALS) at Berkeley which provides tuneable synchrotron radiation to photoionize the products from neutral–neutral reactions. The ionized products are then analyzed by time of flight or quadrupole mass spectrometry (Osborn et al. 2008; Soorkia et al. 2008). In addition, to our knowledge, no quantitative experimental investigations of the branching ratios of reactions involving atomic nitrogen have been made at low temperature.

For ion–molecule reactions, even though the experimental and theoretical work is plentiful for reactions at 300 K, the information is still incomplete at this temperature. However, with some exceptions, most reaction rate constants are equal or close to the Langevin rate, which is independent of temperature and is the maximum value of the rate constant for target molecules with no permanent dipole. The reactivity of the long-lived N^+ (^1D) metastable state and of the relevant doubly charged ions is still very poorly known. This lack of information can explain why these reactions have not yet been included in models of planetary atmospheres. In summary, the N_2^+ reactions with hydrocarbons produce mainly charge transfer (dissociative or non dissociative) and minor N_2H^+ products via H transfer, whereas the N^+ (^3P) reactions involve significant chemical reactions, in particular the formation of C-N bonds. The few N^+ (^1D) metastable state reactions which have been investigated give the same ion products as the N^+ (^3P) ground state reactions, but their branching ratios are different, with a higher yield for products arising from charge transfer. Let us note that the data concerning the products of ion–molecule reactions is much more complete than for neutral reactions, due to the fact that they can be easily detected by mass spectrometry. However, information concerning the neutral products associated with product ions is sometimes lacking and requires more theoretical or experimental work. More information is also desirable about the isomeric structure of products, as their further reactions can be affected. For example, the production of HCN and HNC in Titan's upper atmosphere has been recently modeled (Hébrard et al. 2012). This study reveals the need for more experimental measurements to improve the chemistry of these two isomers. It is also the case for the corresponding ions, as a very different reactivity is expected for HCN^+ and HNC^+ isomeric ions, because of their peculiar thermo-chemistry, as HNC^+ is more stable than HCN^+ by 0.98 eV and HNC is less stable than HCN by 0.58 eV (Hansel et al. 1998a, 1998b). For doubly charged ions, there are experimental studies for only very few reactions, which all show that their rate constant is equal to the Langevin rate. The dominant process for the N_2^{++} reactivity is single charge transfer, both non-dissociative and dissociative, but surprisingly minor products coming from chemical reactions involving bond rearrangement are also observed. With hydrocarbons, there are only preliminary experiments for reactions of N_2^{++} with methane and ethylene, so a huge effort should be made, in particular to

measure the ion products with coincidence methods, as those developed by Price et al. (Lockyear et al. 2011; Price 2003, 2007).

The N_2^+ + e dissociative recombination reaction is still not well understood, as discrepancies remain between the different experimental and theoretical studies: this reaction certainly deserves further work to determine more precise N (^2D)/N (^2P)/N (^4S) yields. The N_2^{++} + e reaction also needs further investigation, as some questions are still unresolved, such as the electronic state of the N^+ and N products formed by electron dissociative recombination or the branching ratio between the dissociative electron recombination (N^+ + N) and the dissociation induced by electrons without electron capture (N^+ + N^+).

The study of isotope effects is a highlighted topic among planetary scientists for the last few years. Isotope effects can give a lot of information about the evolution of a planet's atmosphere. Fractionation of the ^{12}C/^{13}C and D/H ratios in methane or ^{15}N/^{14}N in molecular nitrogen have been recently investigated for Titan (Mandt et al. 2009, 2012; Nixon et al. 2012). This fractionation, due to atmospheric escape over geological times, requires an excellent knowledge of the isotopically resolved physicochemical processes, in particular the kinetic isotope effect, i.e. the difference of reactivity between isotopic species. For bimolecular reactions, D/H isotope effects can play a significant role and were reviewed in this paper, even though many data are still lacking as it can be seen in Tables 16 and 17. For carbon and nitrogen, the reactivity is the same for the different isotopic species. Indeed species labeled with ^{13}C and/or ^{15}N atoms are often used as an experimental route to better identify the reaction products, as was mentioned several times in this paper. However, it would be important to better address the question of atom exchange and scrambling of atoms involving carbon and/or nitrogen atoms in reactions, in order to better identify the route of isotopic molecular species in the chain of chemical reactions.

This paper is focused on the principal reactions which are the first steps in the chemistry of Titan's atmosphere. In the future, it would be important to make also a critical review of other reactions which play an important role later in the chemical chain. Studies should also be extended to reactions with other molecules present in Titan's atmosphere, such as HCN, which is more abundant than C_2H_6 and C_3H_8, or other unsaturated hydrocarbons such as C_3H_4, C_3H_6, or C_4H_2, aromatics such as C_6H_6, nitriles such as C_2N_2, CH_3CN, HC_3N, species, all of which are present in Titan's atmosphere (Bézard 2009; Magee et al. 2009; Teanby et al. 2008, 2009). Studies should involve reactions of other species, in particular radical or ionic hydrocarbons, as well as negative ions, which play an essential role in molecular growth in Titan's atmosphere. Such a review would help to address the important issue of the formation of complex molecules and aerosols in Titan's atmosphere. We must also note that we did not review in this paper neither the termolecular reactions that are present in Titan's atmosphere at low altitudes, nor reactions on surfaces.

Termolecular reactions of N atoms are not relevant for Titan's atmosphere, as N atoms are mainly formed by photodissociation above 1000 km altitude, where the pressure is too low for triple collisions to occur. However at low altitudes, termolecular chemistry can occur with ions formed by galactic cosmic rays (Gronoff et al. 2009a, 2009b, 2011; Molina-Cuberos et al. 1999). Anicich & McEwan (Anicich & McEwan 2001; Anicich et al. 2000; Milligan et al. 2001) studied experimentally termolecular

ion–molecule reactions of the main ions of Titan's atmosphere. Vacher et al. (1997, 2000) and Anicich & McEwan (2001) found in particular a substantial clustering of HCNH$^+$ ions with N$_2$ molecules by triple collisions which could be very effective at altitudes below 90 km, according to Anicich & McEwan (2001).

Heterogeneous reactions of nitrogen species in Titan's atmosphere involve most likely interactions with surfaces of aerosols, i.e., surfaces composed of organic (C–H–N) compounds The different heterogeneous processes have been recently described in the book on Titan to be published by Cambridge University Press (Vuitton et al. 2012). For nitrogen species, very few experimental studies have been performed in conditions relevant to Titan. When N$_2$ adsorbs on a surface at high temperature, it can dissociate (Ertl 1980) and the produced atomic nitrogen can proceed to further chemical reactions. This interaction is well known since the beginning of the 20th century and has been used for the catalytic production of ammonia and nitrogen-rich fertilizers (Haber–Bosch process) with substantial socio-economical consequences. However, it is possible to overcome the requirement of high temperature if the surface interacts with N$_2$ molecular ions (Lancaster & Rabalais 1979). Concerning neutral nitrogen surface reactions, a very effective heterogeneous chemistry has been indirectly observed in experimental simulations at low temperatures of the first steps of Titan's ion chemistry (Thissen et al. 2009). The experimental results could not been interpreted without involving a very effective formation of HCN and NH$_3$ on surfaces, probably induced by N atoms (Thissen et al. 2009). Other studies showed the importance of heterogeneous interaction of hydrogen atoms on the surfaces of Tholins, which can have further implications for the chemical composition of the atmosphere (Lavvas et al. 2008c; Sekine et al. 2008a, 2008b). Information on collisions of N$_2^+$ with Tholins (laboratory analogs of Titan's aerosols) has so far not been available. Related information may be presumably obtained from studies of hyperthermal collisions of nitrogen ions with hydrocarbons layers (C–H compounds, assumed to be C7–C8 chains) covering carbon and other surfaces (Herman et al. 2009, 2012; Keim et al. 2012). The main process is surface neutralization, the survival probability S_a(%) of nitrogen molecular ions being only 0.002%–0.02% (Herman et al. 2009, 2012). The nature of neutral products is not known. Mass spectra of products ions show sputtering of the surface material (Keim et al. 2012), no heterogeneous chemical reactions of N$_2^+$ have been so far clearly identified. For the other nitrogen ions (N$^+$, N$_2^{++}$, N^{++}), the correlation function between S_a and the ionization energy measured for other ions can be used to predict their survival probability (Herman et al. 2009), indicating a value of the same order of magnitude or smaller. At collision energies close to thermal energies, trapping of the incident particles on the surface may be important. Similar studies for other species need to further investigate the heterogeneous interaction of N$_2$ and its ions with the surface of Tholins.

In conclusion, this work of evaluation by experts of all types of reactions is essential for planetary scientists, as well as for astrophysicists. Therefore, the new KIDA database (Wakelam et al. 2012) which includes a critical evaluation of neutral and ion reactions is a very promising and important tool for modelers.

Annex: List of contacts among the authors for the different types of reactions and processes

Reactions of neutrals: Nadia Balucani, Piergiorgio Casavecchia, Sébastien Le Picard, Jean-Christophe Loison

Ion–molecule reactions: Odile Dutuit, Roland Thissen, Christian Alcaraz, Daniela Ascenzi, Pietro Franceschi, Paolo Tosi, Zdenek Herman, Jan Zabka, Stephen Price

Electron recombination reactions: André Canosa

Uncertainty propagation: Nathalie Carrasco, Pascal Pernot

Titan ion and neutral chemistry in models: Véronique Vuitton, Panayotis Lavvas

REFERENCES

Adams, N. G., Poterya, V., & Babcock, L. M. 2006, Mass Spectrom. Rev., 25, 798
Adams, N. G., & Smith, D. 1976, IJMSI, 21, 349
Adams, N. G., & Smith, D. 1981, ApJL, 247, L123
Adams, N. G., & Smith, D. 1985, CPL, 117, 67
Adams, N. G., Smith, D., & Paulson, J. F. 1980, JChPh, 72, 288
Ahmad, M., Lablanquie, P., Penent, F., et al. 2006, JPhB, 39, 3599
Ajello, J. M., Gustin, J., Stewart, I., et al. 2008, GeoRL, 35, L06102
Alcaraz, C., Nicolas, C., Thissen, R., Zabka, J., & Dutuit, O. 2004, JPCA, 108, 9998
Aldrovandi, S. M. V., & Pequignot, D. 1973, A&A, 25, 137
Anicich, V. 2003, JPL Pub. 03-19 (Pasadena, CA: NASA)
Anicich, V. G. 1993, JPCRD, 22, 1469
Anicich, V. G., Huntress, W. T., Jr., & Futrell, J. H. 1977, CPL, 47, 488
Anicich, V. G., & McEwan, M. J. 1997, P&SS, 45, 897
Anicich, V. G., & McEwan, M. J. 2001, Icar, 154, 522
Anicich, V. G., Milligan, D. B., Fairley, D. A., & McEwan, M. J. 2000, Icar, 146, 118
Anicich, V. G., Wilson, P., & McEwan, M. J. 2004, J. Am. Soc. Mass Spectrom., 15, 1148
Aoto, T., Ito, K., Hikosaka, Y., et al. 2006, JChPh, 124, 6
Avakyan, S. V. 1979, Ge&Ae, 18, 652
Bahati, E. M., Jureta, J. J., Belic, D. S., et al. 2001, JPhB, 34, 2963
Bakalian, F. 2006, Icar, 183, 69
Balucani, N., Alagia, M., Cartechini, L., et al. 2000a, JAChS, 122, 4443
Balucani, N., Bergeat, A., Cartechini, L., et al. 2009, JPCA, 113, 11138
Balucani, N., Cartechini, L., Alagia, M., Casavecchia, P., & Volpi, G. G. 2000b, JPCA, 104, 5655
Balucani, N., Cartechini, L., Capozza, G., et al. 2002, PhRvL, 89, 013201
Balucani, N., Casavecchia, P., Banares, L., et al. 2006, JPCA, 110, 817
Balucani, N., Leonori, F., Petrucci, R., et al. 2010, FaDi, 147, 189
Balucani, N., Skouteris, D., Leoneri, F., & Petrucci, R. 2012, JPCA, 116, 10467
Bates, D. R., & Mitchell, J. B. A. 1991, P&SS, 39, 1297
Bell, R. P. 1942, Trans. Faraday Soc., 38, 422
Besnard, M. J., Hellner, L., Dujardin, G., & Winkoun, D. 1988, JChPh, 88, 1752
Bézard, B. 2009, RSPTA, 367, 683
Bhardwaj, A., & Jain, S. K. 2012, Icar, 217, 752
Black, G., Sharpless, R. L., Slanger, T. G., & Lorents, D. C. 1975, JChPh, 62, 4266
Black, G., Slanger, T. G., St. John, G. A., & Young, R. A. 1969, JChPh, 51, 116
Bohmer, E., & Hack, W. 1989, BBGPC, 93, 170
Bohmer, E., & Hack, W. 1991, ZPhys. Chem., 170, 15
Böhringer, H., Durup-Ferguson, M., Ferguson, E. E., & Fahey, D. W. 1983, P&SS, 31, 483
Brehm, B., & de Frênes, G. 1978, Int. J. Mass Spectrom. Ion Phys., 26, 251
Broadfoot, A. L., Hatfield, D. B., Anderson, E. R., et al. 1997, JGR, 102, 11567
Brown, R. L. 1973, Int. J. Chem. Kinetics, 5, 663
Callear, A. B., & Wood, P. M. 1971, Trans. Faraday Soc., 67, 272
Canosa, A., Gomet, J. C., Rowe, B. R., & Queffelec, J. L. 1991, JChPh, 94, 7159
Cao, D. Z., & Setser, D. W. 1985, CPL, 116, 363
Carrasco, N., Alcaraz, C., Dutuit, O., et al. 2008a, P&SS, 56, 1644
Carrasco, N., Dutuit, O., Thissen, R., Banaszkiewicz, M., & Pernot, P. 2007, P&SS, 55, 141
Carrasco, N., & Pernot, P. 2007, JPCA, 111, 3507
Carrasco, N., Plessis, S., Dobrijevic, M., & Pernot, P. 2008b, Int. J. Chem. Kinetics, 40, 699
Carroll, P. K. 1958, CaJPh, 36, 1585
Casavecchia, P., Balucani, N., Cartechini, L., et al. 2001, FaDi, 119, 27
Church, D. A., & Holzscheiter, H. M. 1980, CPL, 76, 109

Cimas, A., & Largo, A. 2006, JPCA, 110, 10912
Clark, W. G., & Setser, D. W. 1980, JPhCh, 84, 2225
Coates, A. J., Crary, F. J., Young, D. T., et al. 2007, GeoRL, 34, L24S05
Cossart, D., Cossart-Magos, C., & Launay, F. 1991, J. Chem. Soc. Faraday Trans., 87, 2525
Cossart, D., Launay, F., Robbe, J. M., & Gandara, G. 1985, JMoSp, 113, 142
Crary, F. J., Magee, B. A., Mandt, K., et al. 2009, P&SS, 57, 1847
Cravens, T. E., Robertson, I. P., Waite, J. H., Jr., et al. 2009, Icar, 199, 174
Cravens, T. E., Robertson, I. P., Waite, J. H., Jr., et al. 2006, GeoRL, 33, L07105
Crowe, A., & McConkey, J. W. 1973, JPhB, 6, 2108
Cui, J., Yelle, R. V., Vuitton, V., et al. 2009, Icar, 200, 581
Cunningham, A. J., & Hobson, R. M. 1972, JPhB, 5, 2328
Dawber, G., McConkey, A. G., Avaldi, L., et al. 1994, JPhB, 27, 2191
de Gouw, J. A., Ding, L. N., Frost, M. J., et al. 1995, CPL, 240, 362
De la Haye, V., Waite, J. H., Jr., Johnson, R. E., et al. 2007, JGRA, 112, A07309
DePrince, A. E., III, & Mazziotti, D. A. 2008, JPCB, 112, 16158
Dheandhanoo, S., Johnsen, R., & Biondi, M. A. 1984, P&SS, 32, 1301
Dobrijevic, M., Carrasco, N., Hebrard, E., & Pernot, P. 2008, P&SS, 56, 1630
Dobrijevic, M., Hébrard, E., Plessis, S., et al. 2010, AdSpR, 45, 77
Donovan, R. J., & Husain, D. 1970, Chem. Rev., 70, 489
Dreyer, J. W., & Perner, D. 1971, CPL, 12, 299
Dreyer, J. W., & Perner, D. 1973, JChPh, 58, 1195
Dryahina, K., Cunha de Miranda, B. K., Spanel, P., et al. 2011, JPCA, 115, 7310
Edberg, N. J. T., Wahlund, J. E., Agren, K., et al. 2010, GeoRL, 37, L20105
Ehresmann, A., Liebel, H., Schmoranzer, H., et al. 2003, JPhB, 36, 3669
Ertl, G. 1980, Catalysis Rev.: Sci. Eng., 21, 201
Ervin, K. M., & Armentrout, P. B. 1985, JChPh, 83, 166
Ervin, K. M., & Armentrout, P. B. 1987, JChPh, 86, 2659
Fang, Z., & Kwong, V. H. S. 1997, PhRvA, 55, 440
Fang, Z., Kwong, V. H. S., & Parkinson, W. H. 1993, ApJL, 413, L141
Fehsenfeld, F. C., Albritton, D. L., Bush, Y. A., et al. 1974, JChPh, 61, 2150
Fehsenfeld, F. C., Schmeltekopf, A. L., & Ferguson, E. E. 1967, JChPh, 46, 2802
Fell, B., Rivas, I. V., & McFadden, D. L. 1981, JPhCh, 85, 224
Ferreira, N., Sigaud, L., de Jesus, V. L. B., et al. 2012, PhRvA, 86, 012702
Florescu-Mitchell, A. I., & Mitchell, J. B. A. 2006, PhR, 430, 277
Fournier, P., van de Runstraat, C. A., Govers, T. R., et al. 1971, CPL, 9, 426
Fox, J. L. 1992, P&SS, 40, 1663
Fox, J. L. 1993, JGRE, 98, 3297
Fox, J. L., & Dalgarno, A. 1979, JGRA, 84, 7315
Fox, J. L., & Dalgarno, A. 1985, JGRA, 90, 7557
Fox, J. L., Rowe, B. R., Mitchell, J. B. A., & Canosa, A. 1993, in Dissociative Recombination: Theory Experiments and Applications (New York: Plenum Press), 219
Franceschi, P., Ascenzi, D., Tosi, P., et al. 2007, JChPh, 126, 4310
Freysinger, W., Khan, F. A., Armentrout, P. B., et al. 1994, JChPh, 101, 3688
Frost, M. J., Kato, S., Bierbaum, V. M., & Leone, S. R. 1994, JChPh, 100, 6359
Fulchignoni, M., Ferri, F., Angrilli, F., et al. 2005, Natur, 438, 785
Ge, S.-H., Cheng, X.-L., Yang, X.-D., Liu, Z.-J., & Wang, W. 2006, Icar, 183, 153
Geoghegan, M., Adams, N. G., & Smith, D. 1991, JPhB, 24, 2589
Gerlich, D. 1989, JChPh, 90, 3574
Gerlich, D. 1993, J. Chem. Soc.: Faraday Trans., 89, 2199
Gianturco, F. A., & Giorgi, P. G. 1997, ApJ, 479, 560
Gichuhi, W. K., & Suits, A. G. 2011, JPCA, 115, 7105
Gilmore, F. 1965, JQSRT, 5, 369
Glosik, J., Luca, A., Mark, S., & Gerlich, D. 2000, JChPh, 112, 7011
Golde, M. F. 1988, Int. J. Chem. Kinetics, 20, 75
Golde, M. F., Ho, G. H., Tao, W., & Thomas, J. M. 1989, JPhCh, 93, 1112
Gronoff, G., Lilensten, J., Desorgher, L., & Flueckiger, E. 2009a, A&A, 506, 955
Gronoff, G., Lilensten, J., & Modolo, R. 2009b, A&A, 506, 965
Gronoff, G., Lilensten, J., Simon, C., et al. 2007, A&A, 465, 641
Gronoff, G., Mertens, C., Lilensten, J., et al. 2011, A&A, 529, A143
Guberman, S. L. 1991, GeoRL, 18, 1051
Guberman, S. L. 2003, in Dissociative Recombination of Molecular Ions with Electrons, ed. B. R. Rowe, J. B. A. Mitchell, & A. Canosa (New York: Kluwer), 187
Guberman, S. L. 2012, JChPh, 137, 074309
Guberman, S. L., Rowe, B. R., Mitchell, J. B. A., & Canosa, A. 1993, in Dissociative Recombination: Theory Experiments and Applications (New York: Plenum Press), 47
Hack, W., Kurzke, H., Ottinger, C., & Wagner, H. G. 1988, CP, 126, 111
Hagstrum, H. D., & Tate, J. T. 1941, PhRv, 59, 354
Halas, S., & Adamczyk, B. 1972, Int. J. Mass Spectrom. Ion Phys., 10, 157
Hansel, A., Glantschnig, M., Scheiring, C., Lindinger, W., & Ferguson, E. E. 1998a, JChPh, 109, 1743

Hansel, A., Scheiring, C., Glantschnig, M., Lindinger, W., & Ferguson, E. E. 1998b, JChPh, 109, 1748
Harrison, A. G., & Myher, J. J. 1967, JChPh, 46, 3276
Hébrard, E., Dobrijevic, M., Bénilan, Y., & Raulin, F. 2006, J. Photochem. Photobiol. C: Photochem. Rev., 7, 211
Hébrard, E., Dobrijevic, M., Bénilan, Y., & Raulin, F. 2007, P&SS, 55, 1470
Hébrard, E., Dobrijevic, M., Loison, J. C., Bergeat, A., & Hickson, K. M. 2012, A&A, 541, 21
Hébrard, E., Dobrijevic, M., Pernot, P., et al. 2009, JPCA, 113, 11227
Helm, H., & Cosby, P. C. 1989, JChPh, 90, 4208
Henri, G., Lavollée, M., Dutuit, O., et al. 1988, JChPh, 88, 6381
Herbst, E., Terzieva, R., & Talbi, D. 2000, MNRAS, 311, 869
Herman, Z., Zabka, J., & Pysanenko, A. 2009, JPCA, 113, 14838
Herman, Z., Zabka, J., & Pysanenko, A. 2012, MolPh, 110, 1669
Herod, A. A., Harrison, A. G., & McAskill, N. A. 1971, CaJCh, 49, 2217
Herron, J. T. 1966, JPhCh, 70, 2803
Herron, J. T. 1999, JPCRD, 28, 1453
Herron, J. T., & Huie, R. E. 1968, JPhCh, 72, 2538
Hiyama, M., & Iwata, S. 1993, CPL, 211, 319
Ho, G. H., & Golde, M. F. 1991, JChPh, 95, 8866
Hochlaf, M. 1996, CP, 207, 159
Honvault, P., & Launay, J. M. 1999, JChPh, 111, 6665
Huntress, W. T., Jr., McEwan, M. J., Karpas, Z., & Anicich, V. G. 1980, ApJS, 44, 481
Husain, D., Kirsch, L. J., & Wiesenfeld, J. R. 1972, Faraday Discuss. Chem. Soc., 53, 201
Husain, D., Mitra, S. K., & Young, A. N. 1974, J. Chem. Soc. Faraday Trans. II, 70, 1721
Itikawa, Y. 2006, JPCRD, 35, 31
Jain, S. K., & Bhardwaj, A. 2011, JGRE, 116, E07005
Johnsen, R. 2011, JPhCS, 300, 012002
Juran, J. M., & Godfrey, A. B. 1999, Quality Handbook (5th ed.; New York: McGraw Hill)
Kasner, W. H. 1967, PhRv, 164, 194
Kato, S., Bierbaum, V. M., & Leone, S. R. 1998, JPCA, 102, 6659
Kato, T., & Asano, E. 1999, NIFS-DATA-54 (Nagoya: National Institute for Fusion Science)
Keim, A., Harnisch, M., Menzel, A., Scheier, P., & Herman, Z. 2012, NIMPR, submitted
Kella, D., Johnson, P. J., Pedersen, H. B., Vejby-Christensen, L., & Andersen, L. H. 1996, PhRvL, 77, 2432
Keller, C. N., Cravens, T. E., & Gan, L. 1992, JGR, 97, 12117
Kieffer, L. J., & van Brunt, R. J. 1967, JChPh, 46, 2728
Kim, J. K., Theard, L. P., & Huntress, W. T., Jr. 1975, JChPh, 62, 45
Kjeldsen, H., Kristensen, B., Brooks, R. L., et al. 2002, ApJS, 138, 219
Knott, W. J., Proch, D., Kompa, K. L., & Rose-Petruck, C. 1995, JChPh, 102, 214
Koskinen, T. T., Yelle, R. V., Snowden, D. S., et al. 2011, Icar, 216, 507
Koyano, I., Tanaka, K., Kato, T., & Suzuki, S. 1987, FaDi, 84, 265
Krasnopolsky, V. A. 2009, Icar, 201, 226
Kurosaki, Y., Takayanagi, T., Sato, K., & Tsunashima, S. 1998, JPCA, 102, 254
Lammer, H., Stumptner, W., Molina-Cuberos, G. J., Bauer, S. J., & Owen, T. 2000, P&SS, 48, 529
Lancaster, G. M., & Rabalais, J. W. 1979, JPhCh, 83, 209
Lavvas, P., Coustenis, A., & Vardavas, I. M. 2008a, P&SS, 56, 27
Lavvas, P., Coustenis, A., & Vardavas, I. M. 2008b, P&SS, 56, 67
Lavvas, P., Galand, M., Yelle, R. V., et al. 2011, Icar, 213, 233
Lavvas, P., Yelle, R. V., & Vuitton, V. 2009, Icar, 201, 626
Lavvas, P. P., Coustenis, A., & Vardavas, I. M. 2008c, P&SS, 56, 67
Leblanc, F., Chaufray, J. Y., & Bertaux, J. L. 2007, GeoRL, 34, L02206
Leblanc, F., Chaufray, J. Y., Lilensten, J., Witasse, O., & Bertaux, J. L. 2006, JGRE, 111, E09s11
Lee, S.-H., Chin, C.-H., Chen, W.-K., Huang, W.-J., & Hsieh, C.-C. 2011, PCCP, 13, 8515
Levron, D., & Phelps, A. V. 1978, JChPh, 69, 2260
Lewis, B. R., Gibson, S. T., Zhang, W., Lefebvre-Brion, H., & Robbe, J. M. 2005, JChPh, 122, 144302
Li, Y.-H., & Harrison, A. G. 1978, Int. J. Mass Spectrom. Ion Process., 28, 289
Lilensten, J., Witasse, O., Simon, C., et al. 2005, GeoRL, 32, L03203
Lin, C.-L., & Kaufman, F. 1971, JChPh, 55, 3760
Lockyear, J. F., Ricketts, C. L., Parkes, M. A., & Price, S. D. 2011, Chem. Sci., 2, 150
Luine, J. A., & Dunn, G. H. 1985, ApJL, 299, L67
Lundqvist, M., Edvardsson, D., Baltzer, P., & Wannberg, B. 1996, JPhB, 29, 1489
Mackie, R. A., Sands, A. M., Scully, S. W. J., et al. 2002, JPhB, 35, 1061
Mackie, R. A., Sands, A. M., Scully, S. W. J., et al. 2003, IJMSp, 223, 67

Magee, B. A., Waite, J. H., Mandt, K. E., et al. 2009, P&SS, 57, 1895
Mahdavi, M. R., Hasted, J. B., & Nakshban, M. M. 1971, JPhB, 4, 1726
Maier, W. B., II, & Murad, E. 1971, JChPh, 55, 2307
Mandt, K. E., Waite, J. H., Lewis, W., et al 2009, P&SS, 57, 1917
Mandt, K. E., Waite, J. H., Teolis, B., et al. 2012, ApJ, 749, 160
Mark, S., & Gerlich, D. 1996, CP, 209, 235
Märk, T. D. 1975, JChPh, 63, 3731
Marquette, J. B., Rebrion, C., & Rowe, B. R. 1988, JChPh, 89, 2041
Marquette, J. B., Rowe, B. R., Dupeyrat, G., & Roueff, E. 1985, A&A, 147, 115
Marston, G., Nesbitt, F. L., Nava, D. F., Payne, W. A., & Stief, L. J. 1989a, JPhCh, 93, 5769
Marston, G., Nesbitt, F. L., & Stief, L. J. 1989b, JChPh, 91, 3483
Mathur, D., Andersen, L. H., Hvelplund, P., Kella, D., & Safvan, C. P. 1995, JPhB, 28, 3415
McAfee, K. B., Szmanda, C. R., & Hozack, R. S. 1981, JPhB, 14, L243
McEwan, M. J., & Anicich, V. G. 2007, Mass Spectrom. Rev., 26, 281
McEwan, M. J., Scott, G. B. I., & Anicich, V. G. 1998, IJMSI, 172, 209
McMahon, T. B., Miasek, P. G., & Beauchamp, J. L. 1976, Int. J. Mass Spectrom. Ion Phys., 21, 63
Mehr, F. J., & Biondi, M. A. 1969, PhRv, 181, 264
Meyer, J. A., Klosterboer, D. H., & Setser, D. W. 1971, JChPh, 55, 2084
Michael, J. V. 1979, CPL, 68, 561
Michael, J. V. 1980, CPL, 76, 129
Michael, J. V., & Lee, J. H. 1977, CPL, 51, 303
Milligan, D. B., Freeman, C. G., Maclagan, R., et al. 2001, J. Am. Soc. Mass Spectrom., 12, 557
Molina-Cuberos, G. J., Lopez-Moreno, J. J., Rodrigo, R., & Lara, L. M. 1999, JGRE, 104, 21997
Morrill, J. S., & Benesch, W. M. 1996, JGRA, 101, 261
Mul, P. M., & McGowan, J. W. 1979, JPhB, 12, 1591
Nahar, S. N., & Pradhan, A. K. 1997, ApJS, 111, 339
Nguyen, M. T., Sengupta, D., & Ha, T. K. 1996, JPhCh, 100, 6499
Nicolas, C. 2002, thesis Orsay, Univ. Paris-Sud
Nicolas, C., Alcaraz, C., Thissen, R., Vervloet, M., & Dutuit, O. 2003a, JPhB, 36, 2239
Nicolas, C., Torrents, R., & Gerlich, D. 2003b, JChPh, 118, 2723
Niemann, H. B., Atreya, S. K., Demick, J. E., et al. 2010, JGR, 115, E12006
Nixon, C. A., Temelso, B., Vinatier, S., et al. 2012, ApJ, 749, 159
Noren, C., Yousif, F. B., & Mitchell, J. B. A. 1989, J. Chem. Soc. Faraday Trans. II, 85, 1697
Oddone, S., Sheldon, J. W., Hardy, K. A., & Peterson, J. R. 1997, PhRvA, 56, 4737
Olsson, B. J. K., G., & Larsson, M. 1988, JChPh, 88, 7501
Osborn, D. L., Zou, P., Johnsen, H., et al. 2008, RScI, 79, 104103
Ouk, C.-M., Zvereva-Loete, N., & Bussery-Honvault, B. 2011, CPL, 515, 13
Payne, W. A., Monks, P. S., Nesbitt, F. L., & Stief, L. J. 1996, JChPh, 104, 9808
Pederson, L. A., Schatz, G. C., Ho, T.-S., et al. 1999, JChPh, 110, 9091
Peng, Z., Dobrijevic, M., Hebrard, E., Carrasco, N., & Pernot, P. 2010, FaDi, 147, 137
Peterson, J. R., Le Padellec, A., Danared, H., et al. 1998, JChPh, 108, 1978
Peterson, J. R., & Moseley, J. T. 1973, JChPh, 58, 172
Phelps, A. V. 1991, JPCRD, 20, 557
Piper, L. G. 1993, JChPh, 99, 3174
Piper, L. G., Donahue, M. E., & Rawlins, W. T. 1987, JPhCh, 91, 3883
Piper, L. G., Marinelli, W. J., Rawlins, W. T., & Green, B. D. 1985, JChPh, 83, 5602
Plessis, S., Carrasco, N., Dobrijevic, M., & Pernot, P. 2012, Icar, 219, 254
Plessis, S., Carrasco, N., & Pernot, P. 2010, JChPh, 133, 134110
Potts, A. W., & Williams, A. T. 1974, JESRP, 3, 3
Prasad, S. S., & Furman, D. R. 1975, JGR, 80, 1360
Praxmarer, C., Hansel, A., Lindinger, W., & Herman, Z. 1998, JChPh, 109, 4246
Price, S. D. 2003, PCCP, 5, 1717
Price, S. D. 2007, IJMSp, 260, 1
Queffelec, J. L., Rowe, B. R., Morlais, M., Gomet, J. C., & Vallee, F. 1985, P&SS, 33, 263
Rakshit, A. B. 1980, ZNatA, 35a, 1218
Ralchenko, Y., Kramida, A. E., Reader, J., & Team, N. A. 2011, NIST Atomic Spectra Database (version 4.1.0; Gaithersburg, MD: NIST), http://physics.nist.gov/asd
Randeniya, L. K., & Smith, M. A. 1991, JChPh, 94, 351
Richard, M. S., Cravens, T. E., Robertson, I. P., et al. 2011, JGRA, 116, 09310
Robertson, I. P., Cravens, T. E., Waite, J. H., et al. 2009, P&SS, 57, 1834
Roithova, J., & Schroder, D. 2007a, PCCP, 9, 2341
Roithova, J., & Schroder, D. 2007b, PCCP, 9, 731
Rosi, M., Falcinelli, S., Balucani, N., et al. 2012, ICCSA 2012, Computational Science and Its Applications (Vol. 7333; Berlin: Springer), 331

Rowe, B. R., Dupeyrat, G., Marquette, J. B., & Gaucherel, P. 1984, JChPh, 80, 4915
Rowe, B. R., Marquette, J. B., Dupeyrat, G., & Ferguson, E. E. 1985, CPL, 113, 403
Rowe, B. R., Marquette, J. B., & Rebrion, C. 1989, J. Chem. Soc. Faraday Trans., 85, 1631
Samson, J. A. R. 1990, PhRvL, 65, 2861
Samson, J. A. R., & Angel, G. C. 1990, PhRvA, 42, 1307
Samson, J. A. R., He, Z. X., Moberg, R., Stolte, W. C., & Cutler, J. N. 1996, CaJPh, 74, 722
Samson, J. A. R., Masuoka, T., Pareek, P. N., & Angel, G. C. 1987, JChPh, 86, 6128
Sato, S., Misawa, K., Kobayashi, Y., et al. 1999, JPCA, 103, 8650
Sato, S., Sugawara, K., & Ishikawa, Y. 1979, CPL, 68, 557
Schmidt, H. U., Wegmann, R., Huebner, W. F., & Boice, D. C. 1988, CoPhC, 49, 17
Schultz, R. H., & Armentrout, P. B. 1992, JChPh, 96, 1036
Schwarzer, M., Hansel, A., Freysinger, W., et al. 1991, JChPh, 95, 7344
Seiersen, K., Heber, O., Jensen, M. J., Safvan, C. P., & Andersen, L. H. 2003, JChPh, 119, 839
Sekine, Y., Imanaka, H., Matsui, T., et al. 2008a, Icar, 194, 186
Sekine, Y., Lebonnois, S., Imanaka, H., et al. 2008b, Icar, 194, 201
Senekowitsch, J., O'Neil, S., Knowles, P., & Werner, H. J. 1991, JPhCh, 95, 2125
Shaw, D. 1992, CP, 166, 379
Sheehan, C. H., & St. Maurice, J. P. 2004, JGRA, 109, A03302
Simon, C., Lilensten, J., Dutuit, O., et al. 2005, AnGeo, 23, 781
Slanger, T. G., & Black, G. 1976, JChPh, 64, 4442
Slanger, T. G., Wood, B. J., & Black, G. 1973, J. Photochem., 2, 63
Smith, D., & Adams, N. G. 1980, CPL, 76, 418
Smith, D., Adams, N. G., & Miller, T. M. 1978, JChPh, 69, 308
Smith, I. W. M. 2008, Chem. Soc. Rev., 37, 812
Sohlberg, K. 1999, CP, 246, 307
Soorkia, S., Liu, C.-L., Savee, J. D., et al. 2008, RSci, 82, 124102
Sperlein, R. F., & Golde, M. F. 1989, JChPh, 91, 6120
Sprengers, J. P., Ubachs, W., Johansson, A., et al. 2004, JChPh, 120, 8973
Stebbings, R. F., & Lindsay, B. G. 2001, JChPh, 114, 4741
Stief, L. J., Nesbitt, F. L., Payne, W. A., et al. 1995, JChPh, 102, 5309
Stockbauer, R. 1973, JChPh, 58, 3800
Stockbauer, R., & Inghram, M. G. 1976, JChPh, 65, 4081
Straub, H. C., Renault, P., Lindsay, B. G., Smith, K. A., & Stebbings, R. F. 1996, PhRvA, 54, 2146
Strobel, D. F., & Shemansky, D. E. 1982, JGR, 87, 1361
Sugawara, K., Ishikawa, Y., & Sato, S. 1980, Bull. Chem. Soc. Japan, 53, 3159
Sun, Y., Zhang, Q. Y., Ai, X. C., Zhang, H. P., & Sun, C. C. 2004, J. Mol. Struct.—Theochem, 686, 123
Sunderlin, L. S., & Armentrout, P. B. 1994, JChPh, 100, 5639
Suzuki, S., Itoh, H., Sekizawa, H., & Ikuta, N. 1993a, JPSJ, 62, 2692
Suzuki, S., Itoh, H., Sekizawa, H., & Ikuta, N. 1997, JaJAP, 36, 4744
Suzuki, T., Shihira, Y., Sato, T., Umemoto, H., & Tsunashima, S. 1993b, J. Chem. Soc.: Faraday Trans., 89, 995
Takayanagi, T., Kurosaki, Y., Misawa, K., et al. 1998a, JPCA, 102, 6251
Takayanagi, T., Kurosaki, Y., Sato, K., & Tsunashima, S. 1998b, JPCA, 102, 10391
Takayanagi, T., Kurosaki, Y., Sato, K., et al. 1999, JPCA, 103, 250
Tawara, H., & Kato, M. 1999, in NIFS-DATA-51 (Nagoya: National Institute for Fusion Science)
Teanby, N. A., Irwin, P. G. J., de Kok, R., et al. 2008, Icar, 193, 595
Teanby, N. A., Irwin, P. G. J., de Kok, R., et al. 2009, Icar, 202, 620
Thissen, R., Soldi-Lose, H., Alcaraz, C., et al. 2004, in XIVth Symp. on Atomic, Cluster, and Surface Physics (SASP), Molecular Dication Reactions of Interest for Planetary Ionospheres, ed. G. C. a. P. Casavecchia (La Thuile: Univ. of Innsbruck, Austria), 50
Thissen, R., Vuitton, V., Lavvas, P., et al. 2009, JPCA, 113, 11211
Thissen, R., Witasse, O., Dutuit, O., et al. 2011, PCCP, 13, 18264
Thomas, J. M., Jeffries, J. B., & Kaufman, F. 1983, CPL, 102, 50
Thomas, J. M., Kaufman, F., & Golde, M. F. 1987, JChPh, 86, 6885
Thomas, R. D. 2008, Mass Spectrom. Rev., 27, 485
Tian, C., & Vidal, C. R. 1998, JPhB, 31, 5369
Tichy, M., Lister, D. G., Rakshit, A. B., et al. 1979, IJMSI, 29, 231
Tomasko, M. G., Doose, L., Engel, S., et al. 2008, P&SS, 56, 669
Torr, M. R., & Torr, D. G. 1979, GeoRL, 6, 775
Tosi, P., Dimitrijev, O., & Bassi, D. 1992, JChPh, 97, 3333
Tosi, P., Dmitriev, O., Bassi, D., Wick, O., & Gerlich, D. 1994, JChPh, 100, 4300
Tosi, P., Lu, W. Y., Bassi, D., & Tarroni, R. 2001, JChPh, 114, 2149

Uiterwaal, C. J. G. J., van Eck, J., & Niehaus, A. 1995, JChPh, 102, 744
Umemoto, H. 2007, JChPh, 127, 014304
Umemoto, H., Hachiya, N., Matsunaga, E., Suda, A., & Kawasaki, M. 1998a, CPL, 296, 203
Umemoto, H., Kimura, Y., & Asai, T. 1997, CPL, 264, 215
Umemoto, H., Nakae, T., Hashimoto, H., Kongo, K., & Kawasaki, M. 1998b, JChPh, 109, 5844
Umemoto, H., Nakagawa, S., Tsunashima, S., & Sato, S. 1986, Bull. Chem. Soc. Japan, 59, 1449
Umemoto, H., Sugiyama, K., Tsunashima, S., & Sato, S. 1985, Bull. Chem. Soc. Japan, 58, 3076
Umemoto, H., Terada, N., & Tanaka, K. 2000, JChPh, 112, 5762
Vacher, J. R., Le Duc, E., & Fitaire, M. 1997, P&SS, 45, 1407
Vacher, J. R., Le Duc, E., & Fitaire, M. 2000, P&SS, 48, 237
Van Brunt, R. J., & Kieffer, L. J. 1975, JChPh, 63, 3216
Vidaud, P. H., Wayne, R. P., Yaron, M., & Vonengel, A. 1976, J. Chem. Soc.: Faraday Trans., 72, 1185
Vigren, E., Semaniak, J., Hamberg, M., et al. 2012, P&SS, 60, 102
Vinatier, S., Bézard, B., Nixon, C. A., et al. 2010, Icar, 205, 559
Vuitton, V., Dutuit, O., Balucani, N., & Smith, M. A. 2012, Titan (Cambridge: Cambridge Univ. Press)
Vuitton, V., Lavvas, P., Yelle, R. V., et al. 2009, P&SS, 57, 1558
Vuitton, V., Yelle, R. V., & Anicich, V. G. 2006, ApJL, 647, L175
Vuitton, V., Yelle, R. V., & Cui, J. 2008, JGR, 113, E05007
Vuitton, V., Yelle, R. V., & McEwan, M. J. 2007, Icar, 191, 722
Wahlund, J.-E., Boström, R., Gustafsson, G., et al. 2005, Sci, 308, 986
Waite, J. H., Niemann, H., Yelle, R. V., et al. 2005, Sci, 308, 982
Wakelam, V., Herbst, E., Loison, J. C., et al. 2012, ApJS, 199, 21
Wakelam, V., Smith, I. W. M., Herbst, E., et al. 2010, SSRv, 156, 13
Walter, C. W., Cosby, P. C., & Helm, H. 1993, JChPh, 99, 3553
Warneck, V. P. 1972, Ber. Bunsenges. Phys. Chem. Chem. Phys., 76, 413
Wehlitz, R. 2010, AAMOP, 58, 1
Westlake, J. H., Waite, J. H., Jr., Mandt, K. E., et al. 2012, JGRE, 117, E01003
Whitefield, P. D., & Hovis, F. E. 1987, CPL, 135, 454
Wiese, W. L., & Fuhr, J. R. 2007, JPCRD, 36, 1287
Wong, A. T., Bacskay, G. B., Hush, N. S., & Bogaard, M. P. 1991, MolPh, 74, 1037
Woodruff, P. R., & Marr, G. V. 1977, RSPSA, 358, 87
Wuerker, R. F., Schmitz, L., Fukuchi, T., & Straus, P. 1988, CPL, 150, 443
Yang, Y., Zhang, W. J., Pei, S. X., et al. 2005, JMoSt, 725, 133
Yelle, R. V., Cui, J., & Müller-Wodarg, I. C. F. 2008, JGR, 113, E10003
Yelle, R. V., Vuitton, V., Lavvas, P., et al. 2010, FaDi, 147, 31
Young, R. A., Black, G., & Slanger, T. G. 1969, JChPh, 50, 303
Young, R. A., & Dunn, O. J. 1975, JChPh, 63, 1150
Yung, Y. L. 1987, Icar, 72, 468
Zabka, J., Roithova, J., Spanel, P., & Herman, Z. 2010, JPCA, 114, 1384
Zipf, E. C. 1980, GeoRL, 7, 645